

Discovery and Structure–Activity Relationship Studies of Novel Adenosine A₁ Receptor-Selective AgonistsBarbara Preti,[#] Anna Suchankova,[#] Giuseppe Deganutti,[#] Michele Leunenberger, Kerry Barkan, Iga Manulak, Xianglin Huang, Sabrina Carvalho, Graham Ladds,* and Martin Lochner*Cite This: <https://doi.org/10.1021/acs.jmedchem.2c01414>

Read Online

ACCESS |



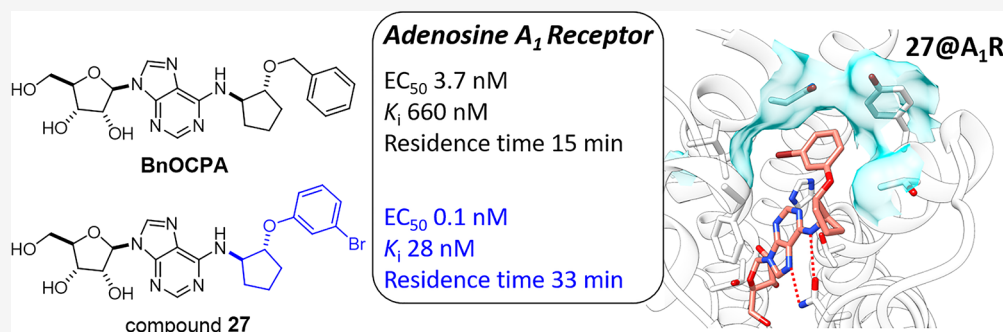
Metrics & More



Article Recommendations



Supporting Information



ABSTRACT: A series of benzyloxy and phenoxy derivatives of the adenosine receptor agonists *N*⁶-cyclopentyl adenosine (CPA) and *N*⁶-cyclopentyl 5'-*N*-ethylcarboxamidoadenosine (CP-NECA) were synthesized, and their potency and selectivity were assessed. We observed that the most potent were the compounds with a halogen in the *meta* position on the aromatic ring of the benzyloxy- or phenoxy-cyclopentyl substituent. In general, the NECA-based compounds displayed greater A₁R selectivity than the adenosine-based compounds, with *N*⁶-2-(3-bromobenzyloxy)cyclopentyl-NECA and *N*⁶-2-(3-methoxyphenoxy)cyclopentyl-NECA showing ~1500-fold improved A₁R selectivity compared to NECA. In addition, we quantified the compounds' affinity and kinetics of binding at both human and rat A₁R using a NanoBRET binding assay and found that the halogen substituent in the benzyloxy- or phenoxy-cyclopentyl moiety seems to confer high affinity for the A₁R. Molecular modeling studies suggested a hydrophobic subpocket as contributing to the A₁R selectivity displayed. We believe that the identified selective potent A₁R agonists are valuable tool compounds for adenosine receptor research.

INTRODUCTION

The adenosine A₁ receptor (A₁R) is a G protein-coupled receptor (GPCR) that belongs to the adenosine receptor family consisting of four receptor subtypes (A₁R, A_{2A}R, A_{2B}R, and A₃R). All four receptor subtypes are nonselectively activated by the endogenous ligand adenosine, a naturally occurring purine nucleoside. The adenosine receptors are widely expressed in the body and therefore implicated in various pathological conditions including cancer; sleep regulation; and cardiovascular, neurodegenerative, and inflammatory diseases.^{1–9} The wide expression pattern has led to the reality that despite more than four decades of intense medicinal research, very few compounds have actually made it to the clinic due to unacceptable side effects based on insufficient subtype selectivity and/or low efficacy, leaving a big untapped need for subtype-selective compounds.^{10,11}

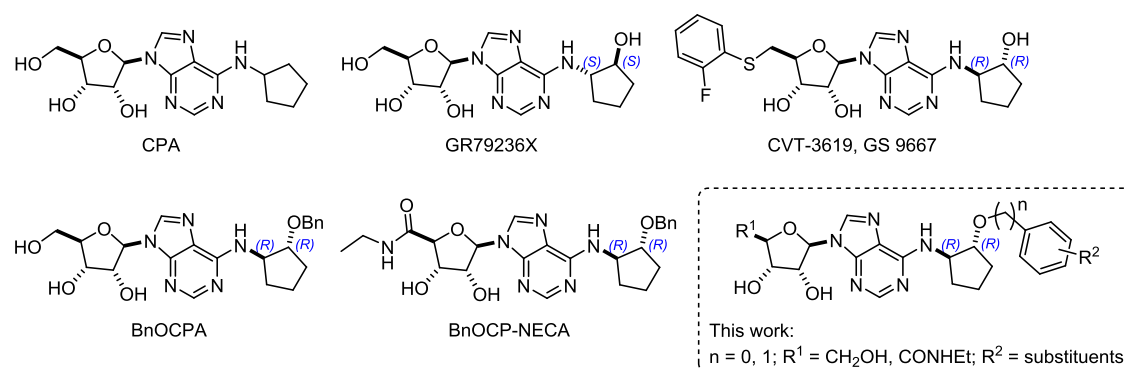
The selective activation of the A₁R, in particular, is a very promising strategy for the treatment of glaucoma, type 2 diabetes mellitus, pain, epilepsy, heart arrhythmias, and cerebral ischemia, in which there are clear unmet clinical needs that could be addressed with novel more selective

therapeutics.^{11,12} Although all members of the adenosine receptor family are activated by endogenous adenosine, the A₁R and A₃R receptors are predominantly G_{i/o}-coupled, while the A_{2A}R and A_{2B}R are predominantly G_s-coupled. The classical pathway following G_{i/o} activation is the inhibition of adenylyl cyclase (AC) and subsequent inhibition of 3',5'-cyclic adenosine monophosphate (cAMP) accumulation in the cell, while activation of G_s activates AC, resulting in the promotion of cAMP accumulation.

Several potent and A₁R-selective agonists are based on the endogenous adenosine scaffold. Substitution at the purine C-2 position, e.g., with chloride, and at the *N*⁶ position with cycloalkyl- and bicycloalkyl groups has led to potent and A₁R-

Received: August 26, 2022

Chart 1. Known N^6 -Cyclopentyl Adenosine A_1R Agonists, Previously Synthesized A_1R Agonists, and Derivatives Presented in This Work



selective agonists.^{11–15} In addition, the ribose moiety has been the focus of synthetic modifications in AR agonist development. The ribose C-5' position tolerates certain substitutions, such as a 5'-carboxamido group in the prototypical, very potent, albeit not highly subtype-selective AR agonist 5'-*N*-ethylcarboxyamidoadenosine (NECA). Small 5'-chlorine substituents have also been used, and it was shown that they, together with N^6 -bicycloalkyl groups, lead to high-affinity and highly selective human A_1R agonists, which have antinociceptive effects in mice without affecting motor or cardiovascular functions.^{16,17} More bulky pyrazole groups have also been employed at this C-5' position and yielded potent and selective A_1R agonists that showed analgesic effects in mice.¹⁵ Other successful selective and CNS active A_1R agonist examples feature conformationally constrained ribose ring systems.¹⁴ Alternatively, non-nucleoside 3,5-dicyanopyridines have been synthetically optimized to yield potent and A_1R -selective full agonists, which have also been developed into PET tracers very recently.¹⁸ Rather than modulating receptor activity by orthosteric exogenous agonists, Christopoulos and collaborators have recently presented MIPSS21, a positive allosteric modulator of the A_1R , with which they were able to show *in vivo* analgesic efficacy in rats.¹⁹ Their cryo-EM structural study of the human A_1R bound to adenosine, MIPSS21, and a G_{12} protein heterotrimer (PDB code 7LD3) revealed the allosteric binding pocket at the lipid interface that could spark structure-based drug design campaigns.

We have previously reported the adenosine-based potent and highly A_1R -selective full agonist BnOCPA (Chart 1), which emerged from a structure–activity relationship (SAR) study with respect to cyclic and bicyclic purine N^6 substituents.¹³ Our SAR study also showed that the synthetic NECA derivatives, such as BnOCP-NECA (Chart 1), were generally less subtype-selective than the adenosine ones. BnOCPA and BnOCP-NECA are extension derivatives of the prototypical, non-subtype-selective AR agonist N^6 -cyclopentyl adenosine (CPA). The N^6 -hydroxycyclopentyl moiety is present in the known A_1R -selective partial agonist CVT-3619 (later renamed GS 9667) and full agonist GR79236X. It should be noted that the stereochemical configuration of the N^6 -hydroxycyclopentyl group in GR79236X is opposite to that in CVT-3619 and BnOCPA (Chart 1). Both GR79236X and CVT-3619 are able to increase insulin sensitivity and thus have been evaluated in clinical trials for the treatment of type II diabetes; however, their development was not successful and later discontinued.^{20,21} Appending a benzyl group to the N^6 -hydroxycyclopentyl moiety, we have found previously that

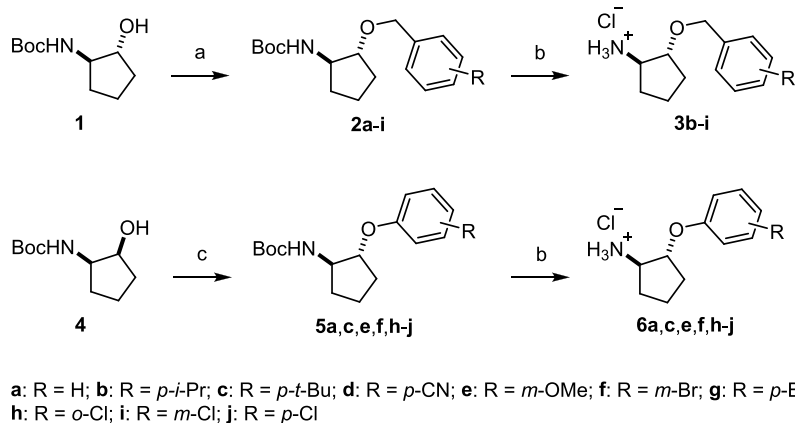
BnOCPA retained high potency at A_1R and displayed very high A_1R selectivity compared to the nonbenzylated congener.¹³

Subsequently, we demonstrated that BnOCPA was able to specifically activate $G_{\alpha_{ob}}$ protein subtype-mediated signaling, which translated into potent *in vivo* analgesia without causing sedation, bradycardia, hypotension, or respiratory depression.²² Molecular dynamics (MD) simulations using the cryo-EM structure of the active adenosine-bound A_1R -heterotrimeric G_{12} protein complex (PDB code 6D9H²³) proposed four binding modes of BnOCPA²² due to the high flexibility of the N^6 -appended benzyloxy group.²⁴

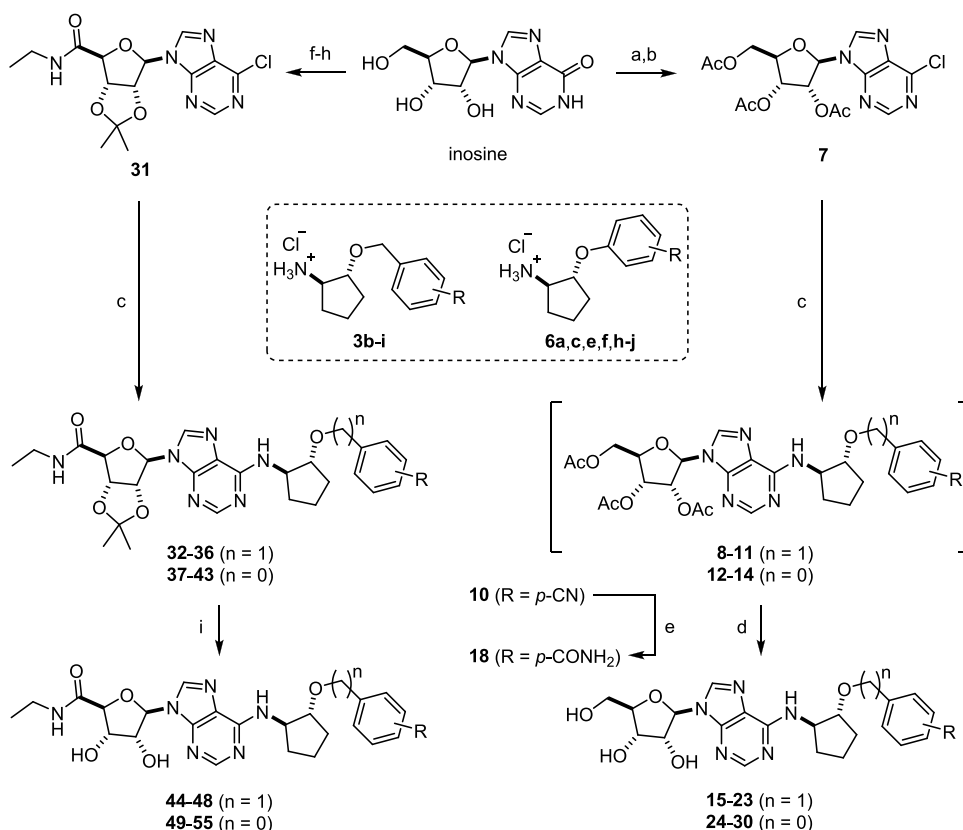
Based on these molecular modeling studies, we have designed a series of adenosine- and NECA-based compounds with extended N^6 -benzyloxy- and N^6 -phenoxy-cyclopentyl substituents (Chart 1) with the aim of improving the potency at A_1R while maintaining or improving the subtype selectivity. To test the potency, selectivity, and affinity of the designed compounds at the adenosine receptors, we have employed the cAMP accumulation and NanoBRET binding assays previously validated and employed at ARs.²⁵ We explored subtype selectivity at human A_1R , $A_{2A}R$, $A_{2B}R$, and A_3R in mammalian CHO-K1 cells and confirmed the binding of the compounds at both human and rat A_1R in HEK293 cells. Kinetic studies were performed to dissect the binding properties of the compounds to h A_1R and r A_1R and outline their structure–kinetic relationship (SKR). Finally, we have also used MD modeling to evaluate the binding pose of some of the agonists and validated the findings using mutagenesis. Together, this approach has identified novel adenosine- and NECA-based derivatives with improved potency, selectivity, and affinity at the A_1R receptor. Hence, these compounds constitute valuable tools for cellular studies of the A_1R receptor and show interesting therapeutic promise.

RESULTS AND DISCUSSION

Chemistry. Our initial synthetic strategy was designed for keeping the route as concise as possible and entailed a projected *O*-alkylation of ribose-protected N^6 -hydroxycyclopentyl adenosine and NECA precursors. After exploring different *O*-alkylation protocols and ribose hydroxyl protecting groups, we abandoned this synthetic plan, as our attempts resulted in low conversions, trace amounts of desired products, and many side products stemming from the loss or migration of protecting groups, elimination reactions, and *N*-alkylation of amine and amide groups (Scheme S1).

Scheme 1. Synthesis of Benzyloxycyclopentyl and Phenoxy-cyclopentyl Amine Building Blocks^a

^aReagents and conditions: (a) R-BnBr (1 equiv), NaH (2 equiv), THF, 0 °C, 2–4 h, 30–91%; (b) HCl (4 M in dioxane), 1,4-dioxane, rt, 4–18 h, 50%-quant; and (c) R-PhOH, PPh₃, DIAD, THF, 0 °C to rt, 18 h, 51–62%.

Scheme 2. Synthesis of Benzyloxy- and Phenoxy-cyclopentyl Adenosine and NECA Derivatives^a

^aReagents and conditions: (a) Ac₂O, pyridine, rt 18 h, quant.; (b) SOCl₂, DMF, CH₂Cl₂, 50 °C, 18 h, 86%; (c) 3b-i or 6a,c,e,f,h-j, NaHCO₃, *i*-PrOH, 105 °C, 18 h, 36%-quant.; (d) K₂CO₃, MeOH, rt, 30 min, 36–93%; (e) K₂CO₃, H₂O₂ (aq. 30%), MeOH, 40 °C, 7 h, 83%; (f) 2,2-dimethoxypropane, *p*-TsOH, acetone, rt, 18 h, 32%; (g) TEMPO, DAIB, MeCN/H₂O, rt, 18 h, 80%; (h) SOCl₂, DMF, CH₂Cl₂, 50 °C, 18 h and then EtNH₂ (2 M in THF), 0 °C to rt, 30 min, 41%; and (i) AcOH, H₂O, 80 °C, 18 h, 43–73%.

We therefore adapted our strategy and carried out the *O*-alkylation on *N*-protected (1*R*,2*R*)-2-aminocyclopentanol **1**²⁶ (Scheme 1). Under optimized conditions, treating a mixture of **1** and benzyl bromide (1 equiv) in THF at 0 °C with sodium hydride (2 equiv) yielded 58% of desired **2a** after 4 h. It was important to monitor this reaction carefully, as after a certain time (2–4 h), side products started to emerge that diminished the isolated yields. These optimized conditions were applied

for the preparation of benzyloxycyclopentyl intermediates **2b**–**i**, which were isolated in moderate to very good yields (30–91%).

For the introduction of the phenoxy substituents on the cyclopentyl ring, we first tosylated epimeric *N*-protected (1*S*,2*R*)-2-aminocyclopentanol **4** (*p*-TsCl, pyridine, rt, 24 h, 57% yield), which was followed by S_N2-type substitution with phenoxide (Figure S1). However, the latter reaction required

Table 1. Affinity (pK_i) and Potency (pEC_{50}) of Extended BnOCPA Derivatives at Human A_1R ^{a,c}

compd	R ¹	R ²	pEC_{50} (hA_1R) ^b	E_{max} ^c	pK_i (hA_1R) ^d
BnOCPA	-CH ₂ OH	H	8.43 ± 0.09	51.49 ± 1.9	6.18 ± 0.09
15	-CH ₂ OH	<i>p-i</i> Pr	7.87 ± 0.16	51.95 ± 3.1	5.77 ± 0.08
16	-CH ₂ OH	<i>p-t</i> Bu	8.20 ± 0.13	54.59 ± 2.8	5.58 ± 0.10
17	-CH ₂ OH	<i>p</i> -CN	7.40 ± 0.19	58.03 ± 4.2	5.85 ± 0.06
18	-CH ₂ OH	<i>p</i> -CONH ₂	7.71 ± 0.13	59.51 ± 4.1	5.98 ± 0.05

^aData are the mean ± SEM of at least three independent repeats conducted in duplicate. ^bThe negative logarithm of the agonist concentration required to produce a half-maximal inhibition response of the 10 μM forskolin-induced cAMP accumulation in CHO-K1- A_1R cells. ^cThe % maximal inhibition of cAMP accumulation for each agonist. Calculated as the % inhibition of the 10 μM forskolin response. ^dBinding affinity (pK_i) determined through the NanoBRET binding assay in HEK293 cells stably expressing human Nluc- A_1R . The resulting concentration-dependent decrease in NanoBRET ratio at 10 min was used to calculate pK_i . Statistical significance (* p < 0.05) determined using one-way ANOVA and Dunnett's post-test and presented as described by Curtis *et al.*³¹

Benzyloxycyclopentyl derivatives

Phenoxycyclopentyl derivatives

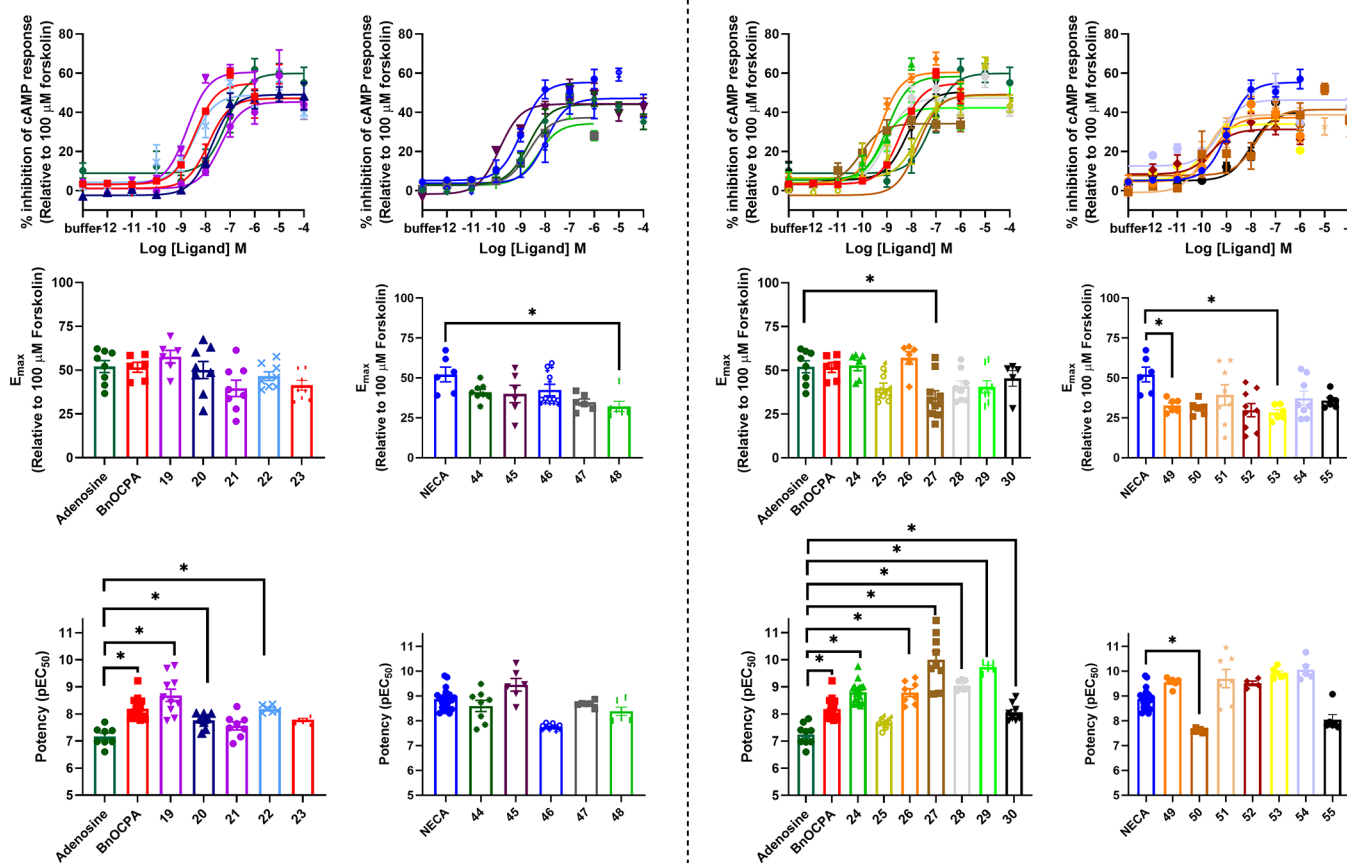


Figure 1. Efficacy and potency of synthetic benzyloxy- and phenoxycyclopentyl adenosine and NECA derivatives at A_1R . cAMP response in CHO-K1 cells stably expressing human A_1R in response to varying concentrations of AR ligands and 10 μM forskolin. E_{max} and pEC_{50} values for individual repeats are plotted at the bottom. Data are the mean ± SEM of at least three independent repeats conducted in duplicate. Statistical significance (* p < 0.05) determined using one-way ANOVA and Dunnett's post-test, presented as described in ref 31.

forcing conditions (phenol, K_2CO_3 , DMF, 70 °C, 3 days) to obtain **5a** with the desired (1*R*,2*R*) stereochemistry in acceptable 61% yield. We therefore sought a milder, more efficient method and hypothesized that the Mitsunobu reaction²⁷ might allow us to directly access protected phenoxycyclopentyl amines **5** from **4** (Scheme 1). The Mitsunobu reaction is commonly used to convert primary

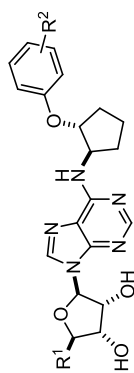
and secondary alcohols to a variety of functional groups with inversion at the alcohol stereogenic center and requires an acidic nucleophile (e.g. carboxylic acids). In rare cases, phenols (pK_a ~9–10) were employed as nucleophiles, but to the best of our knowledge, cyclic secondary alcohols were not reported as Mitsunobu substrates to date. We were therefore pleased to find that adding diisopropyl azodicarboxylate (DIAD) to a

Table 2. Affinity (pK_i) and Potency (pEC_{50}) of Synthetic Adenosine and NECA Benzylcyclopentyl Derivatives

compd	R ¹	R ²	adenosine			NECA			BnOCPA, 19-23, 44-48			
			pEC_{50}^a	E_{max}^b	pK_i^d	pEC_{50}^a	E_{max}^c	pK_i^d	pEC_{50}^a	E_{max}^b	pK_i^d	
adenosine			7.16 ± 0.23	51.09 ± 4.9	7.60 ± 0.11	21.53 ± 0.9	7.28 ± 0.12	59.07 ± 2.9	7.87 ± 0.23	24.71 ± 2.5	6.09 ± 0.06	6.06 ± 0.05
BnOCPA	-CH ₂ OH	H	8.43 ± 0.09*	51.49 ± 1.9	4.95 ± 0.38*	17.13 ± 4.6	N.D. ^e	N.D. ^f	N.R. ^g		6.18 ± 0.09	6.41 ± 0.06*
19	-CH ₂ OH	<i>m</i> -OMe	8.74 ± 0.10*	57.41 ± 2.4	N.D.	N.D.	N.D.	5.98 ± 0.47*	5.98 ± 0.47*	9.52 ± 2.1*	6.67 ± 0.10*	6.55 ± 0.06*
20	-CH ₂ OH	<i>m</i> -Br	7.74 ± 0.13*	51.44 ± 2.8	N.R.	N.D.	N.D.	5.08 ± 0.26*	5.08 ± 0.26*	12.59 ± 1.8*	6.16 ± 0.10	6.13 ± 0.08
21	-CH ₂ OH	<i>p</i> -Br	7.39 ± 0.16	44.25 ± 3.2	N.D.	N.D.	N.D.	N.R.	N.R.		5.94 ± 0.07	6.06 ± 0.07
22	-CH ₂ OH	<i>o</i> -Cl	8.47 ± 0.24*	44.66 ± 4.3	5.17 ± 0.33*	18.55 ± 3.5	4.57 ± 0.12*	96.93 ± 8.1*	N.R.		6.56 ± 0.07*	6.56 ± 0.04*
23	-CH ₂ OH	<i>m</i> -Cl	7.88 ± 0.17	45.97 ± 3.3	N.D.	N.D.	N.D.	N.R.	N.R.		6.15 ± 0.07	6.43 ± 0.03*
NECA			8.96 ± 0.11	50.11 ± 2.4	7.95 ± 0.26	22.03 ± 2.4	7.20 ± 0.07	68.12 ± 2.0	7.83 ± 0.26	34.34 ± 3.7	6.61 ± 0.06	6.38 ± 0.04
44	-CONHET	<i>m</i> -OMe	8.67 ± 0.19	41.15 ± 3.3	N.R.	N.D.	4.42 ± 0.16*	73.07 ± 8.9	5.38 ± 0.09*	46.56 ± 2.1	6.39 ± 0.08	6.11 ± 0.07*
45	-CONHET	<i>m</i> -Br	9.85 ± 0.19	46.12 ± 5.2	N.R.	N.D.	N.D.	N.D.	5.56 ± 0.10*	49.17 ± 2.4*	6.54 ± 0.15	6.46 ± 0.07
46	-CONHET	<i>p</i> -Br	7.97 ± 0.24	43.32 ± 4.5	N.D.	N.D.	N.D.	N.D.	5.82 ± 0.20*	30.56 ± 2.8	6.15 ± 0.06*	6.38 ± 0.03
47	-CONHET	<i>o</i> -Cl	8.67 ± 0.15	34.67 ± 2.2	5.68 ± 0.32	20.34 ± 3.1	5.36 ± 0.08*	87.58 ± 3.3	5.85 ± 0.13*	43.92 ± 2.8	6.63 ± 0.07	6.85 ± 0.05*
48	-CONHET	<i>m</i> -Cl	8.29 ± 0.16	31.57 ± 2.1*	5.04 ± 0.29*	17.18 ± 2.9	4.72 ± 0.11*	96.14 ± 6.8*	5.83 ± 0.39*	31.06 ± 5.7	6.49 ± 0.08	6.90 ± 0.05*

^aThe negative logarithm of the agonist concentration required to produce a half-maximal response in the cAMP accumulation assay in CHO-K1 cells stably expressing a human AR subtype. Forskolin is included in the assay (10 and 1 μ M for A₁R and A₃R, respectively). ^bThe % maximal inhibition of cAMP accumulation for each agonist. Forskolin is included in the assay (10 and 1 μ M for A₁R and A₃R, respectively). ^cThe % maximal accumulation of each agonist relative to 10 μ M forskolin stimulation. ^dBinding affinity (pK_i) determined through the NanoBRET binding assay in HEK293 cells stably expressing human or rat Nluc-A₁R. The resulting concentration-dependent decrease in NanoBRET ratio at 10 min was used to calculate pK_i . ^eN.D., not determined. Full dose-response curve was not feasible. ^fN.R., no response detected in the assay. All data are the mean \pm SEM of at least three independent repeats conducted in duplicate. Statistical significance (* p < 0.05) determined using one-way ANOVA and Dunnett's post-test, presented according to ref 31. Adenosine derivatives were compared to adenosine, while NECA derivatives were compared to NECA.

†

Table 3. Affinity (pK_i) and Potency (pEC_{50}) of Synthetic Adenosine and NECA Phenoxy-cyclopentyl Derivatives

24-30, 49-55

compd	R ¹	R ²	hA ₁ R			hA _{2A} R			hA _{2B} R			hA ₃ R			rA ₁ R		
			pEC_{50}^a	E_{max}^b	pEC_{50}^a	E_{max}^c	pEC_{50}^d	E_{max}^e	pEC_{50}^f	E_{max}^g	pEC_{50}^h	E_{max}^i	pK_i^d	pK_i^d	pK_i^d		
adenosine																	
24	-CH ₂ OH	H	7.16 ± 0.23	51.09 ± 4.9	7.60 ± 0.11	21.53 ± 0.9	7.28 ± 0.12	59.07 ± 2.9	7.87 ± 0.23	24.71 ± 2.5	6.09 ± 0.06	6.06 ± 0.05					
25	-CH ₂ OH	<i>p</i> -t-Bu	8.98 ± 0.14*	52.71 ± 3.1	N.D. ^e		4.90 ± 0.14*	64.19 ± 5.4	5.78 ± 0.42*	17.83 ± 3.7	6.84 ± 0.06*	6.60 ± 0.02*					
26	-CH ₂ OH	<i>m</i> -OMe	7.74 ± 0.28	42.14 ± 5.1	N.D. ^f		N.D.		N.R.		6.35 ± 0.08	6.70 ± 0.05*					
26	-CH ₂ OH	<i>m</i> -OMe	9.28 ± 0.10*	56.74 ± 2.4	5.24 ± 0.55*	17.25 ± 5.0	N.D.		N.R.		6.61 ± 0.07*	6.56 ± 0.06*					
27	-CH ₂ OH	<i>m</i> -Br	10.0 ± 0.24*	30.55 ± 3.3*	N.D.		4.63 ± 0.12*	82.53 ± 6.2	N.R.		7.55 ± 0.11*	6.94 ± 0.08*					
28	-CH ₂ OH	<i>o</i> -Cl	9.03 ± 0.19*	44.15 ± 3.6	5.96 ± 0.28*	17.01 ± 2.2	5.31 ± 0.09*	96.77 ± 4.4*	6.73 ± 0.42	13.42 ± 2.4*	7.17 ± 0.06*	7.28 ± 0.04*					
29	-CH ₂ OH	<i>m</i> -Cl	9.21 ± 0.19*	38.25 ± 3.0	6.26 ± 0.34	13.63 ± 2.1	5.29 ± 0.07*	96.93 ± 8.1*	6.81 ± 0.47	11.77 ± 2.3*	7.19 ± 0.07*	7.36 ± 0.03*					
30	-CH ₂ OH	<i>p</i> -Cl	8.19 ± 0.18*	45.06 ± 3.6	4.86 ± 0.58*	15.15 ± 5.5	N.D.		6.88 ± 0.60	12.5 ± 3.2*	6.23 ± 0.11	6.22 ± 0.06					
NECA			8.96 ± 0.11	50.11 ± 2.4	7.95 ± 0.26	22.03 ± 2.4	7.20 ± 0.07	68.12 ± 2.0	7.83 ± 0.26	34.34 ± 3.7	6.61 ± 0.06	6.38 ± 0.04					
49	-CONH ₂	H	9.53 ± 0.20	32.68 ± 2.5*	5.48 ± 0.42*	15.41 ± 3.0	6.04 ± 0.09*	87.99 ± 3.7*	7.17 ± 0.16	51.24 ± 3.4*	7.30 ± 0.05*	7.41 ± 0.03*					
50	-CONH ₂	<i>p</i> -t-Bu	7.81 ± 0.41*	33.66 ± 6.1	4.84 ± 0.30*	20.11 ± 3.8	4.77 ± 0.08*	96.35 ± 5.0*	6.63 ± 0.19*	39.85 ± 3.2	6.35 ± 0.07	6.85 ± 0.05*					
51	-CONH ₂	<i>m</i> -OMe	9.88 ± 0.29	39.71 ± 5.9	5.20 ± 1.11*	5.16 ± 3.1*	5.10 ± 0.07*	84.76 ± 3.3	5.56 ± 0.14*	59.38 ± 4.0*	7.26 ± 0.14*	6.85 ± 0.06*					
52	-CONH ₂	<i>m</i> -Br	9.62 ± 0.35	39.71 ± 5.9	4.58 ± 0.87*	11.48 ± 6.7	5.37 ± 0.11*	61.12 ± 3.3	5.52 ± 0.12*	68.26 ± 3.8*	7.05 ± 0.16*	6.82 ± 0.10*					
53	-CONH ₂	<i>o</i> -Cl	9.91 ± 0.23	28.65 ± 2.7*	5.67 ± 0.46*	14.69 ± 3.2	6.22 ± 0.09*	80.91 ± 3.1	7.00 ± 0.19*	41.6 ± 3.3	7.39 ± 0.04*	7.60 ± 0.04*					
54	-CONH ₂	<i>m</i> -Cl	9.28 ± 0.28	34.67 ± 2.1	5.86 ± 0.41	13.32 ± 2.6	6.01 ± 0.09*	78.81 ± 3.4	6.79 ± 0.14*	44.20 ± 2.6	7.43 ± 0.05*	7.51 ± 0.06*					
55	-CONH ₂	<i>p</i> -Cl	7.99 ± 0.15	35.07 ± 2.5	4.86 ± 0.32*	25.01 ± 5.2	5.10 ± 0.09*	83.73 ± 4.5	6.92 ± 0.17*	47.16 ± 3.3	6.86 ± 0.10	7.08 ± 0.04*					

^aThe negative logarithm of the agonist concentration required to produce a half-maximal response in the cAMP accumulation assay in CHO-K1 cells stably expressing a human AR subtype. Forskolin is included in the assay (10 and 1 μ M for A₁R and A₃R, respectively). ^bThe % maximal inhibition of cAMP accumulation for each agonist. Forskolin is included in the assay (10 and 1 μ M for A₁R and A₃R, respectively). ^cThe % maximal accumulation of each agonist relative to 10 μ M forskolin stimulation. ^dBinding affinity (pK_i) determined through the NanoBRET binding assay in HEK293 cells stably expressing human or rat Nluc-A₁R. The resulting concentration-dependent decrease in NanoBRET ratio at 10 min was used to calculate pK_i . ^eN.D., not determined. Full dose-response curve was not feasible. ^fN.R., no response detected in the assay. All data are the mean \pm SEM of at least three independent repeats conducted in duplicate. Statistical significance ($*p < 0.05$) determined using one-way ANOVA and Dunnett's post-test, presented according to ref 31. Adenosine derivatives were compared to adenosine, while NECA derivatives were compared to NECA.

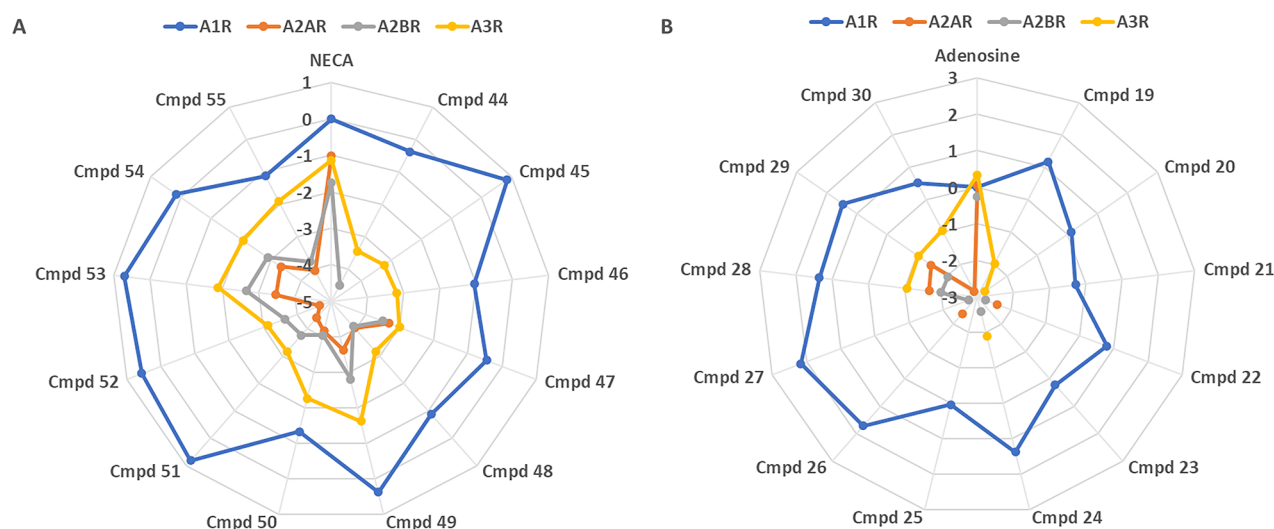


Figure 2. Adenosine and NECA derivatives show selectivity towards A₁R subtype. Log(RA) values of AR ligands at human A₁R, A_{2A}R, A_{2B}R, and A₃R normalized to (A) NECA or (B) adenosine response at A₁R.

solution of **4**, phenol, and triphenylphosphine at 0 °C and subsequent stirring at room temperature overnight delivered **5a** in 60% yield. ¹H NMR spectra of **5a** obtained via Mitsunobu reaction and of **5a** isolated after S_N2 phenoxide substitution of tosylated **4** were identical, confirming full inversion at C-1 during the Mitsunobu reaction (Figure S1). For comparison, reaction with epimeric **1** under identical Mitsunobu conditions yielded the C-1 epimer of **5a** with a distinctively different ¹H NMR spectrum. Overall, our new synthetic strategy efficiently produced phenoxy-cyclopentyl building block **5** in moderate to good yields. Clean removal of the Boc-protecting group from **2** and **5** was achieved with HCl in dioxane to deliver ammonium salts **3** and **6** (Scheme 1).

Nucleophilic aromatic substitution (S_NAr) of 6-chloropurines **7** and **31** with amines **3** and **6** assembled the final agonist scaffolds (Scheme 2). Chloropurines **7** and **31** were synthesized starting from inosine using procedures adopted from Kotra *et al.*²⁸ and Middleton *et al.*,²⁹ with minor experimental modifications. Removal of the acetate groups was carried out with potassium carbonate in methanol at room temperature, while removal of the ribose acetonide group was accomplished with acetic acid in water at 80 °C, yielding final adenosine derivatives **15–30** and NECA derivatives **44–55** in high purity and sufficient quantity.

In the adenosine series, we observed partial cleavage of the acetate groups during the S_NAr reaction for some substrates, which led to complex but separable mixtures of desired nucleosides **8–14** and various deacetylated side products. We found that it was more convenient to take these crude mixtures into the subsequent deprotection step and isolate the fully deacetylated final products **15–30** (Scheme 2). Primary carboxamide derivative **18** was obtained from protected nitrile nucleoside **10** through hydrolysis with basic hydrogen peroxide in methanol at elevated temperatures.³⁰

Biological Activity at the Human A₁ Receptor.

BnOCPA has previously been identified as a high-potency A₁R-selective full agonist.^{13,22} Using insights from BnOCPA MD simulations^{22,24} and with the aim of further improving the A₁R selectivity and potency, we designed extended BnOCPA derivatives **15–18**. Their binding and activity at human A₁R

(hA₁R) were then explored using both a NanoBRET binding assay and a cAMP accumulation assay, respectively (Table 1). To determine the A₁R mediated G_{i/o} response, CHO-K1-A₁R cells were co-stimulated for 30 min with 10 μM forskolin (which promotes cAMP production by activating adenylyl cyclase), and the test compounds **15–18** were added in a range of concentrations (10⁻¹³ to 10⁻⁴ M).

All four compounds were found to be agonists at the hA₁R using the inhibiting forskolin-stimulated cAMP accumulation assay with equivalent E_{max} values to that of the full agonist BnOCPA. **16** showed the highest potency with pEC₅₀ of 8.20 ± 0.13, which was similar to BnOCPA (pEC₅₀ of 8.43 ± 0.09). **15–18** were further tested for their ability to displace the specific binding of CA200645, a fluorescent A₁R/A₃R antagonist, in HEK293 cells stably expressing an N-terminally tagged human Nanoluc-hA₁R (Nluc-hA₁R), as described previously.²⁵ All four explored BnOCPA derivative compounds **15–18** displayed similar affinity for Nluc-hA₁R with K_i in the range of 1–3 μM, which remained similar or lower than BnOCPA (K_i of 0.66 μM). Since none of derivatives **15–18** improved upon BnOCPA potency or affinity at the A₁R, we have decided to not continue with these compounds further and instead designed a new series of compounds based on adenosine (**19–30**) and their structural analogs based on NECA (**44–55**). Full cAMP inhibition curves in the CHO-K1-hA₁R cells were obtained as described above (Figure 1, Tables 2 and 3). Except for **27**, **48**, **49**, and **53**, which showed partial activity, all the tested compounds behaved as full agonists at the hA₁R. **27** was the most potent (pEC₅₀ of 10.0 ± 0.24), closely followed by **26**, **45**, **49**, and **51–54**. Furthermore, all these compounds displayed a higher potency than adenosine, NECA, or BnOCPA, making them very promising candidate compounds. It is interesting to note that, except for **49** and **53**, the most potent compounds have a substituent in the *meta* position and, except for **26**, **49** and **51**, all have a halogen substituent. Therefore, it seems that a halogen in the *meta* position on the aromatic ring confers high potency at the hA₁R. In addition, all most potent hA₁R agonists except **45** feature a N⁶-phenoxy-cyclopentyl moiety.

Subtype Selectivity of Adenosine and NECA Derivatives. As the structural similarity between the orthosteric site

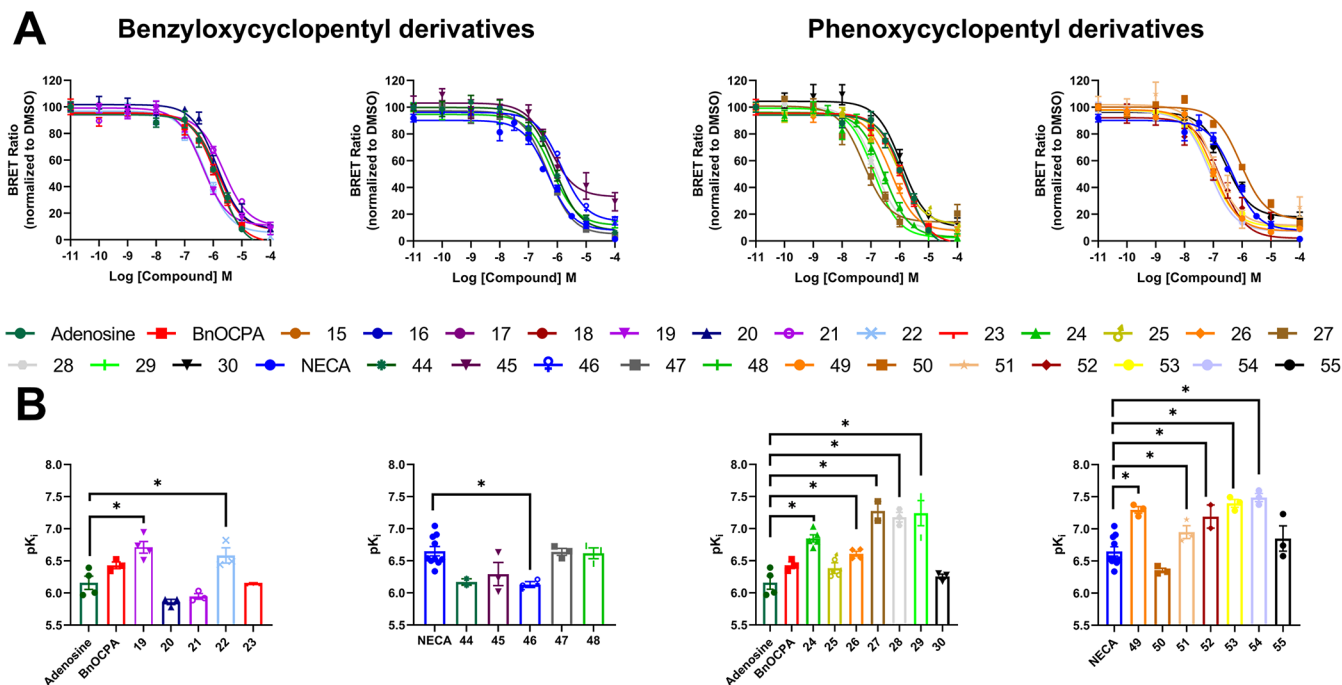
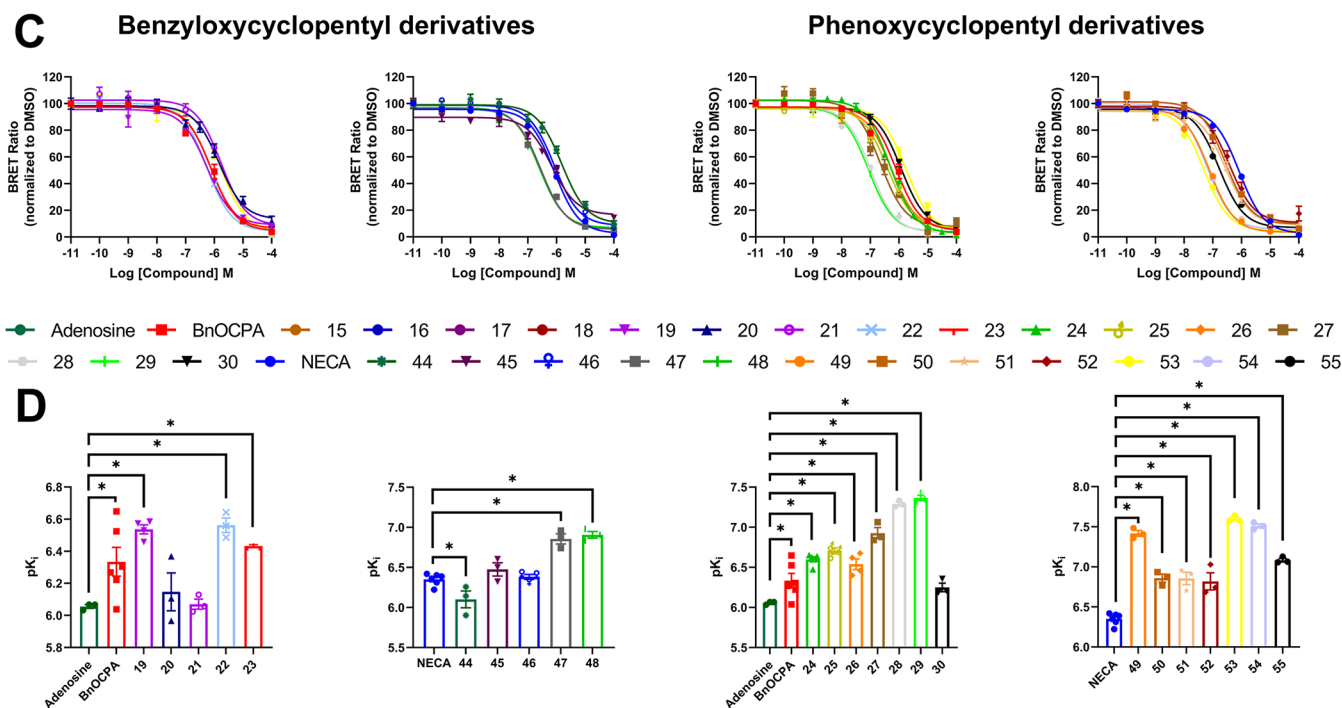
Human A₁RRat A₁R

Figure 3. Binding affinity of AR ligands at human and rat A₁R measured by NanoBRET. HEK293 cells stably expressing (A) human or (C) rat Nluc-A₁R were treated with 20 nM CA200645 and increasing concentrations of unlabeled AR ligand. pK_i values for individual repeats from (B) human A Nluc-A₁R and (D) rat Nluc-A₁R. Data are the mean ± SEM of at least three independent repeats conducted in duplicate. Statistical significance (**p* < 0.05) determined using one-way ANOVA and Dunnett's post-test, presented as described in ref 31.

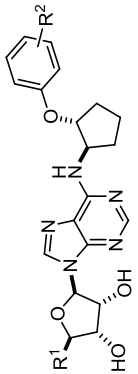
of the four adenosine receptor subtypes often results in reduced selectivity of the compounds targeting them, we utilized CHO-K1 cells stably expressing human A_{2A}R, A_{2B}R, or A₃R (hA_{2A}R, hA_{2B}R, or hA₃R) and incubated them with

increasing concentrations of the tested compounds (10⁻¹³ to 10⁻⁴ M) to measure the cAMP accumulation in the cells in response to the agonists. For the G_{i/o}-coupled hA₃R, 1 μM forskolin was also included. This addition was not required for

Table 4. Kinetics of Binding for Synthetic Adenosine and NECA Benzylloxycyclopentyl Derivatives to the Orthosteric Binding Site at Human and Rat A₁R

compd	R ¹	R ²	adenosine				hA ₁ R				rA ₁ R			
			$k_{on} (k_3) \times 10^5 (M^{-1} min^{-1})^a$	$k_{off} (k_4) (min^{-1})^b$	pK_d^c	RT (min) ^d	$k_{on} (k_3) \times 10^5 (M^{-1} min^{-1})^a$	$k_{off} (k_4) (min^{-1})^b$	pK_d^c	RT (min) ^d	$k_{on} (k_3) \times 10^5 (M^{-1} min^{-1})^a$	$k_{off} (k_4) (min^{-1})^b$	pK_d^c	RT (min) ^d
adenosine			1.65 ± 0.24	0.048 ± 0.002		21.15 ± 0.84	0.52 ± 0.22	0.079 ± 0.007		12.86 ± 1.10				
BnOCPA	-CH ₂ OH	H	1.47 ± 0.33	0.068 ± 0.002		14.75 ± 0.56	1.57 ± 0.54	0.054 ± 0.007		19.42 ± 2.21				
NECA			2.04 ± 0.07	0.049 ± 0.005		20.97 ± 1.98	2.29 ± 0.39	0.066 ± 0.008		15.84 ± 2.05				
19	-CH ₂ OH	<i>m</i> -OMe	2.51 ± 0.36	0.041 ± 0.004		24.64 ± 1.98	2.52 ± 0.31	0.083 ± 0.016		13.22 ± 2.10				
20	-CH ₂ OH	<i>m</i> -Br	0.56 ± 0.12	0.080 ± 0.016		14.84 ± 3.83	1.50 ± 0.29	0.097 ± 0.008		10.56 ± 0.81				
21	-CH ₂ OH	<i>p</i> -Br	0.66 ± 0.02	0.065 ± 0.010		16.72 ± 3.01	1.13 ± 0.09	0.066 ± 0.010		16.05 ± 2.09				
22	-CH ₂ OH	<i>o</i> -Cl	2.75 ± 0.14	0.055 ± 0.012		22.22 ± 6.21	5.07 ± 0.26	0.090 ± 0.015		12.10 ± 2.06				
23	-CH ₂ OH	<i>m</i> -Cl	1.40 ± 0.08	0.051 ± 0.015		24.12 ± 5.29	2.85 ± 0.22	0.060 ± 0.006		17.13 ± 1.54				
44	-CONHEt	<i>m</i> -OMe	1.12 ± 0.09	0.110 ± 0.024		10.59 ± 2.34	1.96 ± 0.13	0.141 ± 0.018		7.41 ± 0.82				
45	-CONHEt	<i>m</i> -Br	0.83 ± 0.06	0.095 ± 0.011		10.78 ± 1.28	2.95 ± 0.41	0.121 ± 0.012		6.38 ± 0.06				
46	-CONHEt	<i>p</i> -Br	1.01 ± 0.06	0.076 ± 0.007		13.55 ± 1.36	2.14 ± 0.14	0.058 ± 0.003		6.56 ± 0.01				
47	-CONHEt	<i>o</i> -Cl	3.64 ± 0.33	0.044 ± 0.009		25.70 ± 4.63	7.31 ± 0.61	0.046 ± 0.002		7.20 ± 0.03				
48	-CONHEt	<i>m</i> -Cl	1.80 ± 0.17	0.040 ± 0.006		27.96 ± 5.57	7.54 ± 0.30	0.073 ± 0.004		7.02 ± 0.03				

^a k_{on} (k_3) for ligands as determined using NanoBRET binding assays using either human or rat Nluuc-A₁R expressing HEK 293 cells and determined through fitting with the "kinetics of competitive binding" model.³⁸ ^b k_{off} (k_4) for ligands determined as in footnote a. ^cKinetic dissociation constant (pK_d) for each ligand as determined from k_{off}/k_{on} . ^dResidence time of each ligand as determined by the reciprocal of the k_{off} . All data are the mean ± SEM of at least three independent repeats conducted in duplicate.

Table 5. Kinetics of Binding for Synthetic Adenosine and NECA Phenoxypropyl Derivatives to the Orthosteric Binding Site at Human and Rat A₁R


24-30, 49-55

compd	R ¹		R ²		hA ₁ R				rA ₁ R			
	-CH ₂ OH	-CH ₂ OH	H		$k_{\text{on}} (k_3) \times 10^5 (M^{-1} \text{min}^{-1})^a$	$k_{\text{off}} (k_4) (\text{min}^{-1})^b$	pK _d ^c	RT (min) ^d	$k_{\text{on}} (k_3) \times 10^5 (M^{-1} \text{min}^{-1})^a$	$k_{\text{off}} (k_4) (\text{min}^{-1})^b$	pK _d ^c	RT (min) ^d
24	-CH ₂ OH	-CH ₂ OH	H		4.78 ± 0.93	0.048 ± 0.004	6.97 ± 0.06	21.56 ± 2.13	2.70 ± 0.34	0.053 ± 0.001	6.70 ± 0.06	18.91 ± 0.30
25	-CH ₂ OH	-CH ₂ OH	<i>p</i> -t-Bu		1.48 ± 0.04	0.054 ± 0.005	6.44 ± 0.03	19.12 ± 2.01	4.84 ± 0.37	0.484 ± 0.173	6.17 ± 0.30	5.53 ± 3.31
26	-CH ₂ OH	-CH ₂ OH	<i>m</i> -OMe		2.97 ± 0.27	0.037 ± 0.003	6.90 ± 0.01	27.61 ± 2.09	3.32 ± 0.52	0.085 ± 0.007	6.58 ± 0.03	12.06 ± 1.03
27	-CH ₂ OH	-CH ₂ OH	<i>m</i> -Br		10.12 ± 1.29	0.038 ± 0.012	7.47 ± 0.09	33.13 ± 10.40	13.30 ± 1.21	0.050 ± 0.005	7.42 ± 0.03	20.40 ± 1.86
28	-CH ₂ OH	-CH ₂ OH	<i>o</i> -Cl		11.61 ± 1.31	0.052 ± 0.004	7.34 ± 0.04	19.55 ± 1.48	17.92 ± 1.30	0.048 ± 0.005	7.58 ± 0.01	21.46 ± 2.08
29	-CH ₂ OH	-CH ₂ OH	<i>m</i> -Cl		25.90 ± 2.14	0.040 ± 0.003	7.81 ± 0.02	25.37 ± 1.70	30.07 ± 4.02	0.071 ± 0.010	7.63 ± 0.12	15.20 ± 2.50
30	-CH ₂ OH	-CH ₂ OH	<i>p</i> -Cl		1.01 ± 0.31	0.056 ± 0.009	6.22 ± 0.13	19.46 ± 3.34	2.51 ± 0.90	0.056 ± 0.001	6.58 ± 0.15	17.90 ± 0.25
49	-CONH ₂	-CONH ₂	H		16.43 ± 2.81	0.028 ± 0.002	7.63 ± 0.01	32.82 ± 1.02	25.12 ± 2.08	0.037 ± 0.002	7.83 ± 0.05	27.61 ± 1.66
50	-CONH ₂	-CONH ₂	<i>p</i> -t-Bu		1.53 ± 0.11	0.091 ± 0.010	6.23 ± 0.06	11.47 ± 1.48	6.29 ± 0.62	0.070 ± 0.007	6.95 ± 0.01	14.76 ± 1.64
51	-CONH ₂	-CONH ₂	<i>m</i> -OMe		4.27 ± 0.03	0.027 ± 0.007	7.23 ± 0.11	42.68 ± 10.88	11.91 ± 1.33	0.030 ± 0.006	7.62 ± 0.11	38.05 ± 8.74
52	-CONH ₂	-CONH ₂	<i>m</i> -Br		5.57 ± 2.56	0.075 ± 0.038	6.91 ± 0.04	27.87 ± 14.23	4.46 ± 1.28	0.056 ± 0.008	6.85 ± 0.13	19.17 ± 2.68
53	-CONH ₂	-CONH ₂	<i>o</i> -Cl		17.27 ± 1.12	0.041 ± 0.010	7.66 ± 0.11	29.44 ± 6.91	37.59 ± 1.91	0.048 ± 0.003	7.90 ± 0.00	21.23 ± 1.22
54	-CONH ₂	-CONH ₂	<i>m</i> -Cl		20.28 ± 1.11	0.043 ± 0.013	7.75 ± 0.16	34.70 ± 13.43	35.85 ± 3.95	0.062 ± 0.007	7.76 ± 0.10	16.78 ± 2.22
55	-CONH ₂	-CONH ₂	<i>p</i> -Cl		3.75 ± 1.04	0.076 ± 0.024	6.71 ± 0.03	17.48 ± 4.79	11.62 ± 0.26	0.064 ± 0.003	7.26 ± 0.01	15.65 ± 0.78

^a $k_{\text{on}} (k_3)$ for ligands as determined using NanoBRET binding assays using either human or rat Nluc-A₁R expressing HEK 293 cells and determined through fitting with the "kinetics of competitive binding" model.³⁵ ^b $k_{\text{off}} (k_4)$ for ligands determined as in footnote a. ^cKinetic dissociation constant (pK_d) for each ligand as determined from $k_{\text{off}}/k_{\text{on}}$. ^dResidence time of each ligand as determined by the reciprocal of the k_{off} . All data are the mean ± SEM of at least three independent repeats conducted in duplicate.

hA_{2A}R or hA_{2B}R since both are G_s-coupled and thus stimulate cAMP production. All the tested compounds displayed only weak efficacy at either the hA_{2A}R or hA_{2B}R, with many failing to generate full dose-dependent response curves at the concentrations tested, resulting in adenosine and NECA remaining as the only potent compounds at these two receptors (Tables 2 and 3). At the hA₃R, the adenosine derivatives showed either a loss of efficacy or partial activity, while all the NECA-based compounds (44–55) behaved as full agonists, although with reduced potency compared to NECA alone. To further assess the compound selectivity, we have calculated the relative activity (RA) for all agonists at the different receptor subtypes (Figure 2).

Overall, all the compounds display at least partial selectivity for hA₁R except adenosine that is close to being an equipotent agonist at all the receptors. From the adenosine-based derivatives, compounds 22, 23, 26, and 27 display the most hA₁R selectivity, while compounds 28–30 also show activity at hA₃R. However, with NECA itself being hA₁R selective by ~10-fold, it is the NECA-based compounds that display the highest hA₁R selectivity, in particular compounds 44, 45, and 51–53. Compounds 45 and 51 are ~1500-fold more hA₁R selective than NECA itself, suggesting >10,000-fold selectivity overall.

Differences between Adenosine and NECA Derivatives. When comparing the adenosine and NECA analogs, the compounds based on NECA seem to be generally more potent at inhibiting cAMP accumulation at the hA₁R receptor. Their potencies are either equivalent to or reduced compared to NECA at the other three AR subtypes. As a result, the NECA-based derivatives are more hA₁R-selective than the adenosine derivatives. When we looked more closely at the adenosine and NECA-derived analog pairs, most of them displayed very similar selectivity across all AR subtypes (Tables 2 and 3). For example, adenosine-derived 29 and its NECA-derived analog 54 are both potent hA₁R full agonists (pEC₅₀ = 9.21 ± 0.19 and 9.28 ± 0.28, respectively), whereas 30 and 55 are relatively less potent dual hA₁R and hA₃R agonists (pEC₅₀ = 8.19 ± 0.18, 7.99 ± 0.15 (hA₁R) and 6.88 ± 0.60, 6.92 ± 0.17 (hA₃R), respectively). Therefore, for these compounds, it seems to be the position of the substituent on the phenoxy group that has the most effect on compound selectivity. For some analog pairs, however, the patterns do not show such a close relationship. 27 and 52 are both potent agonists at hA₁R (pEC₅₀ = 10.0 ± 0.24 and 9.62 ± 0.35, respectively), but 52 also weakly activated hA₃R (pEC₅₀ = 5.52 ± 0.12), while 27 showed no response for this subtype. Consequently, in this case, the ribose C-5' substituent group also affects the selectivity of the compounds, with the adenosine-derived compound being more hA₁R selective.

Kinetics of Binding of Adenosine and NECA Derivatives at Human and Rat A₁R. Since A₁R agonists are promising compounds for the treatment of glaucoma, type 2 diabetes mellitus, pain, epilepsy, and cerebral ischemia, it is important to assess their binding properties at both human and rat A₁R (rA₁R), as the latter is commonly used as a model in preclinical studies.^{2,11,12} We have tested the compounds' ability to displace the specific binding (at equilibrium) of CA200645 in HEK293 cells stably expressing human and rat Nluc-A₁R (Figure 3, Tables 2 and 3).

The NanoBRET binding assay can also enable determination of real-time kinetics and affinities of the compound binding, as was previously described at the ARs.^{25,32–34} Values

were derived using the "kinetics of competitive binding" model³⁵ built into GraphPad Prism v9.1, enabling determinations of the compounds' *k*_{on} and *k*_{off} values (Tables 4 and 5).

The reciprocal of the *k*_{off} enables a determination of the residence time (RT) of a compound.²⁵ RT is a quantification of the time a ligand spends bound to the receptor, and it is increasingly considered in drug design because of its correlation with pharmacodynamics.³⁶ Beyond this, we also determined the p*K*_d of the compounds (*k*_{off}/*k*_{on}) from the kinetics assays and compared these values to those determined from the saturation binding assays. The kinetic parameters for CA200645 binding at the human Nluc-A₁R were determined as *k*_{on} (*k*₁) = 3.67 ± 0.34 × 10⁶ M⁻¹ min⁻¹ and *k*_{off} (*k*₂) = 0.064 ± 0.0023 min⁻¹ with a *K*_d = 18.29 ± 2.4 nM. For the rA₁R, the kinetics of binding for CA200645 were determined as *k*_{on} (*k*₁) = 2.93 ± 0.24 × 10⁶ M⁻¹ min⁻¹ and *k*_{off} (*k*₂) = 0.066 ± 0.0022 min⁻¹ with a *K*_d = 32.96 ± 2.8 nM. With the help of these parameters, we were then able to provide estimates of the kinetics of binding for adenosine and NECA benzyloxycyclopentyl and phenoxy-cyclopentyl derivatives 19–30 and 44–55 at the human and rat A₁R (Tables 4 and 5).

The adenosine and NECA benzyloxycyclopentyl derivatives (Table 4) displayed RT comparable to adenosine and NECA on hA₁R (~21 min), while the phenoxy-cyclopentyl analogs generally had RT > 20 min (Table 5). As a general trend, the compounds are faster binders at rA₁R regardless of linker length. The reason for this could be the divergent amino acid composition of the extracellular loops between hA₁R and rA₁R, which would favor different binding paths to the orthosteric site.²⁴

Overall, the compounds displayed a very similar binding profile across the human and rat A₁R, suggesting that further studies in rats would be highly relevant for the potential use of the compounds in humans. The adenosine and NECA-derived analog pairs also display very similar affinities for both human and rat A₁R, suggesting that it is the R² substituent on the phenoxy or benzyloxy ring that is key in determining the compound affinity for A₁R. At the hA₁R, the compounds with the highest affinity are 27–29, 49, 51, 53, and 54. All of these have higher affinity at hA₁R than adenosine and NECA alone and are all phenoxy-cyclopentyl derivatives. It is interesting to note that except for 49 and 51, all of these compounds have a halogen (chloride or bromide) substituent, mostly in the *meta*-position of the aromatic phenoxy ring. 27, 49, 51, 53, and 54 all also have RT = 29–43 min at the human A₁R, while the RT for the rest of the compounds is lower. By comparison, the benzyloxycyclopentyl derivatives generally display weaker binding and lower RT. At the rA₁R, compounds with the highest affinity are 28, 29, 49, 53, and 54. 27 and 52, which have the bromide substituent on the aromatic ring, display reduced affinity at the rA₁R as well as the hA₁R when compared to 29 and 54, respectively, which bear the chloride substituent at the same position. Considering the substitution position on the phenoxy ring, we observed the highest affinity with the chloride in the *meta*-position (29, 54) followed by *ortho*- (28, 53) and the *para*-position (30, 55). Overall, halogen substituents as the R² group on the aromatic ring seem to confer high affinity for the A₁R, with chloride being preferential over bromide for binding at both the human and rat versions of the receptor.

Finally, we performed a comparison of the affinity data obtained from the NanoBRET binding assay with the potency for inhibition of cAMP accumulation for the hA₁R, which

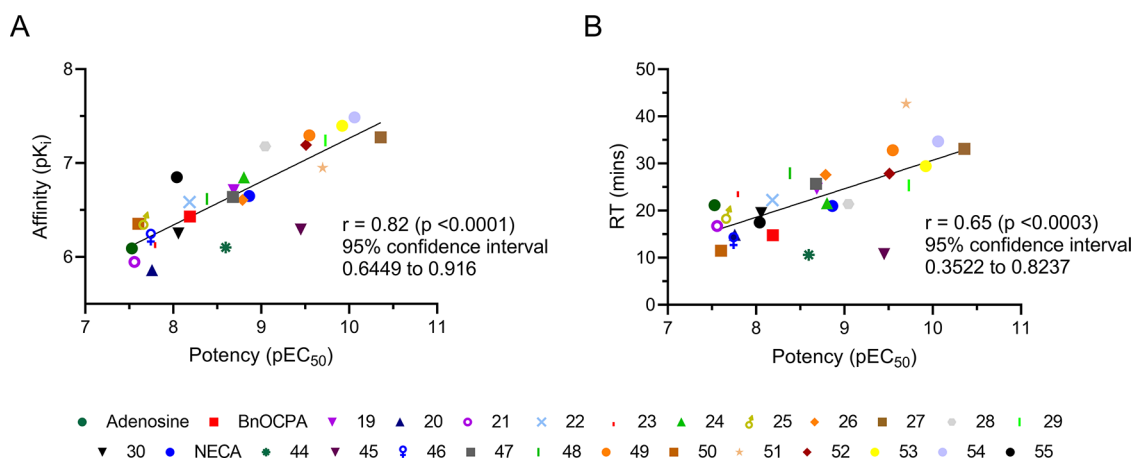


Figure 4. NECA and adenosine derivatives show correlation between potency and affinity or residence time at the hA₁R. (A) Potency pEC₅₀ values of individual compounds from cAMP inhibition experiments plotted against pK_i values from NanoBRET experiments at hA₁R. (B) Potency pEC₅₀ values of individual compounds from cAMP inhibition experiments plotted against RT values from NanoBRET experiments at hA₁R.

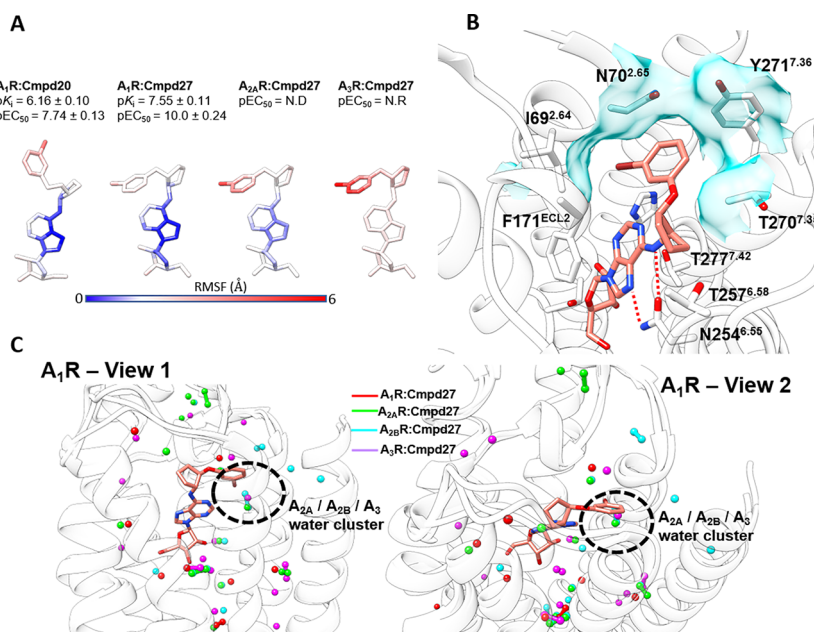


Figure 5. Molecular dynamics docking of **20** and **27**. (A) Atomic root mean square fluctuation (RMSF) of **20** within A₁R and **27** within A₁R, A_{2A}R, and A₃R plotted on the agonists' structure. (B) Compound **27** (salmon stick representation) binding mode within A₁R (white ribbon and sticks); the key hydrogen bonds with N254^{6.55} are shown as red dotted lines, while the hydrophobic subpocket is shown as a cyan transparent surface (coordinates provided in the Supporting Information (A1R_cmpd27_binding_mode.pdb)). (C) Two views (view 1, side; view 2, top) comparing the structural water molecules detected in A₁R (red spheres), A_{2A}R (green), A_{2B}R (cyan), and A₃R (purple). The position of the stable water cluster only present in A_{2A}R, A_{2B}R, and A₃R is highlighted. Binding mode of **27** (salmon sticks) within A₁R is superimposed for reference. Presented data are based on PDB structures 6D9H (A₁R) and 5G53 (A_{2A}R) and AlphaFold2 models of A_{2B}R and A₃R.

showed a clear positive correlation ($r = 0.82$) with compounds **27**, **29**, **49**, and **51–54** identified as both the most potent and strongest binders (Figure 4A). A similar correlation was also observed between potency and compounds' residence time (Figure 4B, $r = 0.65$). Overall, in this work, we have identified high-affinity, very selective potent hA₁R agonists, namely, **27**, **49**, and **51–54**.

Molecular Dynamics Simulations. To retrieve insight into the possible binding mode of the studied agonists and rationalize the selectivity displayed, *in silico* experiments were performed on the phenoxycyclopentyl adenosine derivative **27**, the most A₁R-selective and potent agonist, and its benzyloxycyclopentyl congener **20**. A₁R and A_{2A}R structures solved in complex with adenosine or NECA (or homology models

obtained from them, see the Experimental Section) present a closed conformation of the extracellular vestibule due to the lack of induced fit by N⁶ substituents, not present on adenosine or NECA. This structural feature does not allow molecular docking of compounds bearing bulky N⁶ groups to reproduce the binding mode of AR full agonists (Figure S2), which is characterized by the fundamental hydrogen bonds between the purine scaffold and the conserved Asn residue in position 6.55 and between the ribose ring and the Ser/Thr^{7.42} or His^{7.43}. Therefore, molecular dynamics (MD) simulations of the four ARs subtypes were performed in the absence of any orthosteric agonists to sample receptors' conformations more open at the extracellular loop 2 (ECL2) and ECL3 levels. Molecular docking results for **20** and **27** on the MD-derived AR

Table 6. NanoBRET Competition-Binding Assay at Human Wild-Type and Mutant Nluc-A₁R^a

A ₁ R	pK _i ^a (cmpd)					
	BnOCPA	<i>n</i>	20	<i>n</i>	27	<i>n</i>
WT	6.24 ± 0.04	3	6.38 ± 0.17	3	7.20 ± 0.16	3
I69 ^{2.64} A	5.03 ± 0.02*	3	5.06 ± 0.04*	3	6.37 ± 0.10*	3
N70 ^{2.65} A	6.01 ± 0.05	3	5.48 ± 0.15*	3	7.00 ± 0.24	3
T257 ^{6.58} A	6.93 ± 0.10*	3	6.23 ± 0.02	3	8.09 ± 0.18*	3
Y271 ^{7.36} A	5.40 ± 0.23*	3	5.19 ± 0.13*	3	6.33 ± 0.10*	3

^aCompound affinity (pK_i) determined through NanoBRET competition-binding assays with CA200645 in wild-type (WT) or mutant Nluc-A₁R stably expressing HEK293 cells. The resulting concentration-dependent decrease in BRET ratio at 10 min was used to calculate pK_i. Data are expressed as mean ± SEM obtained in *n* separate experiments. All individual experiments were conducted in duplicate. Statistical significance (**p* < 0.05) compared to WT was determined by one-way ANOVA with Dunnett's post-test and presented according to ref 31.

structures were remarkably enhanced in the case of experimental structures A₁R and A_{2A}R, were slightly improved for the structural A₃R model, and produced very little improvement for the A_{2B}R model (Figure S3).

The best pose (in terms of similarity to adenosine) of **20** within A₁R and the best pose of **27** within A₁R or A_{2A}R were further evaluated during 6 μs of MD simulations. For a complete comparison (Movie S1) of all four ARs subtypes, the best docking pose of **27** obtained on A_{2A}R was superimposed on both A_{2B}R and A₃R and subjected to MD simulations. During the MD trajectories, **27** remained stably bound to A₁R and A_{2A}R but displayed less stable binding modes within A₃R and, in particular, the A_{2B}R orthosteric site (Movie S1, Figure S4A). Compound **20** within A₁R (Movie S2) was steady throughout the simulations (Movie S2), as indicated by RMSD values in line with **27** (Figure S4A). In terms of flexibility, N⁶ substituents explored divergent conformations in the different systems (Figure 5A, Movies S1 and S2): the 3-bromophenyl group of **27** was highly flexible in A₃R or A_{2A}R and more stable in A₁R, while the 3-bromobenzyl group of **20** displayed intermediate flexibility.

Compound **27** bound to A₁R formed key hydrogen bonds with N254^{6.55} and hydrophobic contacts with F171^{ELC2} and oriented the 3-bromophenyl moiety in a hydrophobic subpocket formed by I69^{2.64}, N70^{2.65}, Y271^{7.36}, and T270^{7.35} (Figure 5B, Movies S1 and S2). The bulkier analog **20** was not able to completely accommodate the 3-bromobenzyl group within this pocket and therefore displayed higher flexibility at the N⁶ level (Figure 5A, Movie S2). It is plausible that this contributes to the reduced A₁R affinity and potency of **20** (pK_i = 6.16 ± 0.10, pEC₅₀ = 7.74 ± 0.13) compared to **27** (pK_i = 7.55 ± 0.11, pEC₅₀ = 10.0 ± 0.24). On the other hand, the interaction fingerprints of **20** (bound to A₁R) and **27** are unique for each simulated complex (Figure S4B) and do not allow a straightforward rationalization of the selectivity displayed by the agonists. We therefore focused on the water molecule network present in the apo forms of the four AR subtypes (Figure 5C, Figure S4C–F). Our data suggest the presence of structural water molecules (A_{2A}/A_{2B}/A₃ water cluster in Figure 5C) in the proximity of positions 2.64 and 2.65 of A_{2A}R, A_{2B}R, and A₃R but not A₁R stabilized by the short polar side chain of Ser^{2.65} (Asn^{2.65} in A₁R, Figure S4B). It follows that the hydrophobic subpocket is putatively present only in A₁R; hence, **27** cannot be completely stabilized by the other AR subtypes.

Taken together, computational results suggest that a one-atom linker between the N⁶-cyclopentane and the phenyl rings is optimal for stable binding to the hydrophobic pocket in A₁R. The absence of this pocket and the presence of stable water

molecules competing with the ligands in A_{2A}R, A_{2B}R, and A₃R are probably responsible for the loss in affinity and potency of the tested agonists. The better complementarity with hA₁R could explain why adenosine and NECA benzyloxycyclopentyl derivatives (Table 4) displayed RT comparable to adenosine and NECA at hA₁R (~21 min), while the phenoxycyclopentyl analogs generally had RT > 20 min (Table 5). Indeed, the shorter linker, as present in **27**, would stabilize the compounds and increase the energy required to produce dissociation.

Validating the Predictions from the *In Silico* Experiments for A₁R Bound to **20 and **27**.** As described in Figure 5B, MD simulations suggested that the 3-bromophenyl moiety binds in a hydrophobic subpocket formed by I69^{2.64}, N70^{2.65}, Y271^{7.36}, and T270^{7.35}, while **20** was not able to completely accommodate the 3-bromobenzyl group within this pocket (Movie S2). To test these observations, we made use of previously described mutants (I69^{2.64}A, N70^{2.65}A, Y271^{7.36}A) of the Nluc-A₁R²⁴ that enable comparison of ligand affinities with the wild-type receptor. We also included the mutant T257^{6.58}A since we have previously shown that this residue is a good discriminator between different A₁R agonists.²⁴ We did not consider mutations of N254^{6.55} or F171^{ELC2} since these are known to prevent ligand binding to the A₁R (including CA200645) and therefore cannot be studied.^{24,37} Furthermore, we did not consider mutating T270^{7.35} since, when we compared the sequences of the hA₁R and the rA₁R, we observed that, in the rA₁R, the equivalent residue at position T270^{7.35} is an Ile. Comparison of the binding affinities (pK_i) for **20** and **27** between the hA₁R and the rA₁R shows that **20** is equipotent between the two species while **27** has reduced affinity at the rA₁R (pK_i (hA₁R) = 7.55 ± 0.11; pK_i (rA₁R) = 6.94 ± 0.08). Initially, we determined the K_d for CA200645 at each of the four A₁R mutants (I69^{2.64}A, N70^{2.65}A, T257^{6.58}A, and Y271^{7.36}A) and found the values to show close agreement with those previously reported.²⁴ We next performed a NanoBRET competition binding assay for the four mutants with BnOCPA (as a reference agonist), **20**, and **27** (Table 6, Figure S5).

Consistent with MD simulation predictions, mutation of I69^{2.64} and Y271^{7.36} reduced the affinity of BnOCPA, **20**, and **27**. Interestingly, while the affinity at the A₁R of BnOCPA and **27** was not affected by the mutation of N70^{2.65}, **20** was significantly reduced. A closer analysis of the MD simulations suggested that the side chain of N70^{2.65} orients differently between **20** and **27**. For **20**, simulations predicted N70^{2.65} amidic side chain group interactions with the purine ring (Figure S6, Movie S2), which are lost in N70^{2.65}A. These interactions can comprise water bridges involving the first solvation shell around the purine scaffold of the ligand.³⁸

Conversely, for **27**, the N70^{2.65} amidic side chain group does not interact with the purine ring, but instead, it forms hydrophobic interactions through its methylene group with the bromobenzene ring (Figure S5B, Movie S2), implying that the mutation to Ala does not play a significant role in binding. Finally, as we have previously reported,²⁴ the mutation of T257^{6.58}A did provide a clear discriminator between the three different agonists. **27** together with BnOCPA both showed increases in binding affinity, while **20** displayed no significant change. In our previous studies, we observed that both CPA and BnOCPA displayed increased affinities at the T257^{6.58}A mutant, while NECA showed reduced affinity and there was no change for adenosine. We attributed these changes to an increase in the lipophilicity of the protein environment underneath extracellular loop 3 (ECL3), which surrounds the cyclopentyl groups of the molecules. It is therefore apparent that the small molecule **27** favors a more hydrophobic environment within the binding pocket that is already suitable for **20**.

CONCLUSIONS

Herein, we report the synthesis of novel N⁶-benzyloxycyclopentyl and N⁶-phenoxy-cyclopentyl derivatives of adenosine and NECA. These compounds were evaluated using the cAMP accumulation assay in CHO-K1 cells and the NanoBRET binding assay in HEK293 cells for potency, selectivity, and binding at ARs. Our pharmacology data show that compounds including halogen substituents, chloride in particular, on the aromatic phenoxy and benzyloxy rings confer high affinity for the human and rat A₁R. These compounds also have high potency at the A₁R, particularly ones with a *meta* substituent on the aromatic rings. Furthermore, we also show that NECA-based derivatives have generally higher A₁R selectivity over the other AR subtypes. Molecular modeling studies suggest that the selectivity is driven by a short linker and the absence of stable water molecules within a subpocket of the hA₁R orthosteric site. It is worth noting that compounds **45** and **51** show approximately 1500 times improved A₁R selectivity over NECA itself. Overall, we have identified very selective and very potent A₁R agonists with high affinity for the receptor, namely, phenoxy-cyclopentyl compounds **27**, **49**, and **51–54**, which have great therapeutic promise for overcoming insufficient receptor selectivity and potency that many current compounds face.

EXPERIMENTAL SECTION

General Chemistry. All reactions were performed in dry glassware under an inert argon atmosphere. Anhydrous solvents were purchased as dry over molecular sieves from Sigma-Aldrich (Merck). Solvents were evaporated under reduced pressure at approximately 45 °C using a Büchi Rotavapor or under high vacuum on a Schlenk line. Reagents were purchased from Sigma-Aldrich (Merck), Fluorochem, or Brunschwig and used without further purification. Reactions were monitored by thin layer chromatography (TLC) using aluminum sheets precoated with 0.2 mm silica (Macherey-Nagel ALUGRAM Xtra SII, G/UV₂₅₄) or aluminum oxide (Macherey-Nagel POLYGRAM Alox N/UV₂₅₄). Detection was under a UV light source (λ_{\max} 254 nm or 366 nm) or through staining with a vanillin solution, with subsequent heating. Flash column chromatography was carried out on a Teledyne ISCO CombiFlash using prepacked RediSep Normal-phase Silica Flash Columns.

Proton nuclear magnetic resonance (¹H NMR) and carbon nuclear magnetic resonance (¹³C NMR) spectra were recorded at room temperature using a Bruker Avance IIIHD-400, II-400, or IIIHD-300

spectrometer operating at 400 or 300 MHz, respectively, for ¹H and at 101 and 75 MHz, respectively, for ¹³C. Chemical shifts (δ) are reported in parts per million (ppm) and are referenced to the residual solvent peak (DMSO-*d*₆: $\delta_{\text{H}} = 2.50$ ppm, $\delta_{\text{C}} = 39.52$ ppm; CDCl₃: $\delta_{\text{H}} = 7.26$ ppm, $\delta_{\text{C}} = 77.16$ ppm; methanol-*d*₄: $\delta_{\text{H}} = 3.31$ ppm, $\delta_{\text{C}} = 49.00$ ppm) or Me₄Si ($\delta_{\text{H}} = 0.00$ ppm). The order of citation in parentheses is (1) multiplicity: s (singlet), d (doublet), t (triplet), q (quartet), quint (quintet), m (multiplet), etc., and br (broad); (2) coupling constants (*J*) in hertz (Hz); and (3) number of equivalent nuclei (by integration). COSY, HSQC, and DEPT were routinely used to assign peaks in ¹H and ¹³C NMR spectra. Addition of D₂O was used to confirm the assignment of OH and NH peaks. High-resolution mass spectra (HRMS) were recorded on a Thermo-Scientific LTQ Orbitrap XL spectrometer consisting of a linear ion trap (LTQ) featuring an HCD collision cell, coupled to the Orbitrap mass analyzer, equipped with a nano-electrospray ion source (NSI). HRMS spectra were determined by the Mass Spectrometry Group at the Department of Chemistry, Biochemistry, and Pharmaceutical Sciences, University of Bern, Switzerland (Prof. Dr. S. Schürch).

The purity of the compounds was determined with UPLC-MS on a Dionex UltiMate 3000 Rapid Separation LC system using a reversed-phase column (Acclaim RSLC, 120 C18, 3 × 50 mm, 2.2 μ m, pore size 120 Å, flow rate 1.2 mL/min), which was coupled to a ESI-MS Micromass Platform (quadrupole mass spectrometer). The gradient used was 100% A to 100% D over 7 min, with A = MilliQ H₂O + 0.1% TFA and D = 10% MilliQ H₂O/90% HPLC-grade MeCN + 0.1% TFA. Compounds **24** and **29** were measured on a Thermo-Scientific UltiMate 3000 HPLC equipped with a reverse-phase column (Acclaim 120 C18, 4.6 × 150 mm, 5 μ m, pore size 120 Å) and eluted with a gradient of MilliQ H₂O/HPLC-grade MeCN + 0.1% TFA. Purity was determined by total absorbance at 254 nm. All tested compounds were >95% pure, except for **24** and **29** that were 95 and 94% pure, respectively (Tables S1 and S2).

Established Adenosine Receptor Agonists. Adenosine and 5'-N-ethylcarboxamido-adenosine (NECA) were purchased from R & D Systems (Bristol, UK). Where possible, compounds were prepared as 10 mM stocks in DMSO.

Chemical Synthesis. Intermediates **1**, **7**, and **31** and BnOCPA were synthesized as described previously.^{13,39}

General Procedure A (O-Alkylation) for the Synthesis of Intermediates 2a–i. Boc-protected (1R,2R)-2-aminocyclopentanol **1** and the appropriate benzyl bromide were dissolved in dry THF (50–100 mM). The reaction mixture was cooled to 0 °C, and NaH (60% dispersion in mineral oil) was added. After stirring at 0 °C, the reaction was quenched with MeOH (0.1 mL) and sat. aq. NH₄Cl. The reaction mixture was extracted with EtOAc, and the organic phase was dried over Na₂SO₄ and concentrated under reduced pressure. The crude material was purified by flash column chromatography.

General Procedure B (Mitsunobu) for the Synthesis of Intermediates 5a,c,e,f,h–j. Boc-protected (1S,2R)-2-aminocyclopentanol **4**, the appropriate phenol, and PPh₃ were dissolved in dry THF (50–100 mM) and cooled to 0 °C. DIAD was added dropwise. Cooling was removed, and the reaction mixture was left to warm to room temperature and stirred overnight. Water was added, and the aqueous phase was extracted with EtOAc. The organic phase was dried over Na₂SO₄ and concentrated under reduced pressure. The crude material was purified by flash column chromatography.

General Procedure C (Boc Deprotection) for the Synthesis of Intermediates 3b–i and 6a,c,e,f,h–j. Boc-protected precursors **2b–i** and **5a,c,e,f,h–j** were dissolved in dioxane (85–830 mM), and HCl (4 M in dioxane) was added. After stirring the reaction mixture at room temperature, the solvent was removed under reduced pressure. The residual ammonium chloride salt was co-evaporated with CH₂Cl₂ and dried.

General Procedure D (S_NAr Reaction) for the Synthesis of Intermediates 8–14 and 32–43. The appropriate 6-chloropurine (**7** or **31**) and the appropriate benzyloxy- or phenoxy-cyclopentyl amine intermediate (**3b–i** or **6a,c,e,f,h–j**) were dissolved in *i*-PrOH (11–36 mM). NaHCO₃ was added, and the reaction mixture was heated at

reflux (ca. 105 °C) overnight. After cooling, the solid was filtered off and washed with EtOH, and the solvents were removed under reduced pressure. The crude material was purified by flash column chromatography. In some examples, loss of acetate groups on the secondary alcohols was observed during the S_NAr reaction with 7. In these cases, the crude material was subjected directly to the deprotection protocol (see general procedure G).

General Procedure E (Acetate Deprotection) for the Synthesis of Compounds 15–17, 19, 24, 26, and 30. Acetate-protected intermediates 8–14 were dissolved in MeOH (9–22 mM), and K_2CO_3 was added. The reaction mixture was stirred at room temperature, filtered, and concentrated under reduced pressure. The crude material was purified by flash column chromatography.

General Procedure F (Acetonide Deprotection) for the Synthesis of Compounds 44–55. Acetonide-protected intermediates 32–43 were dissolved in water (38–75 mM) and acetic acid and stirred at 80 °C overnight. The water and acetic acid were removed in vacuo, and the crude material was purified by flash column chromatography.

General Procedure G (S_NAr Reaction and Subsequent Acetate Deprotection) for the Synthesis of Compounds 20–23, 25, and 27–29. 6-Chloropurine 7 and the appropriate benzyloxy- or phenoxy-cyclopentyl amine intermediate (3f–i or 6c,f,h,i) were dissolved in *i*-PrOH (23–46 mM). $NaHCO_3$ was added, and the reaction mixture was heated at reflux (ca. 105 °C) overnight. After cooling, the solid was filtered off and washed with EtOH, and the solvents were removed under reduced pressure. The crude material was dissolved in MeOH (11–17 mM), and K_2CO_3 was added. The reaction mixture was stirred at room temperature, filtered, and concentrated under reduced pressure. The crude material was purified by flash column chromatography.

***tert*-Butyl ((1*R*,2*R*)-2-(*Benzyl*oxy)cyclopentyl)carbamate (2a).** 2a was synthesized according to general procedure A using 1 (0.497 mmol), benzyl bromide (0.497 mmol), and NaH (0.994 mmol). The reaction was run for 2 h. After purification with flash column chromatography (EtOAc/cHex, 15%), 2a was obtained (83 mg, 0.285 mmol, 58%). 1H NMR: (300 MHz, DMSO- d_6) δ 7.30 (m, 5H), 6.90 (d, J = 7.7, 1H), 4.53 (d, J = 12.2, 1H), 4.58–4.41 (m, 1H), 3.82–3.74 (m, 1H), 3.73–3.66 (m, 1H), 1.95–1.73 (m, 2H), 1.60 (m, 3H), 1.43–1.36 (m, 1H) 1.40 (s, 9H). ^{13}C NMR: (75 MHz, DMSO- d_6) δ 155.5, 139.4, 128.6, 127.8, 127.7, 85.0, 78.0, 70.3, 56.9, 30.6, 30.5, 28.8, 21.8. HRMS: (NSI+) m/z calcd for $C_{17}H_{26}NO_3$ [$M + H$] $^+$ 292.1902, found 292.1907.

***tert*-Butyl ((1*R*,2*R*)-2-(*Isopropylbenzyl*oxy)cyclopentyl)carbamate (2b).** 2b was synthesized according to general procedure A using 1 (1.242 mmol), 4-isopropylbenzyl bromide (1.242 mmol), and NaH (2.484 mmol). The reaction was run for 1 h 20 min. After purification with flash column chromatography (EtOAc/cHex, 15%), 2b was obtained (135 mg, 0.406 mmol, 33%). 1H NMR: (300 MHz, DMSO- d_6) δ 7.24–7.18 (m, 4H), 6.89 (d, J = 7.8, 1H), 4.5–4.38 (m, 2H), 3.80–3.72 (m, 1H), 3.72–3.65 (m, 1H), 2.87 (sept, J = 6.9, 1H), 1.93–1.73 (m, 2H), 1.67–1.49 (m, 3H), 1.42–1.32 (m, 1H) 1.40 (s, 9H), 1.19 (d, J = 6.9, 6H). HRMS: (NSI+) m/z calcd for $C_{20}H_{32}NO_3$ [$M + H$] $^+$ 334.2369, found 334.2377.

***tert*-Butyl ((1*R*,2*R*)-2-(*tert*-Butylbenzyl)oxy)cyclopentyl)carbamate (2c).** 2c was synthesized according to general procedure A using 1 (1.242 mmol), 4-*tert*-butylbenzyl bromide (1.242 mmol), and NaH (2.484 mmol). The reaction was run for 1 h 30 min. After purification with flash column chromatography (EtOAc/cHex, 20%), 2c was obtained as an oil (126 mg, 0.363 mmol, 30%). 1H NMR: (300 MHz, DMSO- d_6) δ 7.35 (d, J = 8.2, 2H), 7.22 (d, J = 8.2, 2H), 6.89 (d, J = 7.8, 1H), 4.51–4.40 (m, 2H), 3.82–3.72 (m, 1H), 3.71–3.64 (m, 1H), 1.94–1.72 (m, 2H), 1.65–1.51 (m, 3H), 1.45–1.33 (m, 1H), 1.40 (s, 9H), 1.27 (s, 9H). ^{13}C NMR: (101 MHz, DMSO- d_6) δ 155.4, 150.1, 136.3, 127.8, 125.3, 84.8, 78.0, 70.1, 56.9, 34.7, 31.6, 30.7, 30.6, 28.8, 21.9. HRMS: (NSI+) m/z calcd for $C_{21}H_{34}NO_3$ [$M + H$] $^+$ 348.2533, found 348.2533.

***tert*-Butyl ((1*R*,2*R*)-2-(*4*-Cyanobenzyl)oxy)cyclopentyl)carbamate (2d).** 2d was synthesized according to general procedure A using 1 (1 mmol), 4-(bromomethyl)benzotrile (1 mmol), and NaH (2 mmol). The reaction was run for 6 h 30 min. After

purification with flash column chromatography (EtOAc/cHex, 20%), 2d was obtained as an oil (287 mg, 0.91 mmol, 91%). 1H NMR: (300 MHz, methanol- d_4) δ 7.69 (d, J = 8.3, 2H), 7.58–7.47 (m, 2H), 4.71–4.56 (m, 2H), 3.96–3.83 (m, 1H), 3.83–3.71 (m, 1H), 2.14–1.61 (m, 5H), 1.44 (s, 10H). ^{13}C NMR: (101 MHz, methanol- d_4) δ 151.2, 146.3, 133.2, 129.0, 118.9, 87.0, 71.0, 58.2, 31.3, 31.3, 28.8, 22.5. HRMS: (NSI+) m/z calcd for $C_{18}H_{25}N_2O_3$ [$M + H$] $^+$ 317.1860, found 317.1858.

***tert*-Butyl ((1*R*,2*R*)-2-(*3*-Methoxybenzyl)oxy)cyclopentyl)carbamate (2e).** 2e was synthesized according to general procedure A using 1 (0.497 mmol), 3-methoxybenzyl bromide (0.497 mmol), and NaH (0.994 mmol). The reaction was run for 3 h. After purification with flash column chromatography (EtOAc/cHex, 20%), 2e was obtained (76 mg, 0.235 mmol, 47%). 1H NMR: (300 MHz, DMSO- d_6) δ 7.24 (t, J = 8.0, 1H), 6.93–6.80 (m, 3H), 4.53–4.42 (m, 2H), 3.82–3.72 (m, 1H), 3.75 (s, 3H), 3.72–3.65 (m, 1H), 1.95–1.73 (m, 2H), 1.69–1.49 (m, 3H), 1.44–1.32 (m, 1H), 1.39 (s, 9H). ^{13}C NMR: (75 MHz, DMSO- d_6) δ 159.7, 155.5, 141.0, 129.7, 119.9, 113.2, 84.8, 78.0, 70.1, 56.9, 55.4, 30.6, 30.5, 28.7, 21.8. HRMS: (NSI+) m/z calcd for $C_{18}H_{28}NO_4$ [$M + H$] $^+$ 322.2021, found 322.2013.

***tert*-Butyl ((1*R*,2*R*)-2-(*3*-Bromobenzyl)oxy)cyclopentyl)carbamate (2f).** 2f was synthesized according to general procedure A using 1 (1.242 mmol), 3-bromobenzyl bromide (1.242 mmol), and NaH (2.484 mmol). The reaction was run for 3 h. After purification with flash column chromatography (EtOAc/cHex, 15–20%), 2f was obtained (268 mg, 0.725 mmol, 58%). 1H NMR: (300 MHz, DMSO- d_6) δ 7.51–7.46 (m, 1H), 7.38–7.31 (m, 1H), 7.27–7.13 (m, 2H), 6.91 (d, J = 7.7, 1H), 4.57–4.45 (m, 2H), 3.81–3.72 (m, 1H), 3.72–3.64 (m, 1H), 1.95–1.75 (m, 2H), 1.68–1.49 (m, 3H), 1.46–1.33 (m, 1H), 1.40 (s, 9H). ^{13}C NMR: (75 MHz, methanol- d_4) δ 156.5, 141.5, 130.1, 130.1, 129.7, 125.9, 121.9, 85.2, 78.6, 69.7, 56.7, 30.0, 27.5, 26.6, 21.1. HRMS: (NSI+) m/z calcd for $C_{17}H_{24}BrNNO_3$ [$M + Na$] $^+$ 392.0830, found 392.0832.

***tert*-Butyl ((1*R*,2*R*)-2-(*4*-Bromobenzyl)oxy)cyclopentyl)carbamate (2g).** 2g was synthesized according to general procedure A using 1 (0.8 mmol), 4-bromobenzyl bromide (0.8 mmol), and NaH (1.6 mmol). The reaction was run for 3 h. After purification with flash column chromatography (EtOAc/cHex, 20%), 2g was obtained (198 mg, 0.535 mmol, 67%). 1H NMR: (300 MHz, DMSO- d_6) δ 7.52 (d, J = 8.4, 2H), 7.27 (d, J = 8.4, 2H), 4.48 (m, 2H), 3.82–3.78 (m, 1H), 3.70–3.59 (m, 1H), 1.94–1.74 (m, 2H), 1.59 (m, 3H), 1.44–1.34 (m, 1H), 1.39 (s, 9H). ^{13}C NMR: (101 MHz, methanol- d_4) δ 156.5, 144.9, 131.8, 127.6, 118.4, 110.6, 85.6, 78.6, 69.6, 56.8, 29.9, 27.4, 21.1.

***tert*-Butyl ((1*R*,2*R*)-2-(*2*-Chlorobenzyl)oxy)cyclopentyl)carbamate (2h).** 2h was synthesized according to general procedure A using 1 (0.994 mmol), 2-chlorobenzyl bromide (0.994 mmol), and NaH (1.987 mmol). The reaction was run for 1.5 h at 0 °C and then for another 1.5 h at room temperature. After purification with flash column chromatography (EtOAc/cHex, 20%), 2h was obtained (178 mg, 0.504 mmol, 51%). 1H NMR: (300 MHz, DMSO- d_6) δ 7.53–7.40 (m, 2H), 7.37–7.29 (m, 2H), 6.94 (d, J = 7.7, 1H), 4.65–4.50 (m, 2H), 3.85–3.70 (m, 2H), 1.99–1.78 (m, 2H), 1.68–1.53 (m, J = 9.3, 3H), 1.46–1.35 (m, 1H), 1.40 (s, 9H). ^{13}C NMR: (75 MHz, methanol- d_4) δ 156.5, 136.3, 132.6, 129.05, 128.8, 128.5, 126.5, 85.6, 78.6, 67.9, 56.8, 30.0, 29.8, 27.4, 21.0. HRMS: (NSI+) m/z calcd for $C_{17}H_{24}ClNNO_3$ [$M + Na$] $^+$ 348.1336, found 348.1337.

***tert*-Butyl ((1*R*,2*R*)-2-(*3*-Chlorobenzyl)oxy)cyclopentyl)carbamate (2i).** 2i was synthesized according to general procedure A using 1 (0.994 mmol), 3-chlorobenzyl bromide (0.994 mmol), and NaH (1.987 mmol). The reaction was run for 3 h. After purification with flash column chromatography (EtOAc/cHex, 20%), 2i was obtained (224 mg, 0.688 mmol, 70%). 1H NMR: (300 MHz, DMSO- d_6) δ 7.42–7.23 (m, 4H), 6.91 (d, J = 7.7, 1H), 4.58–4.45 (m, 2H), 3.81–3.73 (m, 1H), 3.73–3.65 (m, 1H), 1.96–1.71 (m, 2H), 1.68–1.47 (m, 3H), 1.46–1.33 (m, 1H), 1.40 (s, 9H). ^{13}C NMR: (75 MHz, methanol- d_4) δ 156.5, 141.3, 133.8, 129.4, 127.2, 127.1, 125.5, 85.2, 78.6, 69.7, 56.7, 30.0, 29.9, 27.4, 21.1. HRMS: (NSI+) m/z calcd for $C_{17}H_{24}ClNNO_3$ [$M + Na$] $^+$ 348.1338, found 348.1337.

(1*R*,2*R*)-2-((4-Isopropylbenzyl)oxy)cyclopentan-1-aminium Chloride (**3b**). **3b** was synthesized according to general procedure C using **2b** (0.405 mmol) and HCl (2.03 mmol). The reaction was run for 3 h. **3b** was obtained as a solid (100 mg, 0.43 mmol, quant.). ¹H NMR: (300 MHz, DMSO-*d*₆) δ 8.05 (br s, 3H), 7.32–7.19 (m, 4H), 4.54–4.40 (m, 2H), 3.95–3.87 (m, 1H), 3.42 (br s, 1H), 2.88 (sept, *J* = 6.9, 1H), 2.09–1.90 (m, 2H), 1.76–1.45 (m, 4H), 1.20 (d, *J* = 6.9, 6H). HRMS: (NSI+) *m/z* calcd for C₁₅H₂₄NO [M]⁺ 234.1849, found 234.1852.

(1*R*,2*R*)-2-((4-*tert*-Butylbenzyl)oxy)cyclopentan-1-aminium Chloride (**3c**). **3c** was synthesized according to general procedure C using **2c** (0.329 mmol) and HCl (1.649 mmol). The reaction was run for 5 h. **3c** was obtained as a colorless solid (93 mg, 0.328 mmol, 99%). ¹H NMR: (300 MHz, DMSO-*d*₆) δ 8.02 (br s, 3H), 7.38 (d, *J* = 8.4, 2H), 7.28 (d, *J* = 8.4, 2H), 4.54–4.39 (m, 2H), 3.93–3.86 (m, 1H), 3.47–3.36 (m, 1H), 2.11–1.92 (m, 2H), 1.75–1.48 (m, 4H), 1.28 (s, 9H). ¹³C NMR: (75 MHz, DMSO-*d*₆) δ 150.4, 135.7, 128.0, 125.4, 82.8, 70.7, 56.3, 34.7, 31.6, 30.3, 28.9, 21.6. HRMS: (NSI+) *m/z* calcd for C₁₆H₂₆NO [M]⁺ 248.2005, found 248.2009.

(1*R*,2*R*)-2-((4-Cyanobenzyl)oxy)cyclopentan-1-aminium Chloride (**3d**). **3d** was synthesized according to general procedure C using **2d** (0.825 mmol) and HCl (8 mmol). After stirring for 1 h, a colorless precipitate formed. Drops of water were added until all the solid dissolved. The reaction mixture was then stirred for an additional 3 h. **3d** was obtained as a colorless solid (209 mg, 0.825 mmol, quant.). ¹H NMR: (300 MHz, DMSO-*d*₆) δ 8.02 (s, 3H), 7.84 (d, *J* = 8.2, 2H), 7.58 (d, *J* = 8.3, 2H), 4.68–4.57 (m, 2H), 3.99–3.93 (m, 1H), 3.44 (s, 1H), 2.11–1.92 (m, 2H), 1.76–1.49 (m, 4H). HRMS: (NSI+) *m/z* calcd for C₁₃H₁₇N₂O [M]⁺ 217.1335, found 217.1333.

(1*R*,2*R*)-2-((3-Methoxybenzyl)oxy)cyclopentan-1-aminium Chloride (**3e**). **3e** was synthesized according to general procedure C using **2e** (0.69 mmol) and HCl (3.49 mmol). The reaction was run for 4 h. **3e** was obtained as a colorless solid (88 mg, 0.341 mmol, 50%). ¹H NMR: (300 MHz, DMSO-*d*₆) δ 8.20 (br s, 3H), 7.27 (t, *J* = 8.1, 1H), 6.98–6.82 (m, 3H), 4.57–4.42 (m, 2H), 3.98–3.88 (m, 1H), 3.76 (s, 3H), 3.47–3.37 (m, 1H), 1.76–1.49 (m, 2H), 1.76–1.49 (m, 4H). ¹³C NMR: (75 MHz, DMSO-*d*₆) δ 159.7, 140.4, 129.7, 117.5, 113.5, 113.4, 82.9, 70.8, 56.3, 55.5, 30.2, 28.9, 21.6. HRMS: (NSI+) *m/z* calcd for C₁₃H₂₀NO₂ [M]⁺ 222.1491, found 222.1489.

(1*R*,2*R*)-2-((3-Bromobenzyl)oxy)cyclopentan-1-aminium Chloride (**3f**). **3f** was synthesized according to general procedure C using **2f** (0.716 mmol) and HCl (14.3 mmol). The reaction was run for 1 h, after which a few drops of MeOH were added to dissolve precipitate. The reaction mixture was then stirred for another 1.5 h. **3f** was obtained as a solid (224 mg, 0.732 mmol, quant.). ¹H NMR: (300 MHz, methanol-*d*₄) δ 7.48 (t, *J* = 1.9, 1H), 7.37–7.32 (m, 1H), 7.27–7.13 (m, 2H), 4.50 (d, *J* = 12.0, 1H), 4.42 (d, *J* = 12.0, 1H), 3.92–3.80 (m, 1H), 3.45–3.34 (m, 1H), 2.16–1.91 (m, 2H), 1.82–1.44 (m, 4H). ¹³C NMR: (75 MHz, methanol-*d*₄) δ 140.7, 130.4, 130.3, 129.9, 126.1, 122.0, 82.8, 70.3, 56.6, 29.1, 27.6, 20.3. HRMS: (NSI+) *m/z* calcd for C₁₂H₁₇BrNO [M]⁺ 270.0489, found 270.0488.

(1*R*,2*R*)-2-((4-Bromobenzyl)oxy)cyclopentan-1-aminium Chloride (**3g**). **3g** was synthesized according to general procedure C using **2g** (0.481 mmol) and HCl (9.61 mmol). The reaction was run for 30 min, after which a few drops of MeOH were added to dissolve precipitate. The reaction mixture was then stirred for another 30 min. **3g** was obtained as a solid (114 mg, 0.373 mmol, 77%). ¹H NMR (300 MHz, methanol-*d*₄) δ 7.40 (d, *J* = 8.4, 2H), 7.21 (d, *J* = 8.1, 2H), 4.51–4.37 (m, 2H), 3.89–3.80 (m, 1H), 3.44–3.34 (m, 1H), 2.17–1.90 (m, 2H), 1.79–1.41 (m, 4H). ¹³C NMR: (75 MHz, methanol-*d*₄) δ 137.3, 131.1, 129.4, 121.1, 82.7, 70.4, 56.6, 29.1, 27.6, 20.3. HRMS: (NSI+) *m/z* calcd for C₁₂H₁₇BrNO [M]⁺ 270.0493, found 270.0488.

(1*R*,2*R*)-2-((2-Chlorobenzyl)oxy)cyclopentan-1-aminium Chloride (**3h**). **3h** was synthesized according to general procedure C using **2h** (0.467 mmol) and HCl (9.33 mmol). The reaction was run for 45 min, after which a few drops of MeOH were added to dissolve precipitate. The reaction mixture was then stirred for another 1.5 h. **3h** was obtained as a solid (121 mg, 0.462 mmol, 99%). ¹H NMR:

(300 MHz, methanol-*d*₄) δ 7.50–7.41 (m, 1H), 7.34–7.12 (m, 3H), 4.63–4.49 (m, 2H), 4.00–3.89 (m, 1H), 3.49–3.35 (m, 1H), 2.20–1.94 (m, 2H), 1.85–1.48 (m, 4H). ¹³C NMR: (75 MHz, methanol-*d*₄) δ 132.8, 129.5, 128.93, 128.92, 126.7, 83.2, 68.5, 56.6, 29.2, 27.7, 20.4. HRMS: (NSI+) *m/z* calcd for C₁₂H₁₇ClNO [M]⁺ 226.0995, found 226.0993.

(1*R*,2*R*)-2-((3-Chlorobenzyl)oxy)cyclopentan-1-aminium Chloride (**3i**). **3i** was synthesized according to general procedure C using **2i** (0.687 mmol) and HCl (13.75 mmol). The reaction was run for 45 min, after which a few drops of MeOH were added to dissolve the precipitate. The reaction mixture was then stirred for another 1.5 h. **3i** was obtained as a solid (176 mg, 0.671 mmol, 97%). ¹H NMR: (300 MHz, DMSO-*d*₆) δ 8.26 (br s, 3H), 7.48–7.29 (m, 4H), 4.60–4.46 (m, 2H), 4.00–3.92 (m, 1H), 3.49–3.37 (m, 1H), 2.09–1.93 (m, 2H), 1.80–1.50 (m, 4H). ¹³C NMR: (75 MHz, methanol-*d*₄) δ 140.5, 133.9, 129.6, 127.4, 127.3, 125.7, 82.8, 66.8, 56.6, 29.1, 27.6, 20.3. HRMS: (NSI+) *m/z* calcd for C₁₂H₁₇ClNO [M]⁺ 226.1002, found 226.0993.

tert-Butyl ((1*R*,2*R*)-2-Phenoxy)cyclopentyl)carbamate (**5a**). **5a** was synthesized according to general procedure B using **4** (0.994 mmol), phenol (1.242 mmol), PPh₃ (1.242 mmol), and DIAD (1.242 mmol). The reaction was run for 21 h. After purification with flash column chromatography (EtOAc/cHex, 20%), **5a** was obtained (165 mg, 0.594 mmol, 60%). ¹H NMR: (300 MHz, DMSO-*d*₆) δ 7.33–7.23 (m, 2H), 7.04 (d, *J* = 7.3, 1H), 6.99–6.86 (m, 3H), 4.57–4.48 (m, 1H), 3.89–3.79 (m, 1H), 2.09–1.87 (m, 2H), 1.79–1.42 (m, 4H), 1.39 (s, 9H). ¹³C NMR: (101 MHz, DMSO-*d*₆) δ 157.6, 155.2, 129.4, 120.4, 115.3, 82.2, 77.7, 56.54, 29.8, 29.6, 28.2, 21.2. HRMS: (NSI+) *m/z* calcd for C₁₆H₂₄NO₃ [M + H]⁺ 278.1756, found 278.1747.

tert-Butyl ((1*R*,2*R*)-2-(4-*tert*-Butylphenoxy)cyclopentyl)carbamate (**5c**). **5c** was synthesized according to general procedure B using **4** (0.994 mmol), 4-*tert*-butylphenol (1.242 mmol), PPh₃ (1.242 mmol), and DIAD (1.242 mmol). The reaction was run for 19 h. After purification with flash column chromatography (EtOAc/cHex, 20%), **5c** was obtained (189 mg, 0.567 mmol, 57%). ¹H NMR: (300 MHz, DMSO-*d*₆) δ 7.31–7.24 (m, 2H), 7.02 (d, *J* = 7.3, 1H), 6.86 (d, *J* = 8.5, 2H), 4.52–4.45 (m, 1H), 3.88–3.75 (m, 1H), 2.07–1.89 (m, 2H), 1.80–1.43 (m, 4H), 1.39 (s, 9H), 1.25 (s, 9H). ¹³C NMR: (75 MHz, methanol-*d*₄) δ 156.5, 155.7, 143.0, 125.7, 114.8, 82.6, 78.7, 56.9, 33.5, 30.6, 29.8, 29.7, 27.4, 21.0. HRMS: (NSI+) *m/z* calcd for C₂₀H₃₂NO₃ [M + H]⁺ 334.2364, found 334.2377.

tert-Butyl ((1*R*,2*R*)-2-(3-Methoxyphenoxy)cyclopentyl)carbamate (**5e**). **5e** was synthesized according to general procedure B using **4** (1.987 mmol), 3-methoxyphenol (2.484 mmol), PPh₃ (2.484 mmol), and DIAD (2.484 mmol). The reaction was run for 18 h. After purification with flash column chromatography (EtOAc/cHex, 20%), **5e** was obtained (381 mg, 1.236 mmol, 62%). ¹H NMR: (300 MHz, DMSO-*d*₆) δ 7.15 (t, *J* = 8.2, 1H), 7.05 (d, *J* = 7.3, 1H), 6.58–6.44 (m, 3H), 4.54–4.47 (m, 1H), 3.88–3.78 (m, 1H), 3.73 (s, 3H), 2.05–1.87 (m, 2H), 1.77–1.54 (m, 3H), 1.53–1.42 (m, 1H), 1.39 (s, 9H). ¹³C NMR: (101 MHz, methanol-*d*₄) δ 161.0, 159.2, 156.5, 129.4, 107.6, 106.1, 101.4, 82.7, 78.7, 56.9, 54.3, 29.8, 27.4, 21.1. HRMS: (NSI+) *m/z* calcd for C₁₇H₂₅NNaO₄ [M + Na]⁺ 330.1683, found 330.1687.

tert-Butyl ((1*R*,2*R*)-2-(3-Bromophenoxy)cyclopentyl)carbamate (**5f**). **5f** was synthesized according to general procedure B using **4** (0.497 mmol), 3-bromophenol (0.621 mmol), PPh₃ (0.621 mmol), and DIAD (0.621 mmol). The reaction was run for 18 h. After purification with flash column chromatography (EtOAc/cHex, 20%), **5f** was obtained (90 mg, 0.253 mmol, 51%). ¹H NMR: (300 MHz, DMSO-*d*₆) δ 7.26–6.91 (m, 4H), 4.58–4.51 (m, 1H), 3.88–3.76 (m, 1H), 2.09–1.86 (m, 2H), 1.80–1.42 (m, 4H), 1.39 (s, 9H). ¹³C NMR: (75 MHz, methanol-*d*₄) δ 158.9, 156.4, 130.4, 123.33, 122.3, 118.6, 114.2, 83.2, 78.7, 56.9, 29.8, 29.7, 21.1, 20.4. HRMS: (NSI+) *m/z* calcd for C₁₆H₂₂BrNNaO₃ [M + Na]⁺ 378.0686, found 378.0675.

tert-Butyl ((1*R*,2*R*)-2-(2-Chlorophenoxy)cyclopentyl)carbamate (**5h**). **5h** was synthesized according to general procedure B using **4** (0.994 mmol), 2-chlorophenol (1.242 mmol), PPh₃ (1.242 mmol), and DIAD (1.242 mmol). The reaction was run for 19 h. After

purification with flash column chromatography (EtOAc/cHex, 10%), **5h** was obtained (187 mg, 0.597 mmol, 60%). ¹H NMR: (300 MHz, DMSO-*d*₆) δ 7.44–7.38 (m, 1H), 7.32–7.20 (m, 2H), 7.06 (d, *J* = 7.2, 1H), 6.98–6.90 (m, 1H), 4.64–4.57 (m, 1H), 3.92–3.81 (br s, 1H), 2.08–1.91 (m, 2H), 1.82–1.44 (m, 4H), 1.39 (s, 9H). ¹³C NMR: (75 MHz, methanol-*d*₄) δ 156.4, 153.5, 129.8, 127.5, 123.2, 121.2, 115.3, 83.9, 78.7, 56.8, 29.9, 29.6, 27.4, 21.1. HRMS: (NSI+) *m/z* calcd for C₁₆H₂₃ClNO₃ [M + H]⁺ 312.1359, found 312.1361.

tert-Butyl ((1*R*,2*R*)-2-(3-Chlorophenoxy)cyclopentyl)carbamate (5i). **5i** was synthesized according to general procedure B using **4** (0.994 mmol), 3-chlorophenol (1.242 mmol), PPh₃ (1.242 mmol), and DIAD (1.242 mmol). The reaction was run for 18 h. After purification with flash column chromatography (EtOAc/cHex, 10%), **5i** was obtained (170 mg, 0.544 mmol, 55%). ¹H NMR: (300 MHz, DMSO-*d*₆) δ 7.29 (t, *J* = 8.1, 1H), 7.11–6.90 (m, 4H), 4.59–4.52 (m, 1H), 3.89–3.77 (m, 1H), 2.12–1.86 (m, 2H), 1.81–1.42 (m, 4H), 1.39 (s, 9H). ¹³C NMR: (75 MHz, methanol-*d*₄) δ 158.9, 156.5, 134.4, 130.1, 120.3, 115.59, 113.8, 83.2, 78.7, 56.9, 29.74, 29.65, 27.4, 21.1. HRMS: (NSI+) *m/z* calcd for C₁₆H₂₃ClNO₃ [M + H]⁺ 312.1354, found 312.1361.

tert-Butyl ((1*R*,2*R*)-2-(4-Chlorophenoxy)cyclopentyl)carbamate (5j). **5j** was synthesized according to general procedure B using **4** (0.994 mmol), 4-chlorophenol (1.242 mmol), PPh₃ (1.242 mmol), and DIAD (1.242 mmol). The reaction was run for 20 h. After purification with flash column chromatography (EtOAc/cHex, 10%), **5j** was obtained (191 mg, 0.611 mmol, 62%). ¹H NMR: (300 MHz, DMSO-*d*₆) δ 7.30 (d, *J* = 9.0, 2H), 7.05 (d, *J* = 7.3, 1H), 6.98 (d, *J* = 8.9, 2H), 4.56–4.47 (m, 1H), 3.87–3.77 (m, 1H), 2.08–1.86 (m, 2H), 1.78–1.43 (m, 4H), 1.38 (s, 9H). ¹³C NMR: (75 MHz, DMSO-*d*₆) δ 157.0, 155.6, 129.7, 124.6, 117.6, 83.2, 78.3, 57.0, 30.2, 30.0, 28.7, 21.6. HRMS: (NSI+) *m/z* calcd for C₁₆H₂₂ClNO₃ [M + Na]⁺ 334.1182, found 334.1180.

(1*R*,2*R*)-2-Phenoxy-cyclopentan-1-aminium chloride (6a). **6a** was synthesized according to general procedure C using **5a** (0.804 mmol) and HCl (16.09 mmol). The reaction was run for 18 h. **6a** was obtained as a solid (173 mg, 0.809 mmol, quant.). ¹H NMR: (300 MHz, DMSO-*d*₆) δ 8.20 (s, 3H), 7.39–7.25 (m, 2H), 7.04–6.91 (m, 3H), 4.77–4.68 (m, 1H), 3.64–3.55 (m, 1H), 2.25–2.02 (m, 2H), 1.83–1.56 (m, 4H). ¹³C NMR: (75 MHz, methanol-*d*₄) δ 157.3, 129.3, 121.1, 115.3, 80.6, 57.0, 29.4, 28.0, 20.7. HRMS: (NSI+) *m/z* calcd for C₁₁H₁₆NO [M]⁺ 178.1228, found 178.1226.

(1*R*,2*R*)-2-(4-(tert-Butylphenoxy)cyclopentan-1-aminium Chloride (6c). **6c** was synthesized according to general procedure C using **5c** (0.507 mmol) and HCl (10.14 mmol). The reaction was run for 20 h, after which a few drops of MeOH were added to dissolve the precipitate. Stirring was continued for another 21 h, and more 4 M HCl in dioxane (1 mL) was added to bring the reaction to completion. **6c** was obtained as a solid (117 mg, 0.432 mmol, 85%). ¹H NMR: (300 MHz, DMSO-*d*₆) δ 8.11 (br s, 3H), 7.37–7.28 (m, 2H), 6.92–6.85 (m, 2H), 4.69–4.63 (m, 1H), 3.65–3.53 (m, 1H), 2.23–2.02 (m, 2H), 1.84–1.54 (m, 4H), 1.26 (s, 9H). ¹³C NMR: (75 MHz, methanol-*d*₄) δ 155.0, 144.0, 126.0, 114.9, 80.7, 57.0, 33.6, 30.6, 29.5, 28.0, 20.7. HRMS: (NSI+) *m/z* calcd for C₁₅H₂₄NO [M]⁺ 234.1850, found 234.1852.

(1*R*,2*R*)-2-(3-Methoxyphenoxy)cyclopentan-1-aminium chloride (6e). **6e** was synthesized according to general procedure C using **5e** (1.236 mmol) and HCl (6.18 mmol). The reaction was run for 19 h, after which more 4 M HCl in dioxane (2 mL) was added to bring the reaction to completion. **6e** was obtained as a solid (322 mg, 1.23 mmol, quant.). ¹H NMR: (300 MHz, DMSO-*d*₆) δ 8.33 (br s, 3H), 7.21 (t, *J* = 8.2, 1H), 6.61–6.47 (m, 3H), 4.80–4.71 (m, 1H), 3.74 (s, 3H), 3.61–3.51 (m, 1H), 2.25–2.04 (m, 2H), 1.86–1.59 (m, 4H). ¹³C NMR: (101 MHz, methanol-*d*₄) δ 161.1, 158.5, 129.8, 107.4, 106.6, 102.0, 80.8, 57.0, 54.4, 29.5, 27.9, 20.7. HRMS: (NSI+) *m/z* calcd for C₁₂H₁₈NO₂ [M]⁺ 208.1329, found 208.1332.

(1*R*,2*R*)-2-(3-Bromophenoxy)cyclopentan-1-aminium chloride (6f). **6f** was synthesized according to general procedure C using **5f** (0.253 mmol) and HCl (5.05 mmol). The reaction was run for 1 h, after which a few drops of MeOH were added to dissolve precipitate. Stirring was then continued for another 19 h. **6f** was obtained as a

solid (74 mg, 0.252 mmol, quant.). ¹H NMR: (300 MHz, DMSO-*d*₆) δ 8.20 (br s, 3H), 7.29 (t, *J* = 8.3, 1H), 7.20–7.15 (m, 2H), 7.03–6.96 (m, 1H), 4.77–4.71 (m, 1H), 3.63–3.53 (m, 1H), 2.24–2.03 (m, 2H), 1.84–1.56 (m, 4H). ¹³C NMR: (101 MHz, methanol-*d*₄) δ 158.2, 130.7, 124.2, 122.4, 118.7, 114.2, 81.1, 56.9, 29.3, 27.9, 20.7. HRMS: (NSI+) *m/z* calcd for C₁₁H₁₅BrNO [M]⁺ 256.0330, found 256.0332.

(1*R*,2*R*)-2-(2-Chlorophenoxy)cyclopentan-1-aminium chloride (6h). **6h** was synthesized according to general procedure C using **5h** (0.6 mmol) and HCl (12 mmol). The reaction was run for 69 h. **6h** was obtained as a solid (149 mg, 0.6 mmol, quant.). ¹H NMR: (300 MHz, DMSO-*d*₆) δ 8.30 (br s, 3H), 7.46 (dd, *J* = 7.9, 1.6, 1H), 7.36–7.30 (m, 1H), 7.23 (dd, *J* = 8.4, 1.5, 1H), 7.05–6.97 (m, 1H), 4.90–4.83 (m, 1H), 3.68–3.59 (m, 1H), 2.24–2.09 (m, 2H), 1.86–1.62 (m, 4H). ¹³C NMR: (75 MHz, methanol-*d*₄) δ 152.7, 130.1, 127.8, 123.4, 122.2, 115.6, 82.1, 57.0, 29.6, 28.4, 21.0. HRMS: (NSI+) *m/z* calcd for C₁₁H₁₅ClNO [M]⁺ 212.0832, found 212.0837.

(1*R*,2*R*)-2-(3-Chlorophenoxy)cyclopentan-1-aminium chloride (6i). **6i** was synthesized according to general procedure C using **5i** (0.481 mmol) and HCl (4.81 mmol). The reaction was run for 48 h. **6i** was obtained as a solid (118 mg, 0.476 mmol, 99%). ¹H NMR: (300 MHz, methanol-*d*₄) δ 7.29 (t, *J* = 8.1, 1H), 7.06–6.91 (m, 3H), 4.90–4.80 (m, 1H), 3.78–3.69 (m, 1H), 2.38–2.23 (m, 2H), 1.99–1.67 (m, 4H). ¹³C NMR: (75 MHz, methanol-*d*₄) δ 158.2, 134.6, 130.5, 121.2, 115.85, 113.9, 81.0, 57.0, 29.4, 28.1, 20.9. HRMS: (NSI+) *m/z* calcd for C₁₁H₁₅ClNO [M]⁺ 212.0830, found 212.0837.

(1*R*,2*R*)-2-(4-Chlorophenoxy)cyclopentan-1-aminium chloride (6j). **6j** was synthesized according to general procedure C using **5j** (0.611 mmol) and HCl (12.22 mmol). The reaction was run for 1.5 h, after which a few drops of MeOH were added to dissolve the precipitate. Stirring was continued for another hour. **6j** was obtained as a solid (150 mg, 0.604 mmol, 99%). ¹H NMR: (300 MHz, DMSO-*d*₆) δ 8.59 (br s, 3H), 7.38–7.29 (m, 2H), 7.07–6.93 (m, 2H), 4.85–4.75 (m, 1H), 3.59–3.50 (m, 1H), 2.29–2.01 (m, 2H), 1.87–1.57 (m, 4H). ¹³C NMR: (75 MHz, DMSO-*d*₆) δ 156.4, 129.8, 125.2, 117.8, 81.5, 56.4, 30.0, 28.7, 21.6. HRMS: (NSI+) *m/z* calcd for C₁₁H₁₅ClNO [M]⁺ 212.0840, found 212.0837.

(2*R*,3*R*,4*R*,5*R*)-2-(Acetoxymethyl)-5-(6-(((1*R*,2*R*)-2-((4-isopropylbenzyl)oxy)cyclopentyl)amino)-9H-purin-9-yl)-tetrahydrofuran-3,4-diyl Diacetate (8). **8** was synthesized according to general procedure D using **7** (0.286 mmol), **3b** (0.428 mmol), and NaHCO₃ (0.857 mmol). The reaction was heated at reflux overnight. After purification with flash column chromatography (MeOH/EtOAc, 2%), **8** was obtained as a ~1:1 mixture with starting material **7** (determined by ¹H NMR). This mixture was used in the next step without further purification to obtain **15**.

(2*R*,3*R*,4*R*,5*R*)-2-(Acetoxymethyl)-5-(6-(((1*R*,2*R*)-2-((tert-butyl)benzyl)oxy)cyclopentyl)amino)-9H-purin-9-yl)-tetrahydrofuran-3,4-diyl Diacetate (9). **9** was synthesized according to general procedure D using **7** (0.235 mmol), **3c** (0.352 mmol), and NaHCO₃ (0.705 mmol). The reaction was heated at reflux for 15 h. After purification with flash column chromatography (EtOAc/cHex, 80%), **9** was obtained as a solid (53 mg, 0.0845 mmol, 36%). ¹H NMR: (300 MHz, methanol-*d*₄) δ 8.31 (s, 1H), 8.24 (s, 1H), 7.32 (d, *J* = 8.5, 2H), 7.23 (d, *J* = 8.4, 2H), 6.25 (d, *J* = 5.3, 1H), 6.03 (t, *J* = 5.5, 1H), 5.74–5.71 (m, 1H), 4.75–4.65 (m, 1H), 4.63 (s, 2H), 4.50–4.35 (m, 3H), 4.04–3.98 (m, 1H), 2.32–2.19 (m, 1H), 2.16 (s, 3H), 2.08 (s, 3H), 2.07 (s, 3H), 2.05–1.99 (m, 1H), 1.90–1.57 (m, 4H), 1.29 (s, 9H). ¹³C NMR: (101 MHz, methanol-*d*₄) δ 170.8, 170.0, 169.7, 154.3, 152.9, 150.2, 148.5, 139.2, 135.5, 127.34, 124.7, 119.5, 86.4, 84.7, 80.2, 78.0, 73.0, 70.7, 70.6, 62.8, 33.9, 30.4, 30.3, 30.0, 21.1, 19.2, 19.0, 18.9. HRMS: (NSI+) *m/z* calcd for C₃₂H₄₂N₅O₈ [M + H]⁺ 624.3012, found 624.3028.

(2*R*,3*R*,4*R*,5*R*)-2-(Acetoxymethyl)-5-(6-(((1*R*,2*R*)-2-((4-cyanobenzyl)oxy)cyclopentyl)amino)-9H-purin-9-yl)-tetrahydrofuran-3,4-diyl Diacetate (10). **10** was synthesized according to general procedure D using **7** (0.83 mmol), **3d** (0.83 mmol), and NaHCO₃ (2.5 mmol). The reaction was heated at reflux for 16 h. After purification with flash column chromatography (EtOAc/cHex, 80%), **10** was obtained as a solid (492 mg, 0.83 mmol, quant.). ¹H NMR: (300 MHz, DMSO-*d*₆) δ 8.37 (s, 1H), 8.27 (s,

1H), 7.99 (d, *J* = 6.0, 1H), 7.75 (d, *J* = 7.8, 2H), 7.47 (d, *J* = 7.8, 2H), 6.21 (d, *J* = 5.4, 1H), 6.04 (t, *J* = 5.6, 1H), 5.63 (t, *J* = 5.2, 1H), 4.70–4.52 (m, 1H), 4.66 (s, 2H), 4.45–4.32 (m, 2H), 4.28–4.19 (m, 1H), 4.02–3.87 (m, 1H), 2.15–1.88 (m, 2H), 2.12 (s, 3H), 2.04 (s, 3H), 2.01 (s, 3H), 1.81–1.54 (m, 4H). ¹³C NMR (101 MHz, CDCl₃) δ 170.4, 169.7, 169.5, 153.8, 149.4, 144.5, 138.7, 132.2, 127.8, 120.3, 119.0, 111.2, 86.5, 85.69, 85.67, 80.5, 77.4, 73.4, 70.7, 70.5, 63.2, 31.02, 30.99, 30.5, 21.7, 20.9, 20.6, 20.5. HRMS: (NSI+) *m/z* calcd for C₂₉H₃₃N₆O₈ [M + H]⁺ 593.2360, found 593.2362.

(2*R*,3*R*,4*R*,5*R*)-2-(Acetoxymethyl)-5-(6-(((1*R*,2*R*)-2-((3-methoxybenzyl)oxy)cyclopentyl)amino)-9*H*-purin-9-yl)-tetrahydrofuran-3,4-diyl Diacetate (**11**). **11** was synthesized according to general procedure D using **7** (0.18 mmol), **3e** (0.271 mmol), and NaHCO₃ (0.542 mmol). The reaction was heated at reflux for 23 h. After purification with flash column chromatography (EtOAc/cHex, 80%), **11** was obtained (68 mg, 0.114 mmol, 67%). ¹H NMR: (300 MHz, methanol-*d*₄) δ 8.37 (s, 1H), 8.26 (s, 1H), 7.98 (d, *J* = 7.9, 1H), 7.19 (t, *J* = 7.8, 1H), 6.89–6.75 (m, 3H), 6.22 (d, *J* = 5.4, 1H), 6.04 (t, *J* = 5.7, 1H), 5.64 (t, *J* = 5.3, 1H), 4.66–4.57 (m, 1H), 4.54 (s, 2H), 4.46–4.33 (m, 3H), 4.28–4.21 (m, 1H), 4.02–3.96 (m, 1H) 3.66 (s, 3H), 2.13 (s, 3H), 2.10–1.88 (m, 2H), 2.04 (s, 3H), 2.01 (s, 3H) 1.77–1.55 (m, 4H). ¹³C NMR: (101 MHz, methanol-*d*₄) δ 170.8, 170.0, 169.8, 159.7, 154.3, 152.8, 148.5, 140.3, 139.2, 128.8, 119.7, 119.5, 112.62, 112.61, 86.4, 84.9, 80.2, 73.0, 70.9, 70.6, 62.8, 57.0, 54.1, 30.2, 30.0, 21.1, 19.2, 19.0, 18.9. HRMS: (NSI+) *m/z* calcd for C₂₉H₃₆N₅O₉ [M + H]⁺ 598.2506, found 598.2508.

(2*R*,3*R*,4*R*,5*R*)-2-(Acetoxymethyl)-5-(6-(((1*R*,2*R*)-2-phenyloxycyclopentyl)amino)-9*H*-purin-9-yl)-tetrahydrofuran-3,4-diyl Diacetate (**12**). **12** was synthesized according to general procedure D using **7** (0.137 mmol), **6a** (0.206 mmol), and NaHCO₃ (0.412 mmol). The reaction was heated at reflux for 18 h. After purification with flash column chromatography (EtOAc, 100%), **12** was obtained (50 mg, 0.09 mmol, 65%). ¹H NMR: (300 MHz, methanol-*d*₄) δ 8.30 (s, 1H), 8.22 (s, 1H), 7.22 (t, *J* = 7.7, 2H), 7.06–6.82 (m, 3H), 6.24 (d, *J* = 5.2, 1H), 6.02 (t, *J* = 5.6, 1H), 5.72 (t, *J* = 5.2, 1H), 4.85–4.73 (m, 2H), 4.50–4.33 (m, 3H), 2.38–2.18 (m, 2H), 2.15 (s, 3H), 2.07 (s, 6H), 1.98–1.69 (m, 4H). ¹³C NMR: (101 MHz, methanol-*d*₄) δ 170.8, 170.0, 169.8, 158.0, 154.4, 152.8, 148.6, 139.4, 129.0, 120.3, 119.5, 115.4, 86.4, 82.5, 80.2, 73.0, 70.6, 62.8, 57.1, 30.0, 29.7, 21.1, 19.2, 19.0, 18.9. HRMS: (NSI+) *m/z* calcd for C₂₇H₃₂N₅O₈ [M + H]⁺ 554.2239, found 554.2245.

(2*R*,3*R*,4*R*,5*R*)-2-(Acetoxymethyl)-5-(6-(((1*R*,2*R*)-2-(3-methoxyphenoxy)cyclopentyl)amino)-9*H*-purin-9-yl)-tetrahydrofuran-3,4-diyl Diacetate (**13**). **13** was synthesized according to general procedure D using **7** (0.196 mmol), **6e** (0.197 mmol), and NaHCO₃ (0.394 mmol). The reaction was heated at reflux for 23 h. After purification with flash column chromatography (EtOAc/cHex, 80%), **13** was obtained (63 mg, 0.108 mmol, 55%). ¹H NMR: (300 MHz, DMSO-*d*₆) δ 8.38 (s, 1H), 8.26 (s, 1H), 8.15 (d, *J* = 6.5, 1H), 7.14 (t, *J* = 8.1, 1H), 6.57–6.44 (m, 3H), 6.22 (d, *J* = 5.4, 1H), 6.07–6.01 (m, 1H), 5.66–5.61 (m, 1H), 4.89–4.83 (m, 1H), 4.70–4.60 (m, 1H), 4.46–4.34 (m, 2H), 4.28–4.20 (m, 1H), 3.67 (s, 3H), 2.23–2.13 (m, 2H), 2.12 (s, 3H), 2.04 (s, 3H), 2.02 (s, 3H), 1.89–1.62 (m, 4H). ¹³C NMR: (75 MHz, methanol-*d*₄) δ 170.8, 170.0, 169.8, 160.9, 159.1, 154.3, 152.8, 139.4, 129.4, 119.5, 107.8, 106.0, 101.7, 86.4, 82.6, 80.2, 73.0, 70.6, 62.8, 57.0, 54.3, 30.0, 29.8, 21.1, 19.2, 19.1, 18.9. HRMS: (NSI+) *m/z* calcd for C₂₈H₃₄N₅O₉ [M + H]⁺ 584.2343, found 584.2351.

(2*R*,3*R*,4*R*,5*R*)-2-(Acetoxymethyl)-5-(6-(((1*R*,2*R*)-2-(4-chlorophenoxy)cyclopentyl)amino)-9*H*-purin-9-yl)-tetrahydrofuran-3,4-diyl Diacetate (**14**). **14** was synthesized according to general procedure D using **7** (0.347 mmol), **6j** (0.52 mmol), and NaHCO₃ (1.04 mmol). The reaction was heated at reflux for 17 h. After purification with flash column chromatography (EtOAc/cHex, 80%), **14** was obtained (192 mg, 0.327 mmol, 82%). ¹H NMR: (300 MHz, methanol-*d*₄) δ 8.19 (s, 1H), 8.10 (s, 1H), 7.12–7.04 (m, 2H), 6.94–6.84 (m, 2H), 6.12 (d, *J* = 5.2, 1H), 5.91 (t, *J* = 5.5, 1H), 5.60 (t, *J* = 5.5, 1H), 4.68–4.63 (m, 1H), 4.63–4.55 (m, 1H), 4.35–4.22 (m, 3H), 2.23–2.05 (m, 2H), 2.03 (s, 3H), 1.95 (s, 6H), 1.87–1.55 (m, 4H). ¹³C NMR: (75 MHz, methanol-*d*₄) δ 170.8, 170.0, 169.8, 156.7, 154.3, 152.8, 139.4, 128.8, 125.1, 119.5, 116.9,

86.4, 82.9, 80.2, 73.0, 70.6, 62.8, 56.9, 29.8, 29.6, 21.0, 19.3, 19.1, 18.9. HRMS: (NSI+) *m/z* calcd for C₂₇H₃₁ClN₅O₈ [M + H]⁺ 588.1854, found 588.1856.

(2*R*,3*S*,4*R*,5*R*)-2-(Hydroxymethyl)-5-(6-(((1*R*,2*R*)-2-((4-isopropylbenzyl)oxy)cyclopentyl)amino)-9*H*-purin-9-yl)-tetrahydrofuran-3,4-diol (**15**). **15** was synthesized according to general procedure E using the ~1:1 mixture of **7** and **8** from above and K₂CO₃ (0.137 mmol). The reaction was run for 1.5 h. After purification with flash column chromatography (MeOH/EtOAc, 2%), **15** was obtained as a colorless solid (27 mg, 0.055 mmol, 19% over two steps). ¹H NMR: (300 MHz, DMSO-*d*₆) δ 8.37 (s, 1H), 8.23 (br s, 1H), 7.93 (d, *J* = 5.6, 1H), 7.22–7.12 (m, 4H), 5.89 (d, *J* = 6.1, 1H), 5.46–5.37 (m, 2H), 5.18 (d, *J* = 4.6, 1H), 4.66–4.44 (m, 3H), 4.62 (q, *J* = 6.0, 1H), 4.18–4.12 (m, 1H), 4.04–3.94 (m, 2H), 3.72–3.63 range (m, 1H), 3.61–3.50 (m, 1H), 2.84 (sept, *J* = 6.7, 1H), 2.13–1.88 (m, 2H), 1.78–1.56 (m, 4H), 1.17 (d, *J* = 6.9, 6H). HRMS: (NSI+) *m/z* calcd for C₂₅H₃₄N₅O₅ [M + H]⁺ 484.2539, found 484.2554. UPLC analysis: *t*_R = 2.87 min; peak area > 95% (detection at 254 nm).

(2*R*,3*R*,4*S*,5*R*)-2-(6-(((1*R*,2*R*)-2-((4-*tert*-Butyl)benzyl)oxy)cyclopentyl)amino)-9*H*-purin-9-yl)-5-(hydroxymethyl)-tetrahydrofuran-3,4-diol (**16**). **16** was synthesized according to general procedure E using **9** (0.083 mmol) and K₂CO₃ (0.05 mmol). The reaction was run for 30 min. After purification with flash column chromatography (MeOH/CH₂Cl₂, 5%), **16** was obtained as a colorless solid (30 mg, 0.06 mmol, 73%). ¹H NMR: (300 MHz, methanol-*d*₄) δ 8.16 (s, 2H), 7.21 (d, *J* = 8.4, 2H), 7.11 (d, *J* = 8.3, 2H), 5.85 (d, *J* = 6.5, 1H), 4.60–4.44 (m, 4H), 4.22 (dd, *J* = 5.1, 2.5, 1H), 4.06–4.09 (m, 1H), 3.87–3.91 (m, 1H), 3.79 (dd, *J* = 12.6, 2.5, 1H), 3.64 (dd, *J* = 12.5, 2.6, 1H), 2.20–2.09 (m, 1H), 1.99–1.85 (m, 1H), 1.80–1.45 (m, 3H), 1.58–1.18 (m, 1H) 1.18 (s, 9H). ¹³C NMR: (101 MHz, methanol-*d*₄) δ 154.5, 152.2, 150.2, 147.8, 140.1, 135.5, 127.3, 124.7, 120.0, 90.0, 86.9, 84.6, 74.1, 71.3, 70.7, 62.1, 56.9, 33.9, 30.4, 30.2, 30.0, 21.1. HRMS: (NSI+) *m/z* calcd for C₂₆H₃₆N₅O₅ [M + H]⁺ 498.2690, found 498.2711. UPLC analysis: *t*_R = 3.01 min; peak area > 95% (detection at 254 nm).

4-(((1*R*,2*R*)-2-((9-((2*R*,3*R*,4*S*,5*R*)-3,4-Dihydroxy-5-(hydroxymethyl)tetrahydrofuran-2-yl)-9*H*-purin-6-yl)amino)cyclopentyl)oxy)methyl)benzamide (**17**). **17** was synthesized according to general procedure E using **10** (0.552 mmol) and K₂CO₃ (0.552 mmol). The reaction was run for 3 h. After purification with flash column chromatography (EtOAc, 100%), **17** was obtained as a colorless solid (183 mg, 0.392 mmol, 71%). ¹H NMR: (300 MHz, DMSO-*d*₆) δ 8.37 (s, 1H), 8.23 (s, 1H), 7.93 (d, *J* = 6.0, 1H), 7.76 (d, *J* = 8.3, 2H), 7.48 (d, *J* = 8.0, 2H), 5.89 (d, *J* = 6.2, 1H), 5.42 (d, *J* = 6.3, 1H), 5.38 (dd, *J* = 7.1, 4.5, 1H), 5.18 (d, *J* = 4.7, 1H), 4.69–4.50 (m, 1H), 4.67 (s, 2H), 4.61 (q, *J* = 5.9, 1H), 4.28–4.11 (m, 1H), 4.08–3.88 (m, 2H), 3.68 (dt, *J* = 12.0, 4.1, 1H), 3.55 (ddd, *J* = 11.7, 7.2, 3.7, 1H), 2.10–2.01 (m, 1H), 2.00–1.89 (m, 1H), 1.89–1.55 (m, 4H). HRMS: (NSI+) *m/z* calcd for C₂₃H₂₇N₆O₅ [M + H]⁺ 467.2037, found 467.2031. UPLC analysis: *t*_R = 2.28 min; peak area > 95% (detection at 254 nm).

4-(((1*R*,2*R*)-2-((9-((2*R*,3*R*,4*S*,5*R*)-3,4-Dihydroxy-5-(hydroxymethyl)tetrahydrofuran-2-yl)-9*H*-purin-6-yl)amino)cyclopentyl)oxy)methyl)benzamide (**18**). **18** (0.186 mmol) was dissolved in MeOH (15 mL) and K₂CO₃ (0.186 mmol) was added. The reaction mixture was stirred at room temperature for 4 h and concentrated under reduced pressure. The residue was dissolved in MeOH (1.5 mL), and aq. 30% H₂O₂ (0.15 mL) was added. The solution was heated to 40 °C and stirred for 3 h. The volatiles were removed under reduced pressure. After purification with flash column chromatography (MeOH/EtOAc, 20%), **18** was obtained as a colorless solid (75 mg, 0.155 mmol, 83%). ¹H NMR: (400 MHz, methanol-*d*₄) δ 8.24 (s, 2H), 7.76 (d, *J* = 8.3, 2H), 7.39 (d, *J* = 7.9, 2H), 5.95 (d, *J* = 6.5, 1H), 4.76 (dd, *J* = 6.5, 5.1, 1H), 4.75–4.56 (m, 1H), 4.71 (s, 2H), 4.33 (dd, *J* = 5.1, 2.5, 1H), 4.17 (q, *J* = 2.6, 1H), 4.00 (dt, *J* = 6.5, 4.1, 1H), 3.89 (dd, *J* = 12.6, 2.5, 1H), 3.75 (dd, *J* = 12.6, 2.7, 1H), 2.29–2.18 (m, 1H), 2.14–1.96 (m, 1H), 1.96–1.72 (m, 3H), 1.72–1.55 (m, 1H). ¹³C NMR: (101 MHz, methanol-*d*₄) δ 172.1, 155.8, 153.5, 149.2, 144.5, 141.5, 133.8, 128.6, 128.4, 121.4, 91.4, 88.2, 86.6, 75.4, 72.7, 71.7, 63.5, 58.3, 31.5, 31.4, 22.5. HRMS:

(NSI+) m/z calcd for $C_{23}H_{28}N_6NaO_6 [M + Na]^+$ 485.2143, found 485.2156. UPLC analysis: $t_R = 1.79$ min; peak area > 95% (detection at 254 nm).

(2*R*,3*S*,4*R*,5*R*)-2-(Hydroxymethyl)-5-(6-(((1*R*,2*R*)-2-((3-methoxybenzyl)oxy)cyclopentyl)amino)-9*H*-purin-9-yl)-tetrahydrofuran-3,4-diol (**19**). **19** was synthesized according to general procedure E using **11** (0.084 mmol) and K_2CO_3 (0.05 mmol). The reaction was run for 30 min. After purification with flash column chromatography (MeOH/EtOAc, 5–10%), **19** was obtained as a colorless solid (36 mg, 0.076 mmol, 93%). 1H NMR: (300 MHz, DMSO- d_6) δ 8.36 (s, 1H), 8.23 (s, 1H), 7.93 (d, $J = 4.9$, 1H), 7.20 (t, $J = 7.7$, 1H), 6.89–6.73 (m, 3H), 5.89 (d, $J = 6.2$, 1H), 5.46–5.37 (m, 2H), 5.18 (d, $J = 4.6$, 1H), 4.71–4.56 (m, 2H), 4.54 (s, 2H), 4.18–4.11 (m, 1H), 4.06–3.92 (m, 2H), 3.72–3.67 (m, 1H), 3.67 (s, 3H), 3.61–3.52 (m, 1H), 2.12–1.89 (m, 2H), 1.76–1.57 (m, 4H). ^{13}C NMR: (101 MHz, methanol- d_4) δ 159.8, 154.4, 152.1, 147.8, 140.2, 140.0, 128.8, 120.0, 119.5, 112.7, 112.6, 90.0, 86.9, 84.8, 74.1, 71.3, 70.8, 62.1, 56.7, 54.1, 30.1, 30.0, 21.1. HRMS: (NSI+) m/z calcd for $C_{23}H_{30}N_6O_6 [M + H]^+$ 472.2186, found 472.2191. UPLC analysis: $t_R = 2.33$ min; peak area > 95% (detection at 254 nm).

(2*R*,3*R*,4*S*,5*R*)-2-(6-(((1*R*,2*R*)-2-((3-Bromobenzyl)oxy)cyclopentyl)amino)-9*H*-purin-9-yl)-5-(hydroxymethyl)tetrahydrofuran-3,4-diol (**20**). **20** was synthesized according to general procedure G using **7** (0.296 mmol), **3f** (0.326 mmol), and $NaHCO_3$ (0.652 mmol). The reaction was heated at reflux for 18 h. After purification with flash column chromatography (EtOAc, 100%) a mixture of the substitution product and fully and semi-deacetylated products was isolated (53 mg). This mixture was dissolved in MeOH (5 mL), and K_2CO_3 (0.05 mmol) was added. After stirring for 30 min at room temperature, the reaction mixture was filtered and concentrated under reduced pressure. After purification with flash column chromatography (MeOH/EtOAc, 5%), **20** was obtained as a colorless solid (33 mg, 0.063 mmol, 66% over two steps). 1H NMR: (300 MHz, methanol- d_4) δ 8.15 (s, 1H), 8.14 (s, 1H), 7.37–7.32 (m, 1H), 7.25–6.99 (m, 3H), 5.85 (d, $J = 6.5$, 1H), 4.69–4.62 (m, 1H), 4.62–4.45 (m, 3H), 4.25–4.20 (m, 1H), 4.07 (q, $J = 2.5$, 1H), 3.89–3.82 (m, 1H), 3.79 (dd, $J = 12.6$, 2.4, 1H), 3.64 (dd, $J = 12.6$, 2.6, 1H), 2.19–2.05 (m, 1H), 1.97–1.85 (m, 1H), 1.81–1.45 (m, 4H). ^{13}C NMR: (75 MHz, methanol- d_4) δ 154.4, 152.2, 141.5, 140.1, 130.1, 130.0, 129.6, 125.8, 121.9, 120.0, 90.0, 86.9, 85.1, 74.1, 71.3, 70.0, 62.2, 56.7, 30.1, 29.9, 21.1. HRMS: (NSI+) m/z calcd for $C_{22}H_{27}BrN_5O_5 [M + H]^+$ 520.1189, found 520.1189. UPLC analysis: $t_R = 2.58$ min; peak area > 95% (detection at 254 nm).

(2*R*,3*R*,4*S*,5*R*)-2-(6-(((1*R*,2*R*)-2-((4-Bromobenzyl)oxy)cyclopentyl)amino)-9*H*-purin-9-yl)-5-(hydroxymethyl)tetrahydrofuran-3,4-diol (**21**). **21** was synthesized according to general procedure G using **7** (0.209 mmol), **3g** (0.209 mmol), and $NaHCO_3$ (0.417 mmol). The reaction was heated at reflux for 18 h. The crude material was deacetylated using K_2CO_3 (0.125 mmol) in MeOH for 30 min at room temperature. After purification with flash column chromatography (MeOH/EtOAc, 5%), **21** was obtained (25 mg, 0.048 mmol, 23% over two steps). 1H NMR (300 MHz, methanol- d_4) δ 8.15 (s, 1H), 8.14 (s, 1H), 7.29 (d, $J = 8.4$, 2H), 7.11 (d, $J = 8.3$, 2H), 5.85 (d, $J = 6.4$, 1H), 4.65 (dd, $J = 6.4$, 5.1, 1H), 4.62–4.51 (m, 1H), 4.49 (s, 2H), 4.23 (dd, $J = 5.1$, 2.5, 1H), 4.07 (q, $J = 2.5$, 1H), 3.90–3.84 (m, 1H), 3.79 (dd, $J = 12.6$, 2.5, 1H), 3.64 (dd, $J = 12.6$, 2.6, 1H), 2.19–2.07 (m, 1H), 1.97–1.84 (m, 1H), 1.80–1.44 (m, 4H). ^{13}C NMR: (75 MHz, methanol- d_4) δ 154.4, 152.1, 140.1, 138.1, 130.9, 129.1, 120.7, 120.0, 90.0, 86.9, 85.0, 74.1, 71.3, 70.1, 62.1, 56.9, 30.1, 30.0, 21.1. HRMS: (NSI+) m/z calcd for $C_{22}H_{27}BrN_5O_5 [M + H]^+$ 520.1187, found 520.1190. UPLC analysis: $t_R = 2.64$ min; peak area > 99% (detection at 254 nm).

(2*R*,3*R*,4*S*,5*R*)-2-(6-(((1*R*,2*R*)-2-((2-Chlorobenzyl)oxy)cyclopentyl)amino)-9*H*-purin-9-yl)-5-(hydroxymethyl)tetrahydrofuran-3,4-diol (**22**). **22** was synthesized according to general procedure G using **7** (0.229 mmol), **3h** (0.229 mmol), and $NaHCO_3$ (0.458 mmol). The reaction was heated at reflux for 19 h. The crude material was deacetylated using K_2CO_3 (0.22 mmol) in MeOH for 30 min at room temperature. After purification with flash column chromatography (MeOH/EtOAc, 5%), **22** was obtained (51 mg, 0.107 mmol, 47% over two steps). 1H NMR: (300 MHz, methanol- d_4) δ 8.13 (br s,

2H), 7.39–7.32 (m, 1H), 7.22–7.02 (m, 3H), 5.84 (d, $J = 6.5$, 1H), 4.71–4.47 (m, 4H), 4.25–4.20 (m, 1H), 4.07 (q, $J = 2.5$, 1H), 3.94–3.87 (m, 1H), 3.84–3.72 (m, 1H), 3.67–3.59 (m, 1H), 2.20–2.06 (m, 1H), 2.00–1.85 (m, 1H), 1.82–1.62 (m, 3H), 1.61–1.45 (m, 1H). ^{13}C NMR: (75 MHz, methanol- d_4) δ 154.4, 152.1, 147.8, 140.0, 136.3, 132.5, 128.9, 128.7, 128.4, 126.5, 120.0, 90.0, 86.9, 85.5, 74.1, 71.3, 68.1, 62.2, 56.7, 30.1, 30.0, 21.2. HRMS: (NSI+) m/z calcd for $C_{22}H_{27}ClN_5O_5 [M + H]^+$ 476.1673, found 476.1695. UPLC analysis: $t_R = 2.51$ min; peak area > 99% (detection at 254 nm).

(2*R*,3*R*,4*S*,5*R*)-2-(6-(((1*R*,2*R*)-2-((3-Chlorobenzyl)oxy)cyclopentyl)amino)-9*H*-purin-9-yl)-5-(hydroxymethyl)tetrahydrofuran-3,4-diol (**23**). **23** was synthesized according to general procedure G using **7** (0.336 mmol), **3i** (0.336 mmol), and $NaHCO_3$ (0.732 mmol). The reaction was heated at reflux for 19 h. The crude material was deacetylated using K_2CO_3 (0.22 mmol) in MeOH for 30 min at room temperature. After purification with flash column chromatography (MeOH/EtOAc, 4%), **23** was obtained (45 mg, 0.095 mmol, 26% over two steps). 1H NMR: (300 MHz, methanol- d_4) δ 8.14 (s, 1H), 8.13 (s, 1H), 7.19 (s, 1H), 7.04–7.03 (m, 3H), 5.85 (d, $J = 6.4$, 1H), 4.69–4.61 (m, 1H), 4.61–4.44 (m, 3H), 4.26–4.20 (m, 1H), 4.07 (q, $J = 2.5$, 1H), 3.89–3.82 (m, 1H), 3.82–3.74 (m, 1H), 3.69–3.60 (m, 1H), 2.18–2.05 (m, 1H), 1.96–1.79 (m, 2H), 1.78–1.45 (m, 4H). ^{13}C NMR: (75 MHz, methanol- d_4) δ 154.4, 152.2, 148.0, 141.3, 140.1, 133.8, 129.3, 127.1, 127.0, 125.4, 120.0, 90.0, 86.9, 85.1, 74.1, 71.3, 70.0, 62.15, 56.8, 30.1, 29.9, 21.1. HRMS: (NSI+) m/z calcd for $C_{22}H_{27}ClN_5O_5 [M + H]^+$ 476.1699, found 476.1695. UPLC analysis: $t_R = 2.56$ min; peak area > 99% (detection at 254 nm).

(2*R*,3*S*,4*R*,5*R*)-2-(Hydroxymethyl)-5-(6-(((1*R*,2*R*)-2-phenoxycyclopentyl)amino)-9*H*-purin-9-yl)tetrahydrofuran-3,4-diol (**24**). **24** was synthesized according to general procedure E using **12** (0.089 mmol) and K_2CO_3 (0.053 mmol). The reaction was run for 30 min. After purification with flash column chromatography (EtOAc, 100%), **24** was obtained as a colorless solid (16 mg, 0.038 mmol, 42%). 1H NMR (400 MHz, methanol- d_4) δ 8.15 (s, 1H), 8.15 (s, 1H), 7.11 (t, $J = 7.9$, 2H), 6.94–6.87 (m, 2H), 6.77 (t, $J = 7.3$, 1H), 5.85 (d, $J = 6.4$, 1H), 4.72–4.67 (m, 1H), 4.66–4.54 (m, 2H), 4.22 (dd, $J = 5.1$, 2.5, 1H), 4.07 (q, $J = 2.6$, 1H), 3.79 (dd, $J = 12.6$, 2.5, 1H), 3.64 (dd, $J = 12.5$, 2.7, 1H), 2.26–2.05 (m, 2H), 1.60–1.56 (m, 4H). ^{13}C NMR: (75 MHz, methanol- d_4) δ 158.0, 154.5, 152.1, 148.0, 140.1, 129.0, 120.4, 120.0, 115.4, 89.9, 86.8, 82.5, 74.1, 71.3, 62.1, 57.2, 29.9, 29.7, 21.0. HRMS: (NSI+) m/z calcd for $C_{21}H_{26}N_5O_5 [M + H]^+$ 428.1924, found 428.1928. HPLC analysis: $t_R = 7.22$ min; peak area 95% (detection at 254 nm).

(2*R*,3*R*,4*S*,5*R*)-2-(6-(((1*R*,2*R*)-2-(4-(tert-Butyl)phenoxy)cyclopentyl)amino)-9*H*-purin-9-yl)-5-(hydroxymethyl)tetrahydrofuran-3,4-diol (**25**). **25** was synthesized according to general procedure G using **7** (0.241 mmol), **6c** (0.241 mmol), and $NaHCO_3$ (0.482 mmol). The reaction was heated at reflux for 19 h. The crude material was deacetylated using K_2CO_3 (0.144 mmol) in MeOH for 30 min at room temperature. After purification with flash column chromatography (MeOH/EtOAc, 3%), **25** was obtained (46 mg, 0.095 mmol, 40% over two steps). 1H NMR: (300 MHz, methanol- d_4) δ 8.14 (s, 1H), 8.13 (s, 1H), 7.16–7.09 (m, 2H), 6.84–6.77 (m, 2H), 5.85 (d, $J = 6.4$, 1H), 4.68–4.51 (m, 3H), 4.25–4.20 (dd, $J = 5.1$, 2.5, 1H), 4.07 (q, $J = 2.3$, 1H), 3.78 (dd, $J = 12.6$, 2.5, 1H), 3.63 (dd, $J = 12.6$, 2.7, 1H), 2.24–1.98 (m, 2H), 1.85–1.54 (m, 4H), 1.14 (s, 9H). ^{13}C NMR: (75 MHz, methanol- d_4) δ 155.6, 154.4, 152.1, 147.9, 143.1, 140.1, 125.7, 120.0, 115.0, 90.0, 86.8, 82.5, 74.1, 71.3, 62.1, 57.0, 33.5, 30.6, 30.0, 29.7, 21.1. HRMS: (NSI+) m/z calcd for $C_{25}H_{34}N_5O_5 [M + H]^+$ 484.2568, found 484.2554. UPLC analysis: $t_R = 3.21$ min; peak area > 99% (detection at 254 nm).

(2*R*,3*S*,4*R*,5*R*)-2-(Hydroxymethyl)-5-(6-(((1*R*,2*R*)-2-(3-methoxyphenoxy)cyclopentyl)amino)-9*H*-purin-9-yl)-tetrahydrofuran-3,4-diol (**26**). **26** was synthesized according to general procedure E using **13** (0.12 mmol) and K_2CO_3 (0.072 mmol). The reaction was run for 30 min. After purification with flash column chromatography (EtOAc, 100%), **26** was obtained as a solid (36 mg, 0.079 mmol, 66%). 1H NMR: (300 MHz, DMSO- d_6) δ 8.38 (s, 1H), 8.23 (s, 1H), 8.10 (d, $J = 7.6$, 1H), 7.14 (t, $J = 8.1$, 1H), 6.57–6.42 (m, 3H), 5.89 (d, $J = 6.1$, 1H), 5.44 (d, $J = 6.2$, 1H), 5.41–5.35 (m,

1H), 5.19 (d, *J* = 4.7, 1H), 4.90–4.82 (m, 1H), 4.74–4.64 (m, 1H), 4.64–4.56 (m, 1H), 4.15 (q, *J* = 4.5, 1H), 3.99–3.94 (m, 1H), 3.73–3.64 (m, 1H), 3.68 (s, 3H), 3.60–3.51 (m, 1H), 2.23–2.09 (m, 2H), 1.87–1.62 (m, 4H). ¹³C NMR: (75 MHz, methanol-*d*₄) δ 160.9, 159.1, 154.4, 152.1, 140.1, 129.4, 120.0, 107.8, 105.9, 101.7, 90.0, 86.8, 82.6, 74.1, 71.3, 62.1, 57.1, 54.3, 29.9, 29.8, 21.1. HRMS: (NSI+) *m/z* calcd for C₂₂H₂₈N₅O₆ [M + H]⁺ 458.2030, found 458.2034. UPLC analysis: *t*_R = 2.50 min; peak area > 95% (detection at 254 nm).

(2*R*,3*R*,4*S*,5*R*)-2-(6-(((1*R*,2*R*)-2-(3-Bromophenoxy)cyclopentyl)-amino)-9*H*-purin-9-yl)-5-(hydroxymethyl)tetrahydrofuran-3,4-diol (**27**). **27** was synthesized according to general procedure G using **7** (0.12 mmol), **6f** (0.12 mmol), and NaHCO₃ (0.239 mmol). The reaction was heated at reflux for 18 h. After purification with flash column chromatography (EtOAc, 100%), a mixture of the substitution product and fully and semi-deacetylated products was isolated (40 mg). This mixture was dissolved in MeOH (5 mL), and K₂CO₃ (0.033 mmol) was added. After stirring for 30 min at room temperature, the reaction mixture was filtered and concentrated under reduced pressure. After purification with flash column chromatography (EtOAc, 100%), **27** was obtained as a solid (21 mg, 0.042 mmol, 35% over two steps). ¹H NMR (300 MHz, methanol-*d*₄) δ 8.24 (s, 1H), 8.16 (s, 1H), 7.49 (br s, 1H), 7.02 (t, *J* = 8.0, 1H), 6.96–6.82 (m, 2H), 5.86 (d, *J* = 6.4, 1H), 4.70–4.62 (m, 2H), 4.61–4.51 (m, 1H), 4.23 (dd, *J* = 5.1, 2.5, 1H), 4.09–4.05 (m, 1H), 3.79 (dd, *J* = 12.6, 2.5, 1H), 3.65 (dd, *J* = 12.5, 2.6, 1H), 2.23–1.97 (m, 2H), 1.90–1.58 (m, 4H). ¹³C NMR: (75 MHz, methanol-*d*₄) δ 158.9, 154.3, 152.2, 140.2, 130.3, 123.3, 122.3, 120.0, 118.4, 114.8, 90.0, 86.9, 82.8, 74.1, 71.3, 62.1, 56.6, 29.6, 29.4, 21.0. HRMS: (NSI+) *m/z* calcd for C₂₁H₂₅BrN₅O₅ [M + H]⁺ 506.1025, found 506.1034. UPLC analysis: *t*_R = 2.83 min; peak area > 95% (detection at 254 nm).

(2*R*,3*R*,4*S*,5*R*)-2-(6-(((1*R*,2*R*)-2-(2-Chlorophenoxy)cyclopentyl)-amino)-9*H*-purin-9-yl)-5-(hydroxymethyl)tetrahydrofuran-3,4-diol (**28**). **28** was synthesized according to general procedure G using **7** (0.322 mmol), **6h** (0.322 mmol), and NaHCO₃ (0.644 mmol). The reaction was heated at reflux for 18 h. The crude material was deacetylated using K₂CO₃ (0.193 mmol) in MeOH for 45 min at room temperature. After purification with flash column chromatography (EtOAc, 100%), **28** was obtained (29 mg, 0.063 mmol, 20% over two steps). ¹H NMR (300 MHz, methanol-*d*₄) δ 8.15 (s, 1H), 8.14 (s, 1H), 7.30–7.01 (m, 3H), 6.80–6.71 (m, 1H), 5.85 (d, *J* = 6.4, 1H), 4.76–4.72 (m, 1H), 4.70–4.60 (m, *J* = 6.4, 5.1, 2H), 4.22 (dd, *J* = 5.1, 2.5, 1H), 4.07 (q, *J* = 2.5, 1H), 3.79 (dd, *J* = 12.6, 2.5, 1H), 3.64 (dd, *J* = 12.6, 2.6, 1H), 2.31–2.19 (m, 1H), 2.13–2.00 (m, 1H), 1.93–1.75 (m, 3H), 1.70–1.57 (m, 1H). ¹³C NMR: (75 MHz, methanol-*d*₄) δ 154.4, 153.5, 152.1, 140.2, 129.8, 127.4, 123.2, 121.3, 120.0, 115.6, 89.9, 86.8, 83.8, 74.1, 71.3, 62.1, 56.9, 29.7, 29.6, 21.1. HRMS: (NSI+) *m/z* calcd for C₂₁H₂₅ClN₅O₅ [M + H]⁺ 462.1529, found 462.1539. UPLC analysis: *t*_R = 2.72 min; peak area > 99% (detection at 254 nm).

(2*R*,3*R*,4*S*,5*R*)-2-(6-(((1*R*,2*R*)-2-(3-Chlorophenoxy)cyclopentyl)-amino)-9*H*-purin-9-yl)-5-(hydroxymethyl)tetrahydrofuran-3,4-diol (**29**). **29** was synthesized according to general procedure G using **7** (0.234 mmol), **6i** (0.234 mmol), and NaHCO₃ (0.467 mmol). The reaction was heated at reflux for 18 h. The crude material was deacetylated using K₂CO₃ (0.138 mmol) in MeOH for 2 h at room temperature. After purification with flash column chromatography (MeOH/EtOAc, 6%), **29** was obtained (36 mg, 0.078 mmol, 33% over two steps). ¹H NMR: (300 MHz, DMSO-*d*₆) δ 8.39 (s, 1H), 8.27 (s, 1H), 8.09 (d, *J* = 7.1, 1H), 7.28 (t, *J* = 8.2, 2H), 7.00–6.91 (m, 2H), 5.90 (d, *J* = 6.1, 1H), 5.43 (d, *J* = 6.2, 1H), 5.41–5.34 (m, 1H), 5.19 (d, *J* = 4.7, 1H), 4.91–4.83 (m, 1H), 4.71–4.57 (m, 2H), 4.15 (q, *J* = 4.7, 2H), 4.00–3.95 (m, 1H), 3.73–3.64 (m, 1H), 3.61–3.51 (m, 1H), 2.22–2.07 (m, 2H), 1.88–1.64 (m, 4H). ¹³C NMR: (101 MHz, methanol-*d*₄) δ 158.9, 154.4, 152.1, 152.1, 140.2, 134.4, 130.0, 120.3, 120.0, 115.6, 114.3, 90.0, 86.8, 82.9, 74.1, 71.3, 62.1, 56.8, 29.6, 29.5, 21.0. HRMS: (NSI+) *m/z* calcd for C₂₁H₂₅ClN₅O₅ [M + H]⁺ 462.1543, found 462.1539. HPLC analysis: *t*_R = 7.16 min; peak area 94% (detection at 254 nm).

(2*R*,3*R*,4*S*,5*R*)-2-(6-(((1*R*,2*R*)-2-(4-Chlorophenoxy)cyclopentyl)-amino)-9*H*-purin-9-yl)-5-(hydroxymethyl)tetrahydrofuran-3,4-diol (**30**). **30** was synthesized according to general procedure E using **14** (0.325 mmol) and K₂CO₃ (0.195 mmol). The reaction was run for 45 min. After purification with flash column chromatography (MeOH/EtOAc, 10%), **30** was obtained as a solid (54 mg, 0.117 mmol, 36%). ¹H NMR: (300 MHz, DMSO-*d*₆) δ 8.38 (s, 1H), 8.25 (s, 1H), 8.08 (d, *J* = 7.5, 1H), 7.30 (d, *J* = 8.9, 2H), 7.03 (d, *J* = 8.3, 2H), 5.90 (d, *J* = 6.1, 1H), 5.43 (d, *J* = 6.0, 1H), 5.40–5.33 (m, 1H), 5.18 (d, *J* = 4.6, 1H), 4.87–4.80 (m, 1H), 4.74–4.56 (m, 2H), 4.15 (q, *J* = 4.2, 1H), 3.97 (dd, *J* = 9.9, 3.3, 2H), 3.72–3.63 (m, 1H), 3.59–3.50 (m, 1H), 2.24–2.06 (m, 2H), 1.88–1.60 (m, 4H). ¹³C NMR: (75 MHz, methanol-*d*₄) δ 156.7, 154.4, 152.1, 148.0, 140.2, 128.8, 125.2, 120.0, 116.9, 89.9, 86.8, 82.9, 74.1, 71.3, 62.1, 57.0, 29.7, 29.6, 21.0. HRMS: (NSI+) *m/z* calcd for C₂₁H₂₅ClN₅O₅ [M + H]⁺ 462.1525, found 462.1539. UPLC analysis: *t*_R = 2.81 min; peak area > 99% (detection at 254 nm).

(3*aS*,4*S*,6*R*,6*aR*)-*N*-Ethyl-6-(6-(((1*R*,2*R*)-2-(3-methoxybenzyl)oxy)cyclopentyl)amino)-9*H*-purin-9-yl)-2,2-dimethyltetrahydrofuro[3,4-*d*][1,3]dioxole-4-carboxamide (**32**). **32** was synthesized according to general procedure D using **31** (0.256 mmol), **3e** (0.256 mmol), and NaHCO₃ (0.698 mmol). The reaction was heated at reflux for 19 h. After purification with flash column chromatography (MeOH/EtOAc, 3%), **32** was obtained (92 mg, 0.166 mmol, 71%). ¹H NMR: (300 MHz, methanol-*d*₄) δ 8.25 (s, 1H), 8.17 (s, 1H), 7.16 (t, *J* = 8.1, 1H), 6.89–6.82 (m, 2H), 6.77–6.72 (m, 1H), 6.32 (d, *J* = 1.4, 1H), 5.60 (dd, *J* = 6.1, 1.9, 1H), 5.48 (dd, *J* = 6.1, 1.0, 1H), 4.72–4.57 (m, 1H), 4.63 (d, *J* = 1.9, 1H), 4.60 (s, 2H), 4.01–3.94 (m, 1H), 3.71 (s, 3H), 2.95–2.74 (m, 2H), 2.30–2.17 (m, 1H), 2.06–1.96 (m, 1H), 1.91–1.69 (m, 3H), 1.67–1.59 (m, 1H), 1.58 (s, 3H), 1.39 (s, 3H), 0.63 (t, *J* = 7.3, 3H). ¹³C NMR: (75 MHz, methanol-*d*₄) δ 170.0, 159.7, 154.3, 152.7, 148.3, 140.4, 140.3, 128.9, 119.5, 119.3, 113.5, 112.7, 112.5, 91.0, 87.2, 84.8, 83.8, 83.7, 70.7, 56.8, 54.2, 33.4, 30.2, 30.0, 25.8, 24.0, 21.1, 12.8. HRMS: (NSI+) *m/z* calcd for C₂₈H₃₇N₆O₆ [M + H]⁺ 553.2774, found 553.2769.

(3*aS*,4*S*,6*R*,6*aR*)-6-(6-(((1*R*,2*R*)-2-(3-Bromobenzyl)oxy)cyclopentyl)amino)-9*H*-purin-9-yl)-*N*-ethyl-2,2-dimethyltetrahydrofuro[3,4-*d*][1,3]dioxole-4-carboxamide (**33**). **33** was synthesized according to general procedure D using **31** (0.359 mmol), **3f** (0.326 mmol), and NaHCO₃ (0.978 mmol). The reaction was heated at reflux for 18 h. After purification with flash column chromatography (EtOAc, 100%), **33** was obtained (119 mg, 0.198 mmol, 55%). ¹H NMR: (300 MHz, methanol-*d*₄) δ 8.14 (s, 1H), 8.07 (s, 1H), 7.32 (br s, 1H), 7.23–6.97 (m, 3H), 6.20 (d, *J* = 1.6, 1H), 5.47 (dd, *J* = 6.1, 1.9, 1H), 5.39–5.32 (m, 1H), 4.62–4.42 (m, 4H), 3.87–3.80 (m, 1H), 2.85–2.65 (m, 2H), 2.17–2.02 (m, 1H), 1.94–1.82 (m, 1H), 1.77–1.56 (m, 3H), 1.55–1.46 (m, 1H), 1.45 (s, 3H), 1.27 (s, 3H), 0.52 (t, *J* = 7.3, 3H). ¹³C NMR: (75 MHz, methanol-*d*₄) δ 170.0, 154.2, 152.7, 148.2, 141.5, 140.5, 130.0, 130.0, 129.7, 125.8, 121.9, 119.3, 113.5, 91.0, 87.2, 85.0, 83.8, 83.7, 69.9, 56.7, 33.4, 30.2, 30.0, 25.8, 24.1, 21.1, 12.8. HRMS: (NSI+) *m/z* calcd for C₂₇H₃₄BrN₆O₅ [M + H]⁺ 601.1767, found 601.1796.

(3*aS*,4*S*,6*R*,6*aR*)-6-(6-(((1*R*,2*R*)-2-(4-Bromobenzyl)oxy)cyclopentyl)amino)-9*H*-purin-9-yl)-*N*-ethyl-2,2-dimethyltetrahydrofuro[3,4-*d*][1,3]dioxole-4-carboxamide (**34**). **34** was synthesized according to general procedure D using **31** (0.163 mmol), **3g** (0.163 mmol), and NaHCO₃ (0.489 mmol). The reaction was heated at reflux for 17 h. After purification with flash column chromatography (EtOAc, 100%), **34** was obtained (65 mg, 0.108 mmol, 66%). ¹H NMR: (300 MHz, methanol-*d*₄) δ 8.12 (s, 1H), 8.07 (s, 1H), 7.29–7.22 (m, 2H), 7.13–7.06 (m, 2H), 6.21 (d, *J* = 1.4, 1H), 5.49 (dd, *J* = 6.1, 1.9, 1H), 5.37 (dd, *J* = 6.1, 1.4, 1H), 4.60–4.42 (m, 4H), 3.90–3.82 (m, 1H), 2.84–2.63 (m, 2H), 2.18–2.04 (m, 1H), 1.98–1.83 (m, 1H), 1.76–1.56 (m, 3H), 1.54–1.42 (m, 1H), 1.46 (s, 3H), 1.28 (s, 3H), 0.51 (t, *J* = 7.3, 3H). ¹³C NMR: (75 MHz, methanol-*d*₄) δ 170.1, 154.2, 152.7, 148.3, 140.5, 138.1, 130.9, 129.1, 120.7, 119.3, 113.5, 91.0, 87.3, 85.0, 83.9, 83.7, 70.1, 56.7, 33.4, 30.2, 30.0, 25.7, 24.0, 21.1, 12.8. HRMS: (NSI+) *m/z* calcd for C₂₇H₃₄BrN₆O₅ [M + H]⁺ 601.1789, found 601.1769.

(3*aS*,4*S*,6*R*,6*aR*)-6-(6-(((1*R*,2*R*)-2-((2-Chlorobenzyl)oxy)cyclopentyl)amino)-9*H*-purin-9-yl)-*N*-ethyl-2,2-dimethyltetrahydrofuro[3,4-*d*][1,3]dioxole-4-carboxamide (35). 35 was synthesized according to general procedure D using 31 (0.221 mmol), 3h (0.221 mmol), and NaHCO₃ (0.663 mmol). The reaction was heated at reflux for 19 h. After purification with flash column chromatography (EtOAc/cHex, 90%), 35 was obtained (79 mg, 0.141 mmol, 64%). ¹H NMR: (300 MHz, methanol-*d*₄) δ 8.13 (s, 1H), 8.06 (s, 1H), 7.40–7.31 (m, 1H), 7.21–7.02 (m, 3H), 6.21 (d, *J* = 1.4, 1H), 5.48 (dd, *J* = 6.1, 1.9, 1H), 5.35 (dd, *J* = 6.1, 1.4, 1H), 4.69–4.52 (m, 3H), 4.51 (d, *J* = 1.9, 1H), 3.94–3.86 (m, 1H), 2.84–2.62 (m, 2H), 2.22–2.05 (m, 1H), 2.00–1.86 (m, 1H), 1.85–1.58 (m, 3H), 1.57–1.45 (m, 1H), 1.45 (s, 3H), 1.27 (s, 3H), 0.51 (t, *J* = 7.3, 3H). ¹³C NMR: (75 MHz, methanol-*d*₄) δ 170.1, 154.2, 152.7, 148.3, 140.5, 136.3, 132.4, 128.9, 128.8, 128.4, 126.5, 119.3, 113.5, 91.0, 87.2, 85.4, 83.8, 83.7, 68.1, 56.9, 33.4, 30.2, 30.0, 25.7, 24.0, 21.2, 12.8. HRMS: (NSI+) *m/z* calcd for C₂₇H₃₄ClN₆O₅ [M + H]⁺ 557.2265, found 557.2274.

(3*aS*,4*S*,6*R*,6*aR*)-6-(6-(((1*R*,2*R*)-2-((3-Chlorobenzyl)oxy)cyclopentyl)amino)-9*H*-purin-9-yl)-*N*-ethyl-2,2-dimethyltetrahydrofuro[3,4-*d*][1,3]dioxole-4-carboxamide (36). 36 was synthesized according to general procedure D using 31 (0.305 mmol), 3i (0.305 mmol), and NaHCO₃ (0.915 mmol). The reaction was heated at reflux for 18 h. After purification with flash column chromatography (EtOAc, 100%), 36 was obtained (115 mg, 0.206 mmol, 68%). ¹H NMR: (300 MHz, methanol-*d*₄) δ 8.26 (s, 1H), 8.19 (s, 1H), 7.30 (br s, 1H), 7.27–7.14 (m, 3H), 6.33 (d, *J* = 1.5, 1H), 5.60 (dd, *J* = 6.1, 1.9, 1H), 5.48 (dd, *J* = 6.1, 1.5, 1H), 4.72–4.57 (m, 4H), 4.00–3.93 (m, 1H), 2.98–2.75 (m, 2H), 2.30–2.17 (m, 1H), 2.08–1.96 (m, 1H), 1.92–1.59 (m, 4H), 1.57 (s, 3H), 1.39 (s, 3H), 0.64 (t, *J* = 7.3, 3H). ¹³C NMR: (75 MHz, methanol-*d*₄) δ 170.0, 154.2, 152.7, 148.2, 141.3, 140.5, 133.7, 129.4, 127.1, 127.0, 125.4, 119.3, 113.5, 91.0, 87.2, 85.0, 83.8, 83.7, 70.0, 56.8, 33.4, 30.2, 29.9, 25.8, 24.0, 21.1, 12.8. HRMS: (NSI+) *m/z* calcd for C₂₇H₃₄ClN₆O₅ [M + H]⁺ 557.2277, found 557.2274.

(3*aS*,4*S*,6*R*,6*aR*)-*N*-Ethyl-2,2-dimethyl-6-(6-(((1*R*,2*R*)-2-phenoxy)cyclopentyl)amino)-9*H*-purin-9-yl)tetrahydrofuro[3,4-*d*][1,3]dioxole-4-carboxamide (37). 37 was synthesized according to general procedure D using 31 (0.234 mmol), 6a (0.234 mmol), and NaHCO₃ (0.702 mmol). The reaction was heated at reflux for 18 h. After purification with flash column chromatography (EtOAc, 100%), 37 was obtained (90 mg, 0.176 mmol, 75%). ¹H NMR: (300 MHz, methanol-*d*₄) δ 8.25 (s, 1H), 8.18 (s, 1H), 7.26–7.17 (m, 2H), 7.05–6.94 (m, 2H), 6.86 (t, *J* = 7.3, 1H), 6.32 (d, *J* = 1.4, 1H), 5.60 (dd, *J* = 6.1, 2.0, 1H), 5.47 (dd, *J* = 6.0, 1.2, 1H), 4.82–4.68 (m, 2H), 4.63 (d, *J* = 1.9, 1H), 2.97–2.74 (m, 2H), 2.35–2.12 (m, 2H), 1.97–1.64 (m, 4H), 1.57 (s, 3H), 1.39 (s, 3H), 0.62 (t, *J* = 7.3, 3H). ¹³C NMR: (75 MHz, methanol-*d*₄) δ 170.0, 157.9, 154.3, 152.6, 148.6, 140.6, 129.0, 120.3, 119.3, 115.4, 113.5, 91.0, 87.2, 83.8, 83.7, 82.4, 57.1, 33.4, 30.0, 29.7, 25.8, 24.1, 21.1, 12.8. HRMS: (NSI+) *m/z* calcd for C₂₆H₃₃N₆O₅ [M + H]⁺ 509.2505, found 509.2507.

(3*aS*,4*S*,6*R*,6*aR*)-6-(6-(((1*R*,2*R*)-2-(4-(*tert*-Butyl)phenoxy)cyclopentyl)amino)-9*H*-purin-9-yl)-*N*-ethyl-2,2-dimethyltetrahydrofuro[3,4-*d*][1,3]dioxole-4-carboxamide (38). 38 was synthesized according to general procedure D using 31 (0.185 mmol), 6c (0.185 mmol), and NaHCO₃ (0.556 mmol). The reaction was heated at reflux for 18 h. After purification with flash column chromatography (EtOAc, 100%), 38 was obtained (58 mg, 0.103 mmol, 56%). ¹H NMR: (300 MHz, methanol-*d*₄) δ 8.12 (s, 1H), 8.07 (s, 1H), 7.12 (d, *J* = 8.8, 2H), 6.78 (d, *J* = 8.8, 2H), 6.21 (d, *J* = 1.4, 1H), 5.49 (dd, *J* = 6.1, 2.0, 1H), 5.36 (dd, *J* = 6.1, 1.4, 1H), 4.67–4.54 (m, 2H), 4.51 (d, *J* = 1.9, 1H), 2.82–2.62 (m, 2H), 2.22–2.02 (m, 2H), 1.87–1.51 (m, 4H), 1.46 (s, 3H), 1.28 (s, 3H), 1.14 (s, 9H), 0.50 (t, *J* = 7.3, 3H). ¹³C NMR: (75 MHz, methanol-*d*₄) δ 170.1, 155.6, 154.3, 152.6, 148.4, 143.1, 140.6, 125.7, 119.3, 114.9, 113.5, 91.0, 87.3, 83.9, 83.71, 82.5, 57.2, 33.5, 33.4, 30.6, 30.1, 29.8, 25.7, 24.0, 21.1, 12.7.

(3*aS*,4*S*,6*R*,6*aR*)-*N*-Ethyl-6-(6-(((1*R*,2*R*)-2-(3-methoxyphenoxy)cyclopentyl)amino)-9*H*-purin-9-yl)-2,2-dimethyltetrahydrofuro[3,4-*d*][1,3]dioxole-4-carboxamide (39). 39 was synthesized according to general procedure D using 31 (0.27 mmol), 6e (0.27 mmol),

and NaHCO₃ (0.738 mmol). The reaction was heated at reflux for 18 h. After purification with flash column chromatography (EtOAc, 100%), 39 was obtained (92 mg, 0.166 mmol, 71%). ¹H NMR: (300 MHz, methanol-*d*₄) δ 8.25 (s, 1H), 8.18 (s, 1H), 7.09 (t, *J* = 8.2, 1H), 6.64–6.53 (m, 2H), 6.48–6.41 (m, 1H), 6.32 (d, *J* = 1.4, 1H), 5.60 (dd, *J* = 6.1, 1.9, 1H), 5.48 (dd, *J* = 6.1, 1.4, 1H), 4.80–4.66 (m, 2H), 4.63 (d, *J* = 1.9, 1H), 3.72 (s, 3H), 2.95–2.74 (m, 2H), 2.34–2.11 (m, 2H), 1.98–1.63 (m, 4H), 1.57 (s, 3H), 1.40 (s, 3H), 0.63 (t, *J* = 7.3, 3H). ¹³C NMR: (75 MHz, methanol-*d*₄) δ 170.0, 160.9, 159.1, 154.3, 152.6, 148.4, 140.6, 129.4, 119.3, 113.5, 107.7, 105.9, 101.7, 91.0, 87.2, 83.8, 83.7, 82.5, 57.3, 54.3, 33.4, 30.0, 29.8, 25.7, 24.0, 21.1, 12.7. HRMS: (NSI+) *m/z* calcd for C₂₇H₃₅N₆O₆ [M + H]⁺ 539.2598, found 539.2613.

(3*aS*,4*S*,6*R*,6*aR*)-6-(6-(((1*R*,2*R*)-2-(3-Bromophenoxy)cyclopentyl)amino)-9*H*-purin-9-yl)-*N*-ethyl-2,2-dimethyltetrahydrofuro[3,4-*d*][1,3]dioxole-4-carboxamide (40). 40 was synthesized according to general procedure D using 31 (0.109 mmol), 6f (0.109 mmol), and NaHCO₃ (0.218 mmol). The reaction was heated at reflux for 18 h. After purification with flash column chromatography (EtOAc, 100%), 40 was obtained (47 mg, 0.081 mmol, 73%). ¹H NMR: (300 MHz, methanol-*d*₄) δ 8.54 (s, 1H), 8.40 (s, 1H), 7.77 (br s, 1H), 7.32 (t, *J* = 8.0, 1H), 7.25–7.12 (m, 2H), 6.53 (d, *J* = 1.4, 1H), 5.81 (dd, *J* = 6.1, 2.0, 1H), 5.68 (dd, *J* = 6.1, 1.4, 1H), 4.99–4.93 (m, 1H), 4.92–4.80 (m, 1H), 4.83 (d, *J* = 1.9, 1H), 3.15–2.94 (m, 2H), 2.53–2.31 (m, 2H), 2.21–1.85 (m, 4H), 1.78 (s, 3H), 1.60 (s, 3H), 0.83 (t, *J* = 7.3, 3H). ¹³C NMR: (75 MHz, methanol-*d*₄) δ 170.1, 158.9, 154.2, 152.7, 148.5, 140.7, 130.3, 123.3, 122.3, 119.3, 118.4, 114.76, 113.5, 91.1, 87.3, 83.9, 83.7, 82.8, 56.7, 33.4, 29.6, 29.5, 25.7, 24.0, 21.0, 12.7. HRMS: (NSI+) *m/z* calcd for C₂₆H₃₂BrN₆O₅ [M + H]⁺ 587.1595, found 587.1612.

(3*aS*,4*S*,6*R*,6*aR*)-6-(6-(((1*R*,2*R*)-2-(2-Chlorophenoxy)cyclopentyl)amino)-9*H*-purin-9-yl)-*N*-ethyl-2,2-dimethyltetrahydrofuro[3,4-*d*][1,3]dioxole-4-carboxamide (41). 41 was synthesized according to general procedure D using 31 (0.282 mmol), 6h (0.282 mmol), and NaHCO₃ (0.846 mmol). The reaction was heated at reflux for 19 h. After purification with flash column chromatography (EtOAc, 100%), 41 was obtained (114 mg, 0.21 mmol, 74%). ¹H NMR: (300 MHz, methanol-*d*₄) δ 8.25 (s, 1H), 8.19 (s, 1H), 7.52 (t, *J* = 5.8, 1H), 7.35–7.26 (m, 2H), 7.23–7.16 (m, 1H), 6.91–6.81 (m, 1H), 6.33 (d, *J* = 1.4, 1H), 5.60 (dd, *J* = 6.1, 1.9, 1H), 5.48 (dd, *J* = 6.1, 1.4, 1H), 4.86–4.80 (m, 1H), 4.80–4.66 (m, 1H), 4.63 (d, *J* = 1.9, 1H), 2.96–2.75 (m, 2H), 2.40–2.27 (m, 1H), 2.23–2.11 (m, 1H), 2.00–1.83 (m, 3H), 1.80–1.65 (m, 1H), 1.57 (s, 3H), 1.39 (s, 3H), 0.63 (t, *J* = 7.3, 3H). ¹³C NMR: (75 MHz, methanol-*d*₄) δ 170.0, 154.2, 153.5, 152.6, 148.4, 140.6, 129.8, 127.5, 123.2, 121.3, 119.3, 115.5, 113.5, 91.0, 87.2, 83.8, 83.8, 83.7, 57.0, 33.4, 29.8, 29.7, 25.8, 24.0, 21.1, 12.8. HRMS: (NSI+) *m/z* calcd for C₂₆H₃₂ClN₆O₅ [M + H]⁺ 543.2106, found 543.2117.

(3*aS*,4*S*,6*R*,6*aR*)-6-(6-(((1*R*,2*R*)-2-(3-Chlorophenoxy)cyclopentyl)amino)-9*H*-purin-9-yl)-*N*-ethyl-2,2-dimethyltetrahydrofuro[3,4-*d*][1,3]dioxole-4-carboxamide (42). 42 was synthesized according to general procedure D using 31 (0.243 mmol), 6i (0.243 mmol), and NaHCO₃ (0.73 mmol). The reaction was heated at reflux for 19 h. After purification with flash column chromatography (EtOAc, 100%), 42 was obtained (101 mg, 0.186 mmol, 78%). ¹H NMR: (300 MHz, methanol-*d*₄) δ 8.31 (s, 1H), 8.20 (s, 1H), 7.38 (br s, 1H), 7.17 (t, *J* = 8.1, 1H), 6.99–6.84 (m, 2H), 6.33 (d, *J* = 1.5, 1H), 5.61 (dd, *J* = 6.1, 2.0, 1H), 5.48 (dd, *J* = 6.0, 1.5, 1H), 4.80–4.72 (m, 1H), 4.71–4.59 (m, 2H), 2.97–2.74 (m, 2H), 2.34–2.09 (m, 2H), 2.00–1.65 (m, 4H), 1.58 (s, 3H), 1.40 (s, 3H), 0.64 (t, *J* = 7.3, 3H). ¹³C NMR: (75 MHz, methanol-*d*₄) δ 170.0, 158.9, 154.2, 152.6, 148.4, 140.6, 134.4, 130.0, 120.3, 119.3, 115.6, 114.2, 113.5, 91.1, 87.2, 83.8, 83.7, 82.8, 56.8, 33.4, 29.6, 29.5, 25.8, 24.0, 21.0, 12.8. HRMS: (NSI+) *m/z* calcd for C₂₆H₃₂ClN₆O₅ [M + H]⁺ 543.2123, found 543.2117.

(3*aS*,4*S*,6*R*,6*aR*)-6-(6-(((1*R*,2*R*)-2-(4-Chlorophenoxy)cyclopentyl)amino)-9*H*-purin-9-yl)-*N*-ethyl-2,2-dimethyltetrahydrofuro[3,4-*d*][1,3]dioxole-4-carboxamide (43). 43 was synthesized according to general procedure D using 31 (0.35 mmol), 6j (0.35 mmol), and NaHCO₃ (1.052 mmol). The reaction was heated at reflux for 20 h. After purification with flash column chromatography (EtOAc, 100%), 43 was obtained (118 mg, 0.217 mmol, 65%). ¹H NMR: (300 MHz,

methanol- d_4) δ 8.25 (s, 1H), 8.19 (s, 1H), 7.21–7.12 (m, 2H), 7.05–6.97 (m, 2H), 6.32 (d, J = 1.4, 1H), 5.60 (dd, J = 6.1, 2.0, 1H), 5.47 (dd, J = 6.1, 1.5, 1H), 4.77–4.65 (m, 2H), 4.63 (d, J = 1.9, 1H), 2.95–2.76 (m, 2H), 2.32–2.11 (m, 2H), 1.97–1.65 (m, 4H), 1.57 (s, 3H), 1.39 (s, 3H), 0.63 (t, J = 7.2, 3H). ^{13}C NMR: (75 MHz, methanol- d_4) δ 170.0, 156.7, 154.2, 152.6, 148.4, 140.6, 128.8, 125.1, 119.3, 116.9, 113.5, 91.0, 87.2, 83.8, 83.7, 82.8, 57.0, 33.39, 29.8, 29.6, 25.8, 24.1, 21.0, 12.8. HRMS: (NSI+) m/z calcd for $\text{C}_{26}\text{H}_{32}\text{ClN}_6\text{O}_5$ [$\text{M} + \text{H}$] $^+$ 543.2109, found 543.2117.

(2*S*,3*S*,4*R*,5*R*)-*N*-Ethyl-3,4-dihydroxy-5-(6-(((1*R*,2*R*)-2-((3-methoxybenzyl)oxy)cyclopentyl)amino)-9*H*-purin-9-yl)-tetrahydrofuran-2-carboxamide (**44**). **44** was synthesized according to general procedure F using **32** (0.075 mmol) and acetic acid (4 mL). The reaction was run for 23 h. After purification with flash column chromatography (MeOH/ CH_2Cl_2 , 6%), **44** was obtained (23 mg, 0.046 mmol, 60%). ^1H NMR: (300 MHz, methanol- d_4) δ 8.20 (s, 1H), 8.13 (s, 1H), 7.04 (t, J = 8.0, 1H), 6.79–6.72 (m, 2H), 6.68–6.62 (m, 1H), 5.90 (d, J = 7.7, 1H), 4.65 (dd, J = 7.7, 4.8, 1H), 4.62–4.52 (m, 1H), 4.51 (s, 2H), 4.37 (d, J = 1.5, 1H), 4.21 (dd, J = 4.8, 1.6, 1H), 3.92–3.85 (m, 1H), 3.60 (s, 3H), 3.32–3.23 (m, 2H), 2.20–2.07 (m, 1H), 1.98–1.82 (m, 1H), 1.79–1.46 (m, 4H), 1.10 (t, J = 7.3, 3H). ^{13}C NMR: (75 MHz, methanol- d_4) δ 170.7, 159.8, 154.4, 152.4, 148.1, 140.6, 140.3, 128.9, 120.1, 119.5, 112.7, 112.6, 89.2, 85.1, 84.8, 73.6, 72.0, 70.8, 58.8, 54.2, 33.7, 30.1, 30.0, 21.1, 13.7. HRMS: (NSI+) m/z calcd for $\text{C}_{25}\text{H}_{33}\text{N}_6\text{O}_6$ [$\text{M} + \text{H}$] $^+$ 513.2441, found 513.2456. UPLC analysis: t_R = 2.59 min; peak area > 99% (detection at 254 nm).

(2*S*,3*S*,4*R*,5*R*)-5-(6-(((1*R*,2*R*)-2-((3-bromobenzyl)oxy)cyclopentyl)amino)-9*H*-purin-9-yl)-*N*-ethyl-3,4-dihydroxytetrahydrofuran-2-carboxamide (**45**). **45** was synthesized according to general procedure F using **33** (0.196 mmol) and acetic acid (16 mL). The reaction was run for 18 h. After purification with flash column chromatography (MeOH/ CH_2Cl_2 , 2%), **45** was obtained (69 mg, 0.123 mmol, 63%). ^1H NMR: (300 MHz, methanol- d_4) δ 8.33 (s, 1H), 8.25 (s, 1H), 7.46 (br s, 1H), 7.37–7.07 (m, 3H), 6.02 (d, J = 7.7, 1H), 4.77 (dd, J = 7.7, 4.8, 1H), 4.71–4.55 (m, 1H), 4.61 (s, 3H), 4.50 (d, J = 1.5, 1H), 4.38–4.28 (m, 1H), 3.42–3.28 (m, 2H), 2.29–2.10 (m, 1H), 1.87–1.59 (m, 4H), 1.21 (t, J = 7.3, 3H). ^{13}C NMR: (75 MHz, methanol- d_4) δ 174.0, 154.4, 152.4, 147.9, 141.5, 140.7, 130.1, 130.0, 129.7, 125.8, 121.9, 120.1, 113.6, 89.2, 85.1, 73.6, 72.1, 70.0, 56.8, 33.7, 30.1, 29.9, 19.5, 13.8. HRMS: (NSI+) m/z calcd for $\text{C}_{24}\text{H}_{30}\text{BrN}_6\text{O}_5$ [$\text{M} + \text{H}$] $^+$ 561.1439, found 561.1456. UPLC analysis: t_R = 2.97 min; peak area > 95% (detection at 254 nm).

(2*S*,3*S*,4*R*,5*R*)-5-(6-(((1*R*,2*R*)-2-((4-bromobenzyl)oxy)cyclopentyl)amino)-9*H*-purin-9-yl)-*N*-ethyl-3,4-dihydroxytetrahydrofuran-2-carboxamide (**46**). **46** was synthesized according to general procedure F using **34** (0.108 mmol) and acetic acid (8 mL). The reaction was run for 20 h. After purification with flash column chromatography (MeOH/ CH_2Cl_2 , 10%), **46** was obtained (36 mg, 0.064 mmol, 64%). ^1H NMR: (300 MHz, methanol- d_4) δ 8.19 (s, 1H), 8.14 (s, 1H), 7.28 (d, J = 8.4, 2H), 7.10 (d, J = 8.3, 2H), 5.90 (d, J = 7.7, 1H), 4.65 (dd, J = 7.7, 4.8, 1H), 4.62–4.46 (m, 1H), 4.49 (s, 2H), 4.37 (d, J = 1.5, 1H), 4.21 (dd, J = 4.8, 1.6, 1H), 3.92–3.82 (m, 1H), 3.32–3.21 (m, 2H), 2.20–2.06 (m, 1H), 1.97–1.84 (m, 1H), 1.78–1.58 (m, 3H), 1.58–1.45 (m, 1H), 1.10 (t, J = 7.3, 3H). ^{13}C NMR: (75 MHz, methanol- d_4) δ 170.7, 154.4, 152.4, 148.1, 140.7, 138.1, 130.9, 129.1, 120.7, 120.1, 89.2, 85.1, 85.0, 73.6, 72.0, 70.1, 56.9, 33.7, 30.1, 30.0, 21.1, 13.7. HRMS: (NSI+) m/z calcd for $\text{C}_{24}\text{H}_{30}\text{BrN}_6\text{O}_5$ [$\text{M} + \text{H}$] $^+$ calculated 561.1458, found 561.1456. UPLC analysis: t_R = 2.94 min; peak area > 99% (detection at 254 nm).

(2*S*,3*S*,4*R*,5*R*)-5-(6-(((1*R*,2*R*)-2-((2-chlorobenzyl)oxy)cyclopentyl)amino)-9*H*-purin-9-yl)-*N*-ethyl-3,4-dihydroxytetrahydrofuran-2-carboxamide (**47**). **47** was synthesized according to general procedure F using **35** (0.141 mmol) and acetic acid (15 mL). The reaction was run for 19 h. After purification with flash column chromatography (MeOH/ CH_2Cl_2 , 8%), **47** was obtained (33 mg, 0.069 mmol, 49%). ^1H NMR: (300 MHz, DMSO- d_6) δ 8.90 (t, J = 5.6, 1H), 8.42 (s, 1H), 8.29 (s, 1H), 8.07 (br s, 1H), 7.50–7.45 (m, 1H), 7.43–7.38 (m, 1H), 7.33–7.27 (m, 2H), 5.98 (d, J = 7.5, 1H), 5.75 (d, J = 4.3, 1H), 5.54 (d, J = 6.5, 1H), 4.75–4.58 (m, 4H), 4.32

(d, J = 1.5, 1H), 4.18–4.12 (m, 1H), 4.10–4.03 (m, 1H), 3.28–3.17 (m, 2H), 2.15–1.94 (m, 2H), 1.84–1.59 (m, 4H), 1.09 (t, J = 7.2, 3H). ^{13}C NMR (101 MHz, DMSO- d_6) δ 169.6, 154.7, 152.6, 148.8, 141.0, 136.8, 132.3, 129.6, 129.5, 129.4, 127.6, 120.5, 88.3, 85.3, 85.1, 73.6, 72.5, 68.0, 56.9, 33.8, 30.8, 30.7, 22.0, 15.2. HRMS: (NSI+) m/z calcd for $\text{C}_{24}\text{H}_{30}\text{ClN}_6\text{O}_5$ [$\text{M} + \text{H}$] $^+$ calculated 517.1943, found 517.1961. UPLC analysis: t_R = 2.82 min; peak area > 99% (detection at 254 nm).

(2*S*,3*S*,4*R*,5*R*)-5-(6-(((1*R*,2*R*)-2-((3-chlorobenzyl)oxy)cyclopentyl)amino)-9*H*-purin-9-yl)-*N*-ethyl-3,4-dihydroxytetrahydrofuran-2-carboxamide (**48**). **48** was synthesized according to general procedure F using **36** (0.206 mmol) and acetic acid (16 mL). The reaction was run for 20 h. After purification with flash column chromatography (MeOH/ CH_2Cl_2 , 8%), **48** was obtained (64 mg, 0.123 mmol, 60%). ^1H NMR: (300 MHz, methanol- d_4) δ 8.32 (s, 1H), 8.24 (s, 1H), 7.32 (br s, 1H), 7.27–7.14 (m, 3H), 6.02 (d, J = 7.7, 1H), 4.77 (dd, J = 7.7, 4.8, 1H), 4.70–4.60 (m, 1H), 4.62 (s, 2H), 4.50 (d, J = 1.5, 1H), 4.34 (dd, J = 4.8, 1.6, 1H), 4.01–3.94 (m, 1H), 3.43–3.29 (m, 2H), 2.31–2.15 (m, 1H), 2.07–1.94 (m, 1H), 1.90–1.58 (m, 4H), 1.21 (t, J = 7.3, 3H). ^{13}C NMR (75 MHz, methanol- d_4) δ 170.6, 154.4, 152.4, 148.0, 141.3, 140.7, 133.7, 129.3, 127.1, 127.0, 125.3, 120.1, 89.2, 85.1, 73.6, 72.0, 70.0, 56.8, 33.7, 30.1, 29.9, 21.1, 13.8. HRMS: (NSI+) m/z calcd for $\text{C}_{24}\text{H}_{30}\text{ClN}_6\text{O}_5$ [$\text{M} + \text{H}$] $^+$ 517.1956, found 517.1961. UPLC analysis: t_R = 2.87 min; peak area > 99% (detection at 254 nm).

(2*S*,3*S*,4*R*,5*R*)-*N*-Ethyl-3,4-dihydroxy-5-(6-(((1*R*,2*R*)-2-phenoxycyclopentyl)amino)-9*H*-purin-9-yl)tetrahydrofuran-2-carboxamide (**49**). **49** was synthesized according to general procedure F using **37** (0.175 mmol) and acetic acid (16 mL). The reaction was run for 23 h. After purification with flash column chromatography (MeOH/ CH_2Cl_2 , 7%), **49** was obtained (56 mg, 0.12 mmol, 68%). ^1H NMR: (300 MHz, methanol- d_4) δ 8.31 (s, 1H), 8.25 (s, 1H), 7.26–7.16 (m, 2H), 7.05–6.96 (m, 2H), 6.87 (t, J = 7.3, 1H), 6.02 (d, J = 7.7, 1H), 4.83–4.66 (m, 3H), 4.49 (d, J = 1.6, 1H), 4.37–4.30 (m, 1H), 3.42–3.31 (m, 2H), 2.39–2.13 (m, 2H), 2.02–1.65 (m, 4H), 1.20 (t, J = 7.3, 3H). ^{13}C NMR: (75 MHz, methanol- d_4) δ 170.6, 157.9, 154.5, 152.4, 148.2, 140.8, 129.0, 120.3, 120.2, 115.4, 89.2, 85.1, 82.5, 73.6, 72.0, 57.1, 33.7, 29.9, 29.7, 21.1, 13.7. HRMS: (NSI+) m/z calcd for $\text{C}_{23}\text{H}_{29}\text{N}_6\text{O}_5$ [$\text{M} + \text{H}$] $^+$ 469.2186, found 469.2194. UPLC analysis: t_R = 2.77 min; peak area > 99% (detection at 254 nm).

(2*S*,3*S*,4*R*,5*R*)-5-(6-(((1*R*,2*R*)-2-(4-(*tert*-butyl)phenoxy)cyclopentyl)amino)-9*H*-purin-9-yl)-*N*-ethyl-3,4-dihydroxytetrahydrofuran-2-carboxamide (**50**). **50** was synthesized according to general procedure F using **38** (0.103 mmol) and acetic acid (8 mL). The reaction was run for 19 h. After purification with flash column chromatography (MeOH/ CH_2Cl_2 , 7%), **50** was obtained (31 mg, 0.059 mmol, 57%). ^1H NMR (300 MHz, DMSO- d_6) δ 8.88 (t, J = 5.6, 1H), 8.43 (s, 1H), 8.30 (s, 1H), 8.17 (d, J = 6.5, 1H), 7.26 (d, J = 8.8, 2H), 6.87 (d, J = 8.3, 2H), 5.98 (d, J = 7.5, 1H), 5.75 (d, J = 4.3, 1H), 5.54 (d, J = 6.5, 1H), 4.88–4.77 (m, 1H), 4.70–4.57 (m, 2H), 4.32 (d, J = 1.6, 1H), 4.17–4.12 (m, 1H), 3.27–3.18 (m, 2H), 2.22–1.97 (m, 2H), 1.87–1.63 (m, 4H), 1.23 (s, 9H), 1.09 (t, J = 7.2, 3H); (300 MHz, methanol- d_4) δ 8.20 (s, 1H), 8.14 (s, 1H), 7.19–7.10 (m, 2H), 6.85–6.73 (m, 2H), 5.90 (d, J = 7.7, 1H), 4.70–4.56 (m, 3H), 4.36 (d, J = 1.6, 1H), 4.21 (dd, J = 4.9, 1.6, 1H), 3.31–3.21 (m, 2H), 2.24–2.02 (m, 2H), 1.90–1.54 (m, 4H), 1.15 (s, 9H), 1.09 (t, J = 7.3, 3H). ^{13}C NMR: (75 MHz, methanol- d_4) δ 170.6, 155.6, 154.5, 152.4, 148.1, 143.1, 140.7, 125.7, 120.2, 115.0, 89.2, 85.1, 82.6, 73.6, 72.0, 57.1, 33.7, 33.5, 30.6, 30.0, 29.8, 21.1, 13.7. HRMS: (NSI+) m/z calcd for $\text{C}_{27}\text{H}_{37}\text{N}_6\text{O}_5$ [$\text{M} + \text{H}$] $^+$ 525.2816, found 525.2820. UPLC analysis: t_R = 3.44 min; peak area > 99% (detection at 254 nm).

(2*S*,3*S*,4*R*,5*R*)-*N*-Ethyl-3,4-dihydroxy-5-(6-(((1*R*,2*R*)-2-(3-methoxyphenoxy)cyclopentyl)amino)-9*H*-purin-9-yl)-tetrahydrofuran-2-carboxamide (**51**). **51** was synthesized according to general procedure F using **39** (0.231 mmol) and acetic acid (16 mL). The reaction was run for 22 h. After purification with flash column chromatography (MeOH/ CH_2Cl_2 , 8%), **51** was obtained (49 mg, 0.099 mmol, 43%). ^1H NMR: (300 MHz, DMSO- d_6) δ 8.87 (t, J = 5.7, 1H), 8.43 (s, 1H), 8.29 (s, 1H), 8.20 (d, J = 7.6, 1H), 7.14 (t, J

= 8.1, 1H), 6.59–6.43 (m, 3H), 5.98 (d, $J = 7.5$, 1H), 5.75 (d, $J = 4.3$, 1H), 5.54 (d, $J = 6.4$, 1H), 4.93–4.84 (m, 1H), 4.76–4.54 (m, 2H), 4.32 (d, $J = 1.6$, 1H), 4.18–4.13 (m, 1H), 3.28–3.20 (m, 2H), 2.25–2.06 (m, 2H), 1.88–1.60 (m, 4H), 1.09 (t, $J = 7.2$, 3H). ^{13}C NMR: (75 MHz, methanol- d_4) δ 170.6, 160.9, 159.1, 154.4, 152.4, 148.1, 140.7, 129.4, 120.2, 107.74, 105.9, 101.7, 89.2, 85.1, 82.6, 73.6, 72.0, 57.1, 54.3, 33.7, 29.9, 29.8, 21.1, 13.7. HRMS: (NSI+) m/z calcd for $\text{C}_{24}\text{H}_{31}\text{N}_6\text{O}_6$ [M + H] $^+$ 499.2296, found 499.2300. UPLC analysis: $t_R = 2.78$ min; peak area > 99% (detection at 254 nm).

(2*S*,3*S*,4*R*,5*R*)-5-(6-(((1*R*,2*R*)-2-(3-Bromophenoxy)cyclopentyl)amino)-9*H*-purin-9-yl)-*N*-ethyl-3,4-dihydroxytetrahydrofuran-2-carboxamide (**52**). **52** was synthesized according to general procedure F using **40** (0.07 mmol) and acetic acid (4 mL). The reaction was run for 18 h. After purification with flash column chromatography (MeOH/CH₂Cl₂, 8%), **52** was obtained (28 mg, 0.052 mmol, 74%). ^1H NMR: (300 MHz, methanol- d_4) δ 8.30 (s, 1H), 8.15 (s, 1H), 7.50 (br s, 1H), 7.01 (t, $J = 8.0$, 1H), 6.94–6.82 (m, 2H), 5.90 (d, $J = 7.7$, 1H), 4.70–4.61 (m, 2H), 4.60–4.48 (m, 1H), 4.36 (d, $J = 1.5$, 1H), 4.25–4.18 (m, 1H), 3.30–3.21 (m, 2H), 2.22–1.98 (m, 2H), 1.93–1.80 (m, 2H), 1.80–1.59 (m, 2H), 1.10 (t, $J = 7.3$, 3H). ^{13}C NMR: (75 MHz, methanol- d_4) δ 170.6, 158.9, 154.4, 152.4, 148.2, 140.8, 130.3, 123.3, 122.3, 118.4, 114.8, 89.2, 85.1, 82.6, 73.6, 72.1, 56.7, 33.7, 29.6, 29.4, 21.0, 13.7. HRMS: (NSI+) m/z calcd for $\text{C}_{23}\text{H}_{28}\text{BrN}_6\text{O}_5$ [M + H] $^+$ 547.1295, found 547.1299. UPLC analysis: $t_R = 3.17$ min; peak area > 99% (detection at 254 nm).

(2*S*,3*S*,4*R*,5*R*)-5-(6-(((1*R*,2*R*)-2-(2-Chlorophenoxy)cyclopentyl)amino)-9*H*-purin-9-yl)-*N*-ethyl-3,4-dihydroxytetrahydrofuran-2-carboxamide (**53**). **53** was synthesized according to general procedure F using **41** (0.21 mmol) and acetic acid (16 mL). The reaction was run for 19 h. After purification with flash column chromatography (MeOH/CH₂Cl₂, 8%), **53** was obtained (55 mg, 0.109 mmol, 52%). ^1H NMR: (300 MHz, DMSO- d_6) δ 8.87 (t, $J = 5.6$, 1H), 8.43 (s, 1H), 8.30 (s, 1H), 8.20 (br s, 1H), 7.42–7.24 (m, 3H), 6.97–6.87 (m, 1H), 5.98 (d, $J = 7.5$, 1H), 5.75 (d, $J = 4.3$, 1H), 5.54 (d, $J = 6.4$, 1H), 4.97–4.90 (m, 1H), 4.77–4.66 (m, 1H), 4.66–4.57 (m, 1H), 4.32 (d, $J = 1.6$, 1H), 4.18–4.12 (m, 1H), 3.29–3.19 (m, 2H), 2.24–2.14 (m, 2H), 1.91–1.67 (m, 4H), 1.09 (t, $J = 7.2$, 3H). ^{13}C NMR (75 MHz, methanol- d_4) δ 170.6, 154.4, 153.4, 152.4, 148.2, 140.8, 129.8, 127.4, 123.2, 121.2, 120.2, 115.5, 89.2, 85.1, 83.8, 73.6, 72.0, 56.9, 33.71, 29.7, 29.6, 21.1, 13.7. HRMS: (NSI+) m/z calcd for $\text{C}_{23}\text{H}_{28}\text{ClN}_6\text{O}_5$ [M + H] $^+$ 503.1810, found 503.1804. UPLC analysis: $t_R = 3.00$ min; peak area > 95% (detection at 254 nm).

(2*S*,3*S*,4*R*,5*R*)-5-(6-(((1*R*,2*R*)-2-(3-Chlorophenoxy)cyclopentyl)amino)-9*H*-purin-9-yl)-*N*-ethyl-3,4-dihydroxytetrahydrofuran-2-carboxamide (**54**). **54** was synthesized according to general procedure F using **42** (0.184 mmol) and acetic acid (16 mL). The reaction was run for 20 h. After purification with flash column chromatography (MeOH/CH₂Cl₂, 8%), **54** was obtained (68 mg, 0.135 mmol, 73%). ^1H NMR: (300 MHz, DMSO- d_6) δ 8.86 (t, $J = 5.6$, 1H), 8.44 (s, 1H), 8.33 (s, 1H), 8.19 (d, $J = 6.4$, 1H), 7.32–7.23 (m, 2H), 6.99–6.92 (m, 2H), 5.98 (d, $J = 7.5$, 1H), 5.75 (d, $J = 4.3$, 1H), 5.54 (d, $J = 6.4$, 1H), 4.94–4.87 (m, 1H), 4.70–4.57 (m, 2H), 4.32 (d, $J = 1.6$, 1H), 4.18–4.13 (m, 1H), 3.29–3.17 (m, 2H), 2.23–2.08 (m, 2H), 1.90–1.64 (m, 4H), 1.09 (t, $J = 7.2$, 3H). ^{13}C NMR (75 MHz, methanol- d_4) δ 170.6, 158.8, 154.3, 152.3, 148.2, 140.8, 134.4, 129.9, 120.3, 120.1, 115.6, 114.3, 89.2, 85.1, 82.8, 73.6, 72.1, 56.7, 33.7, 29.6, 29.4, 21.0, 13.7. HRMS: (NSI+) m/z calcd for $\text{C}_{23}\text{H}_{28}\text{ClN}_6\text{O}_5$ [M + H] $^+$ 503.1780, found 503.1804. UPLC analysis: $t_R = 3.10$ min; peak area > 95% (detection at 254 nm).

(2*S*,3*S*,4*R*,5*R*)-5-(6-(((1*R*,2*R*)-2-(4-Chlorophenoxy)cyclopentyl)amino)-9*H*-purin-9-yl)-*N*-ethyl-3,4-dihydroxytetrahydrofuran-2-carboxamide (**55**). **55** was synthesized according to general procedure F using **43** (0.217 mmol) and acetic acid (8 mL). The reaction was run for 23 h. After purification with flash column chromatography (MeOH/CH₂Cl₂, 7%), **55** was obtained (74 mg, 0.146 mmol, 67%). ^1H NMR: (300 MHz, DMSO- d_6) δ 8.87 (t, $J = 5.7$, 1H), 8.43 (s, 1H), 8.32 (s, 1H), 8.19 (d, $J = 6.5$, 1H), 7.34–7.27 (m, 2H), 7.04 (d, $J = 8.1$, 2H), 5.98 (d, $J = 7.5$, 1H), 5.75 (d, $J = 4.3$, 1H), 5.54 (d, $J = 6.4$, 1H), 4.90–4.80 (m, 1H), 4.76–4.58 (m, 2H), 4.32 (d, $J = 1.6$, 1H), 4.18–4.12 (m, 1H), 3.28–3.17 (m, 2H), 2.26–

2.10 (m, 2H), 1.91–1.57 (m, 4H), 1.09 (t, $J = 7.2$, 3H). ^{13}C NMR: (75 MHz, methanol- d_4) δ 170.6, 156.6, 154.4, 152.4, 148.2, 140.8, 128.8, 125.1, 120.1, 116.8, 89.2, 85.1, 82.8, 73.6, 72.1, 56.9, 33.7, 29.7, 29.6, 21.0, 13.7. HRMS: (NSI+) m/z calcd for $\text{C}_{23}\text{H}_{28}\text{ClN}_6\text{O}_5$ [M + H] $^+$ 503.1789, found 503.1804. UPLC analysis: $t_R = 3.10$ min; peak area > 99% (detection at 254 nm).

Cell Culture. CHO-K1-hA₁R, CHO-K1-hA_{2A}R, CHO-K1-hA_{2B}R, and CHO-K1-hA₃R cells were routinely cultured in Ham's F-12 supplemented with 10% fetal bovine serum (FBS). HEK293 human Nluc-A₁R and HEK293 rat Nluc-A₁R were cultured in Dulbecco's modified Eagle's medium (DMEM)/Nutrient Mixture F12 supplemented with 10% FBS. All cells were maintained at 37 °C with 5% CO₂ in humidified air.

cAMP Accumulation Assay. cAMP accumulation experiments were performed using a LANCE Ultra cAMP detection kit as described previously.^{25,40} Briefly, CHO-K1 cells stably expressing human WT A₁R, A_{2A}R, A_{2B}R, and A₃R were seeded at 2000 cells per well in a white 384-well OptiPlate. Cells were then incubated with adenosine receptor ligands (ranging between 100 μM and 1 pM) for 30 min at room temperature. For A₁R and A₃R expressing cells, 10 and 1 μM forskolin, respectively, was added at the same time as the addition of the adenosine receptor ligands, as we have described previously.^{13,24,25}

NanoBRET Assay for Binding. To determine the affinity (pK_i) of adenosine receptor ligands, a NanoBRET competition binding assay was performed as described previously.^{24,25} Briefly, CA200645 was used at 20 nM. Kinetic data were fitted with the "kinetic of competitive binding" model³⁵ (built into Prism v9.1 (GraphPad Software, San Diego, CA)) to determine affinity (pK_i) values and the association rate constant (k_{on}) and dissociation rates (k_{off}) for AR ligands. In agreement with our previous studies, we determined the K_d of CA200645 to be 18.29 ± 2.4 nM at the human A₁R and 32.96 ± 2.8 nM at the rat A₁R.^{25,40} The "one-site- K_i model" derived from the Cheng and Prusoff correction and available in Prism was fitted with the BRET ratio at 10 min post stimulation, and affinity (pK_i) constant values at equilibrium for adenosine receptor ligands were determined.

Data and Statistical Analysis. Data were analyzed using Prism v9.1 (GraphPad Software, San Diego, CA). Dose–response curves were fitted using a three-parameter logistic equation to calculate response range and pEC_{50} , and normalized to forskolin stimulation (A_{2A}R and A_{2B}R) or forskolin inhibition (A₁R and A₃R), expressed as percentage of 100 μM forskolin. Adenosine and NECA stimulations were used as intrinsic controls across all experiments.

Receptor binding kinetics was determined as described previously²⁵ using the Motulsky and Mahan method³⁵ (built into Prism v9.1) to determine the test compound association rate constant and dissociation rate constant. The k_{on} and k_{off} values for binding of CA200645 were determined to be $k_{on} = 3.67 \pm 0.34 \times 10^6 \text{ M}^{-1} \text{ min}^{-1}$ and $k_{off} = 0.064 \pm 0.0023 \text{ min}^{-1}$ at the human A₁R and $k_{on} = 2.93 \pm 0.24 \times 10^6 \text{ M}^{-1} \text{ min}^{-1}$ and $k_{off} = 0.066 \pm 0.0022 \text{ min}^{-1}$ at the rat A₁R.

To calculate the relative activities (RA) of compounds (Figure 2), eq 1 was used:

$$\text{RA} = \frac{\text{EC}_{50} \times E_{\text{max}}(\text{reference compound})}{\text{EC}_{50} \times E_{\text{max}}(\text{compound})} \quad (1)$$

where E_{max} is the maximal response and EC_{50} is the agonist concentration required to produce a half-maximal response, and web plot was plotted using Microsoft Excel. Since the receptors are expressed in the same cell background and adenosine and NECA are full potent agonists across all the adenosine subtypes, we reasoned that changes in log(RA) for a given ligand, relative to NECA or adenosine at A₁R, would provide a quantitative means of comparing receptor selectivity of individual adenosine receptor ligands.

The statistical analysis was performed in Prism v9.1 using one-way ANOVA with a Dunnett's post-test for multiple comparisons following the guidelines as described by Curtis *et al.*³¹ All experiments were performed in a minimum of three repeats conducted in duplicate, and data were reported as mean \pm SEM.

Adenosine Receptor Structures. The active state A₁R coordinates were retrieved from Protein Data Bank (PDB) database⁴¹ entry 7LD4.¹⁹ PDB ID 5G53⁴² was used for A_{2A}R in active conformation. A_{2B}R in active conformation was modeled using 5G53 as a template through Modeller 9.19.⁴³ The A_{2B}R ECL2 (L142^{ECL2}, K170^{ECL2}) was retrieved from the inactive state model by AlphaFold2⁴⁴ (entry P29275) and inserted in the homology model by superposition. A₃R in active conformation was modeled using 7LD4 as a template through Modeller 9.19.⁴³ The A₃R ECL2 (K152^{ECL2}, S165^{ECL2}) was retrieved from the inactive state model by AlphaFold2 (entry P0DMS8) and inserted in the homology model by superposition. All the ARs structures did not present either the ICL3 or the G protein bound to its intracellular binding site.

Force Field and Ligand Parameters for MD Simulations. The CHARMM36^{45,46}/CGenFF 3.0.1^{47–49} force field combination was employed in this work. The force field, topology, and parameter files for **20** and **27** were obtained from the ParamChem webserver.⁴⁷

System Preparations for MD Simulations. For all systems, hydrogen atoms were added by means of the pdb2pqr⁵⁰ and propka⁵¹ software (considering a simulated pH of 7.0). The protonation of titratable side chains was checked by visual inspection. The resulting receptors were separately inserted in a square 90 × 90 Å 1-palmitoyl-2-oleyl-*sn*-glycerol-3-phosphocholine (POPC) bilayer (previously built by using the VMD Membrane Builder plugin 1.1, Membrane Plugin, Version 1.1. at <http://www.ks.uiuc.edu/Research/vmd/plugins/membrane/>) through an insertion method,⁵² along with their co-crystallized ligand (and the crystallographic water molecules within 5 Å of the ligand). The receptor orientation was obtained by superposing the coordinates on the corresponding structure retrieved from the OPM database.⁵³ Lipids overlapping the receptor transmembrane helical bundle were removed, and TIP3P water molecules⁵⁴ were added to the simulation box by means of the VMD Solvate plugin 1.5 (Solvate Plugin, Version 1.5. at <http://www.ks.uiuc.edu/Research/vmd/plugins/solvate/>). Finally, overall charge neutrality was reached by adding Na⁺/Cl⁻ counterions up to the final concentration of 0.150 M using the VMD Autoionize plugin 1.3 (Autoionize Plugin, Version 1.3. at <http://www.ks.uiuc.edu/Research/vmd/plugins/autoionize/>).

System Equilibration and MD Settings. The MD engine ACEMD⁵⁵ was employed for both the equilibration and productive simulations. The equilibration was achieved in isothermal–isobaric conditions (NPT) using a Berendsen barostat⁵⁶ (target pressure 1 atm) and Langevin thermostat⁵⁷ (target temperature 300 K) with low damping of 1 ps⁻¹. A multistage procedure was performed (integration time step of 2 fs): first, clashes between protein and lipid atoms were reduced through 1500 conjugate-gradient minimization steps, and then 1 kcal mol⁻¹ Å⁻² positional restraints on lipid phosphorus atoms, protein atoms other than C α , and protein C α atoms were gradually removed over 2, 60, and 80 ns, respectively. The last 20 ns of equilibration was performed without any positional restraints. Productive trajectories were computed with an integration time step of 4 fs in the canonical ensemble (NVT). The target temperature was set at 300 K using a thermostat damping of 0.1 ps⁻¹. The M-SHAKE algorithm^{58,59} was employed to constrain the bond lengths involving hydrogen atoms. The cutoff distance for electrostatic interactions was set at 9 Å, with a switching function applied beyond 7.5 Å. Long-range Coulomb interactions were handled using the particle mesh Ewald summation method (PME)⁶⁰ by setting the mesh spacing to 1.0 Å.

Molecular Docking. A first attempt to dock **20** and **27** into all the four ARs subtypes was performed on structures prepared as reported above using Vina⁶¹ in a 30 × 30 × 30 Å cube centered on the atom CZ of the ECL2 conserved phenylalanine residue (F171 in A₁R, F168 in A_{2A}R, F173 in A_{2B}R, and F168 in A₃R). Successive molecular docking simulations of **20** and **27**, with the same settings, were performed into the AR structure extracted from MD simulations (see below). A₁R, A_{2A}R, and A_{2B}R were extracted from adiabatic MD simulations, while the A₃R structure was the equilibrated apo structure.

Adiabatic MD of the apo Adenosine Receptors. The apo AR structures were prepared and equilibrated as reported above. A₁R, A_{2A}R, and A_{2B}R were subjected to 50 ns of adiabatic MD.⁶² A target distance of 13 Å and a force constant of 100 kJ mol⁻¹ Å⁻² were set to favor the opening of the salt bridge between ECL2 and ECL3: E172^{ECL2}(C δ)-K265^{ECL3}(N ζ) on A₁R, E169^{ECL2}(C δ)-H264(H ϵ 2) on A_{2A}R, and E174(C δ)-K265(N ζ) and K267(N ζ) on A_{2B}R.

MD Analysis. Root mean square deviations (RMSD) and fluctuation (RMSF) were computed using VMD.⁶³ Interatomic contacts and hydrogen bonds were detected using the GetContacts scripts tool (<https://getcontacts.github.io>). Contacts and hydrogen bond persistency were quantified as the percentage of frames (over all the frames obtained by merging the different replicas) in which protein residues formed contacts or hydrogen bonds with the ligand. Structural water molecules were detected in the apo ARs using AquaMMapS.⁶⁴ Short 10 ns simulations were performed with a time step 2 fs, restraining the C α atoms and saving a frame every 20 ps of simulation.

Residue Numbering System. Throughout the manuscript, the Ballesteros–Weinstein residue numbering system for GPCRs is adopted.⁶⁵

■ ASSOCIATED CONTENT

Supporting Information

The Supporting Information is available free of charge at <https://pubs.acs.org/doi/10.1021/acs.jmedchem.2c01414>.

Summary of *O*-alkylation studies (Scheme S1); synthetic confirmation of 2-aminocyclopentanol stereochemistry (Figure S1); molecular docking of **20** and **27** (Figures S2–S3); molecular dynamics simulations (Figures S4 and S6); mutagenesis study (Figure S5); purity assessment for all tested compounds (Tables S1 and S2); molecular formula strings of all final compounds (Table S3); and reproduction of ¹H and ¹³C NMR spectra for all tested compounds (PDF)

MD simulations of **27** (orange stick representation) in complex with the four AR subtypes (MP4)

MD simulations of **27** and **20** in complex with A₁R (white transparent ribbon) during three MD simulations of 2 μ s each (MP4)

Coordinates of **27** bound to A₁R (PDB)

Molecular formula strings of all final compounds (CSV)

■ AUTHOR INFORMATION

Corresponding Authors

Graham Ladds – Department of Pharmacology, University of Cambridge, Cambridge CB2 1PD, U.K.; orcid.org/0000-0001-7320-9612; Phone: +44 (0)1223 334 020; Email: grl30@cam.ac.uk

Martin Lochner – Institute of Biochemistry and Molecular Medicine, University of Bern, 3012 Bern, Switzerland; orcid.org/0000-0003-4930-1886; Phone: +41 (0)31 684 3311; Email: martin.lochner@ibmm.unibe.ch

Authors

Barbara Preti – Institute of Biochemistry and Molecular Medicine, University of Bern, 3012 Bern, Switzerland

Anna Suchankova – Department of Pharmacology, University of Cambridge, Cambridge CB2 1PD, U.K.

Giuseppe Deganutti – Centre for Sport, Exercise and Life Sciences, Faculty of Health and Life Sciences, Coventry University, Coventry CV1 5FB, U.K.; orcid.org/0000-0001-8780-2986

Michele Leuenberger – Institute of Biochemistry and Molecular Medicine, University of Bern, 3012 Bern, Switzerland; orcid.org/0000-0003-0641-4338

Kerry Barkan – Department of Pharmacology, University of Cambridge, Cambridge CB2 1PD, U.K.

Iga Manulak – Department of Pharmacology, University of Cambridge, Cambridge CB2 1PD, U.K.

Xianglin Huang – Department of Pharmacology, University of Cambridge, Cambridge CB2 1PD, U.K.

Sabrina Carvalho – Department of Pharmacology, University of Cambridge, Cambridge CB2 1PD, U.K.

Complete contact information is available at:

<https://pubs.acs.org/10.1021/acs.jmedchem.2c01414>

Author Contributions

#B.P., A.S. and G.D. contributed equally to this work. M.Lo. and G.H. also contributed equally.

Notes

The authors declare no competing financial interest.

ACKNOWLEDGMENTS

This study was supported by the Swiss National Science Foundation (B.P., M.Le. and M.Lo.), the Cambridge Trust (A.S.), the Leverhulme Trust (K.B. and G.L.), an AstraZeneca studentship (S.C.), a British Pharmacological Society Vacation Studentship (I.M.), a China Scholarship Council Cambridge International Scholarship (X.H.), and the BBSRC (G.L.). We thank Matt Ladds for his help with proof checking the statistical analysis and the Analytical Services from the Department of Chemistry, Biochemistry, and Pharmaceutical Sciences, University of Bern, Switzerland, for measuring NMR and MS spectra of synthetic intermediates and final compounds.

ABBREVIATIONS USED

AC, adenylyl cyclase; AR, adenosine receptor; A₁R, adenosine A₁ receptor; A_{2A}R, adenosine A_{2A} receptor; A_{2B}R, adenosine A_{2B} receptor; A₃R, adenosine A₃ receptor; BRET, bioluminescence resonance energy transfer; DAIB, (diacetoxyiodo)benzene; DIAD, diisopropyl azodicarboxylate; NECA, S'-N-ethylcarboxamidoadenosine; RA, relative activity; RT, residence time; TEMPO, (2,2,6,6-tetramethylpiperidin-1-yl)oxyl

REFERENCES

- (1) Jacobson, K. A.; Müller, C. E. Medicinal chemistry of adenosine, P2Y and P2X receptors. *Neuropharmacology* **2016**, *104*, 31–49.
- (2) Sawynok, J. Adenosine receptor targets for pain. *Neuroscience* **2016**, *338*, 1–18.
- (3) Huang, Z. L.; Qu, W. M.; Eguchi, N.; Chen, J. F.; Schwarzschild, M. A.; Fredholm, B. B.; Urade, Y.; Hayaishi, O. Adenosine A_{2A}, but not A₁, receptors mediate the arousal effect of caffeine. *Nat. Neurosci.* **2005**, *8*, 858–859.
- (4) Lazarus, M.; Shen, H. Y.; Cherasse, Y.; Qu, W. M.; Huang, Z. L.; Bass, C. E.; Winsky-Sommerer, R.; Semba, K.; Fredholm, B. B.; Boison, D.; Hayaishi, O.; Urade, Y.; Chen, J. F. Arousal effect of caffeine depends on adenosine A_{2A} receptors in the shell of the nucleus accumbens. *J. Neurosci.* **2011**, *31*, 10067–10075.
- (5) Eltzschig, H. K.; Sitkovsky, M. V.; Robson, S. C. Purinergic signaling during inflammation. *N. Engl. J. Med.* **2012**, *367*, 2322–2333.
- (6) Eltzschig, H. K.; Warner, D. S.; Warner, M. A. Adenosine: an old drug newly discovered. *Anesthesiology* **2009**, *111*, 904–915.

(7) Fredholm, B. B. Adenosine, an endogenous distress signal, modulates tissue damage and repair. *Cell Death Differ.* **2007**, *14*, 1315–1323.

(8) Haskó, G.; Linden, J.; Cronstein, B.; Pacher, P. Adenosine receptors: therapeutic aspects for inflammatory and immune diseases. *Nat. Rev. Drug Discov.* **2008**, *7*, 759–770.

(9) Eltzschig, H. K.; Carmeliet, P. Hypoxia and inflammation. *N. Engl. J. Med.* **2011**, *364*, 656–665.

(10) Jacobson, K. A.; Gao, Z. G. Adenosine receptors as therapeutic targets. *Nat. Rev. Drug Discov.* **2006**, *5*, 247–264.

(11) Chen, J. F.; Eltzschig, H. K.; Fredholm, B. B. Adenosine receptors as drug targets - what are the challenges? *Nat. Rev. Drug Discov.* **2013**, *12*, 265–286.

(12) Jacobson, K. A.; Tosh, D. K.; Jain, S.; Gao, Z. G. Historical and current adenosine receptor agonists in preclinical and clinical development. *Front. Cell. Neurosci.* **2019**, *13*, 124.

(13) Knight, A.; Hemmings, J. L.; Winfield, I.; Leuenberger, M.; Frattini, E.; Frenguelli, B. G.; Dowell, S. J.; Lochner, M.; Ladds, G. Discovery of novel adenosine receptor agonists that exhibit subtype selectivity. *J. Med. Chem.* **2016**, *59*, 947–964.

(14) Tosh, D. K.; Rao, H.; Bitant, A.; Salmaso, V.; Mannes, P.; Lieberman, D. I.; Vaughan, K. L.; Mattison, J. A.; Rothwell, A. C.; Auchampach, J. A.; Ciancetta, A.; Liu, N.; Cui, Z.; Gao, Z. G.; Reitman, M. L.; Gavrilova, O.; Jacobson, K. A. Design and in vivo characterization of A₁ adenosine receptor agonists in the native ribose and conformationally constrained (N)-methanocarba series. *J. Med. Chem.* **2019**, *62*, 1502–1522.

(15) Petrelli, R.; Scortichini, M.; Belardo, C.; Boccella, S.; Luongo, L.; Capone, F.; Kachler, S.; Vita, P.; Del Bello, F.; Maione, S.; Lavecchia, A.; Klotz, K. N.; Cappellacci, L. Structure-based design, synthesis, and in vivo antinociceptive effects of selective A₁ adenosine receptor agonists. *J. Med. Chem.* **2018**, *61*, 305–318.

(16) Franchetti, P.; Cappellacci, L.; Vita, P.; Petrelli, R.; Lavecchia, A.; Kachler, S.; Klotz, K.-N.; Marabese, I.; Luongo, L.; Maione, S.; Grifantini, M. N⁶-Cycloalkyl- and N⁶-bicycloalkyl-C5'(C2')-modified adenosine derivatives as high-affinity and selective agonists at the human A₁ adenosine receptor with antinociceptive effects in mice. *J. Med. Chem.* **2009**, *52*, 2393–2406.

(17) Luongo, L.; Petrelli, R.; Gatta, L.; Giordano, C.; Guida, F.; Vita, P.; Franchetti, P.; Grifantini, M.; Novellis, V. D.; Cappellacci, L.; Maione, S. 5'-Chloro-5'-deoxy-(±)-ENBA, a potent and selective adenosine A₁ receptor agonist, alleviates neuropathic pain in mice through functional glial and microglial changes without affecting motor or cardiovascular functions. *Molecules* **2012**, *17*, 13712–13726.

(18) Guo, M.; Bakhoda, A.; Gao, Z. G.; Ramsey, J. M.; Li, Y.; O'Connor, K. A.; Kelleher, A. C.; Eisenberg, S. M.; Kang, Y.; Yan, X.; Javdan, C.; Fowler, J. S.; Rice, K. C.; Hooker, J. M.; Jacobson, K. A.; Kim, S. W.; Volkow, N. D. Discovery of highly potent adenosine A₁ receptor agonists: targeting positron emission tomography probes. *ACS Chem. Neurosci.* **2021**, *12*, 3410–3417.

(19) Draper-Joyce, C. J.; Bhola, R.; Wang, J.; Bhattarai, A.; Nguyen, A. T. N.; Cowie-Kent, I.; O'Sullivan, K.; Chia, L. Y.; Venugopal, H.; Valant, C.; Thal, D. M.; Wootten, D.; Panel, N.; Carlsson, J.; Christie, M. J.; White, P. J.; Scammells, P.; May, L. T.; Sexton, P. M.; Danev, R.; Miao, Y.; Glukhova, A.; Imlach, W. L.; Christopoulos, A. Positive allosteric mechanisms of adenosine A₁ receptor-mediated analgesia. *Nature* **2021**, *597*, 571–576.

(20) Elzein, E.; Zablocki, J. A₁ adenosine receptor agonists and their potential therapeutic applications. *Expert Opin. Invest. Drugs* **2008**, *17*, 1901–1910.

(21) Staehr, P. M.; Dhalla, A. K.; Zack, J.; Wang, X.; Ho, Y. L.; Bingham, J.; Belardinelli, L. Reduction of free fatty acids, safety, and pharmacokinetics of oral GS-9667, an A₁ adenosine receptor partial agonist. *J. Clin. Pharmacol.* **2013**, *53*, 385–392.

(22) Wall, M. J.; Hill, E.; Huckstepp, R.; Barkan, K.; Deganutti, G.; Leuenberger, M.; Preti, B.; Winfield, I.; Carvalho, S.; Suchankowa, A.; Wei, H.; Safitri, D.; Huang, X.; Imlach, W.; La Mache, C.; Dean, E.; Hume, C.; Hayward, S.; Oliver, J.; Zhao, F.-Y.; Spanswick, D.; Reynolds, C. A.; Lochner, M.; Ladds, G.; Frenguelli, B. G. Selective

activation of $G_{\alpha\text{ob}}$ by an adenosine A_1 receptor agonist elicits analgesia without cardiorespiratory depression. *Nat. Commun.* **2022**, *13*, 4150.

(23) Draper-Joyce, C. J.; Khoshouei, M.; Thal, D. M.; Liang, Y.-L.; Nguyen, A. T. N.; Furness, S. G. B.; Venugopal, H.; Baltos, J.-A.; Plitzko, J. M.; Danev, R.; Baumeister, W.; May, L. T.; Wootten, D.; Sexton, P. M.; Glukhova, A.; Christopoulos, A. Structure of the adenosine-bound human adenosine A_1 receptor- G_i complex. *Nature* **2018**, *558*, 559–563.

(24) Deganutti, G.; Barkan, K.; Preti, B.; Leuenerger, M.; Wall, M.; Frenguelli, B. G.; Lochner, M.; Ladds, G.; Reynolds, C. A. Deciphering the agonist binding mechanism to the adenosine A_1 receptor. *ACS Pharmacol. Transl. Sci.* **2021**, *4*, 314–326.

(25) Barkan, K.; Lagarias, P.; Stampelou, M.; Stamatis, D.; Hoare, S.; Safitri, D.; Klotz, K. N.; Vrontaki, E.; Kolocouris, A.; Ladds, G. Pharmacological characterisation of novel adenosine A_3 receptor antagonists. *Sci. Rep.* **2020**, *10*, 20781.

(26) Jagtap, P. Adenosine compounds and their use thereof. WO2011/119919 A1, 2011.

(27) Mitsunobu, O.; Yamada, M. Preparation of esters of carboxylic and phosphoric acid via quaternary phosphonium salts. *Bull. Chem. Soc. Jpn.* **1967**, *40*, 2380–2382.

(28) Kotra, L. P.; Manouilov, K. K.; Cretton-Scott, E.; Sommadossi, J. P.; Boudinot, F. D.; Schinazi, R. F.; Chu, C. K. Synthesis, biotransformation, and pharmacokinetic studies of 9-(β -D-arabinofuranosyl)-6-azidopurine: a prodrug for Ara-A designed to utilize the azide reduction pathway. *J. Med. Chem.* **1996**, *39*, 5202–5207.

(29) Middleton, R. J.; Briddon, S. J.; Cordeaux, Y.; Yates, A. S.; Dale, C. L.; George, M. W.; Baker, J. G.; Hill, S. J.; Kellam, B. New fluorescent adenosine A_1 -receptor agonists that allow quantification of ligand-receptor interactions in microdomains of single living cells. *J. Med. Chem.* **2007**, *50*, 782–793.

(30) Murthy, S.; Desantis, J.; Verheugd, P.; Maksimainen, M. M.; Venkannagari, H.; Massari, S.; Ashok, Y.; Obaji, E.; Nkizinkinko, Y.; Lüscher, B.; Tabarrini, O.; Lehtiö, L. 4-(Phenoxy) and 4-(benzyloxy)-benzamides as potent and selective inhibitors of mono-ADP-ribosyltransferase PARP10/ARTD10. *Eur. J. Med. Chem.* **2018**, *156*, 93–102.

(31) Curtis, M. J.; Alexander, S.; Cirino, G.; Docherty, J. R.; George, C. H.; Giembycz, M. A.; Hoyer, D.; Insel, P. A.; Izzo, A. A.; Ji, Y.; MacEwan, D. J.; Sobey, C. G.; Stanford, S. C.; Teixeira, M. M.; Wonnacott, S.; Ahluwalia, A. Experimental design and analysis and their reporting II: updated and simplified guidance for authors and peer reviewers. *Br. J. Pharmacol.* **2018**, *175*, 987–993.

(32) Guo, D.; Heitman, L. H.; IJzerman, A. P. Kinetic aspects of the interaction between ligand and G protein-coupled receptor: the case of the adenosine receptors. *Chem. Rev.* **2017**, *117*, 38–66.

(33) Sykes, D. A.; Stoddart, L. A.; Kilpatrick, L. E.; Hill, S. J. Binding kinetics of ligands acting at GPCRs. *Mol. Cell. Endocrinol.* **2019**, *485*, 9–19.

(34) Vauquelin, G. Effects of target binding kinetics on *in vivo* drug efficacy: k_{off} , k_{on} and rebinding. *Br. J. Pharmacol.* **2016**, *173*, 2319–2334.

(35) Motulsky, H. J.; Mahan, L. C. The kinetics of competitive radioligand binding predicted by the law of mass action. *Mol. Pharmacol.* **1984**, *25*, 1–9.

(36) Lu, H.; Tonge, P. J. Drug–target residence time: critical information for lead optimization. *Curr. Opin. Chem. Biol.* **2010**, *14*, 467–474.

(37) Suchankova, A.; Stampelou, M.; Koutsouki, K.; Pousias, A.; Dhingra, L.; Barkan, K.; Pouli, N.; Marakos, P.; Tenta, R.; Kolocouris, A.; Lougiakis, N.; Ladds, G. Discovery of a high affinity adenosine A_1/A_3 receptor antagonist with a novel 7-amino-pyrazolo[3,4-*d*]pyridazine scaffold. *ACS Med. Chem. Lett.* **2022**, *13*, 923–934.

(38) Carpenter, B.; Lebon, G. Human adenosine A_{2A} receptor: molecular mechanism of ligand binding and activation. *Front. Pharmacol.* **2017**, *8*, 898.

(39) Frenguelli, B. G.; Wall, M. J. Adenosine receptor agonists. WO2020/188288 A1, 2020.

(40) Deganutti, G.; Barkan, K.; Ladds, G.; Reynolds, C. A. Multisite model of allostery for the adenosine A_1 receptor. *J. Chem. Inf. Model.* **2021**, *61*, 2001–2015.

(41) Berman, H. M.; Westbrook, J.; Feng, Z.; Gilliland, G.; Bhat, T. N.; Weissig, H.; Shindyalov, I. N.; Bourne, P. E. The protein data bank. *Nucleic Acids Res.* **2000**, *28*, 235–242.

(42) Carpenter, B.; Nehmé, R.; Warne, T.; Leslie, A. G. W.; Tate, C. G. Structure of the adenosine A_{2A} receptor bound to an engineered G protein. *Nature* **2016**, *536*, 104–107.

(43) Fiser, A.; Šali, A. Modeller: generation and refinement of homology-based protein structure models. *Methods Enzymol.* **2003**, *374*, 461–491.

(44) Jumper, J.; Evans, R.; Pritzel, A.; Green, T.; Figurnov, M.; Ronneberger, O.; Tunyasuvunakool, K.; Bates, R.; Židek, A.; Potapenko, A.; Bridgland, A.; Meyer, C.; Kohl, S. A. A.; Ballard, A. J.; Cowie, A.; Romera-Paredes, B.; Nikolov, S.; Jain, R.; Adler, J.; Back, T.; Petersen, S.; Reiman, D.; Clancy, E.; Zielsinski, M.; Steinegger, M.; Pacholska, M.; Berghammer, T.; Bodensteiner, S.; Silver, D.; Vinyals, O.; Senior, A. W.; Kavukcuoglu, K.; Kohli, P.; Hassabis, D. Highly accurate protein structure prediction with AlphaFold. *Nature* **2021**, *596*, 583–589.

(45) Huang, J.; MacKerell, A. D., Jr. CHARMM36 all-atom additive protein force field: validation based on comparison to NMR data. *J. Comput. Chem.* **2013**, *34*, 2135–2145.

(46) Huang, J.; Rauscher, S.; Nawrocki, G.; Ran, T.; Feig, M.; de Groot, B. L.; Grubmüller, H.; MacKerell, A. D., Jr. CHARMM36m: an improved force field for folded and intrinsically disordered proteins. *Nat. Methods* **2017**, *14*, 71–73.

(47) Vanommeslaeghe, K.; MacKerell, A. D., Jr. Automation of the CHARMM General Force Field (CGenFF) I: bond perception and atom typing. *J. Chem. Inf. Model.* **2012**, *52*, 3144–3154.

(48) Vanommeslaeghe, K.; Raman, E. P.; MacKerell, A. D., Jr. Automation of the CHARMM General Force Field (CGenFF) II: assignment of bonded parameters and partial atomic charges. *J. Chem. Inf. Model.* **2012**, *52*, 3155–3168.

(49) Yu, W.; He, X.; Vanommeslaeghe, K.; MacKerell, A. D., Jr. Extension of the CHARMM General Force Field to sulfonyl-containing compounds and its utility in biomolecular simulations. *J. Comput. Chem.* **2012**, *33*, 2451–2468.

(50) Dolinsky, T. J.; Nielsen, J. E.; McCammon, J. A.; Baker, N. A. PDB2PQR: an automated pipeline for the setup of Poisson-Boltzmann electrostatics calculations. *Nucleic Acids Res.* **2004**, *32*, W665–W667.

(51) Olsson, M. H. M.; Søndergaard, C. R.; Rostkowski, M.; Jensen, J. H. PROPKA3: consistent treatment of internal and surface residues in empirical pK_a predictions. *J. Chem. Theory Comput.* **2011**, *7*, 525–537.

(52) Sommer, B. Membrane packing problems: a short review on computational membrane modeling methods and tools. *Comput. Struct. Biotechnol. J.* **2013**, *5*, No. e201302014.

(53) Lomize, M. A.; Lomize, A. L.; Pogozheva, I. D.; Mosberg, H. I. OPM: orientations of proteins in membranes database. *Bioinformatics* **2006**, *22*, 623–625.

(54) Jorgensen, W. L.; Chandrasekhar, J.; Madura, J. D.; Impey, R. W.; Klein, M. L. Comparison of simple potential functions for simulating liquid water. *J. Chem. Phys.* **1983**, *79*, 926–935.

(55) Harvey, M. J.; Giupponi, G.; Fabritiis, G. D. ACEMD: accelerating biomolecular dynamics in the microsecond time scale. *J. Chem. Theory Comput.* **2009**, *5*, 1632–1639.

(56) Berendsen, H. J. C.; Postma, J. P. M.; Gunsteren, W. F. v.; DiNola, A.; Haak, J. R. Molecular dynamics with coupling to an external bath. *J. Chem. Phys.* **1984**, *81*, 3684–3690.

(57) Loncharich, R. J.; Brooks, B. R.; Pastor, R. W. Langevin dynamics of peptides: the frictional dependence of isomerization rates of *N*-acetylalanine-*N'*-methylamide. *Biopolymers* **1992**, *32*, 523–535.

(58) Forester, T. R.; Smith, W. SHAKE, rattle, and roll: efficient constraint algorithms for linked rigid bodies. *J. Comput. Chem.* **1998**, *19*, 102–111.

(59) Krätzler, V.; van Gunsteren, W. F.; Hünenberger, P. H. A fast SHAKE algorithm to solve distance constraint equations for small molecules in molecular dynamics simulations. *J. Comput. Chem.* **2001**, *22*, 501–508.

(60) Essmann, U.; Perera, L.; Berkowitz, M. L.; Darden, T.; Lee, H.; Pedersen, L. G. A smooth particle mesh Ewald method. *J. Chem. Phys.* **1995**, *103*, 8577–8593.

(61) Trott, O.; Olson, A. J. AutoDock Vina: improving the speed and accuracy of docking with a new scoring function, efficient optimization, and multithreading. *J. Comput. Chem.* **2010**, *31*, 455–461.

(62) Marchi, M.; Ballone, P. Adiabatic bias molecular dynamics: a method to navigate the conformational space of complex molecular systems. *J. Chem. Phys.* **1999**, *110*, 3697–3702.

(63) Humphrey, W.; Dalke, A.; Schulten, K. VMD: visual molecular dynamics. *J. Mol. Graph.* **1996**, *14*, 33–38.

(64) Cuzzolin, A.; Deganutti, G.; Salmaso, V.; Sturlese, M.; Moro, S. AquaMMapS: an alternative tool to monitor the role of water molecules during protein-ligand association. *ChemMedChem* **2018**, *13*, 522–531.

(65) Ballesteros, J. A.; Weinstein, H. [19] Integrated methods for the construction of three-dimensional models and computational probing of structure-function relations in G protein-coupled receptors. In *Methods in Neurosciences*; Stuart, C. S., Ed.; Academic Press: San Diego, 1995; Vol. 25, pp. 366–428.

Recommended by ACS

Selective A₃ Adenosine Receptor Antagonist Radioligand for Human and Rodent Species

R. Rama Suresh, Kenneth A. Jacobson, *et al.*

MARCH 02, 2022
ACS MEDICINAL CHEMISTRY LETTERS

READ 

Dual A1/A3 Adenosine Receptor Antagonists: Binding Kinetics and Structure–Activity Relationship Studies Using Mutagenesis and Alchemical Binding Free Energy Calcula...

Margarita Stampelou, Antonios Kolocouris, *et al.*

SEPTEMBER 29, 2022
JOURNAL OF MEDICINAL CHEMISTRY

READ 

Truncated (N)-Methanocarba Nucleosides as Partial Agonists at Mouse and Human A₃ Adenosine Receptors: Affinity Enhancement by N⁶-(2-Phenylethyl) Substitution

Dilip K. Tosh, Kenneth A. Jacobson, *et al.*

APRIL 09, 2020
JOURNAL OF MEDICINAL CHEMISTRY

READ 

GPCR Agonist-to-Antagonist Conversion: Enabling the Design of Nucleoside Functional Switches for the A_{2A} Adenosine Receptor

Anna Shiriaeva, Vadim Cherezov, *et al.*

AUGUST 17, 2022
JOURNAL OF MEDICINAL CHEMISTRY

READ 

Get More Suggestions >